Aus dem Institut für Transplantationsdiagnostik und Zelltherapeutika (ITZ)
der Heinrich-Heine-Universität Düsseldorf

Kommissarischer Direktor: Dr. med. Johannes Fischer

Anticancer agents: *in vitro* analysis of their potential and limitations in melanoma cell death

Dissertation

zur Erlangung des Grades eines Doktors der Medizin
der Medizinischen Fakultät der Heinrich-Heine-Universität Düsseldorf

vorgelegt von
Benjamin Bernhard Otto Wolfhart Porzig
2016

Als Inauguraldissertation gedruckt mit Genehmigung der Medizinischen Fakultät der Heinrich-Heine-Universität Düsseldorf

gez. Univ.-Prof. Dr. med. Joachim Windolf
Dekan
Referent: Dr. rer. nat. S. Santourlidis
Korreferent: Univ.-Prof. Dr. rer. nat. S. Wesselborg

Teile dieser Arbeit wurden veröffentlicht:

Denis Selimovic [1], Benjamin B. O. W. Porzig [1], Abdelouahid El-Khattouti [1], Helene E. Badura, Mutmid Ahmad, Foued Ghanjati, Simeon Santourlidis, Youssef Haikel, Mohamed Hassan, October 2012, Bortezomib/proteasome inhibitor triggers both apoptosis and autophagy-dependent pathways in melanoma cells.

Cellular Signalling, 2013 Jan; 25(1):308-18. doi: 10.1016/j.cellsig.2012.10.004. Epub 2012 Oct 15.

Denis Selimovic [1], Benjamin B. O. W. Porzig [1], Abdelouahid El-Khattouti [1], Helene E. Badura, Mutmid Ahmad, Foued Ghanjati, Simeon Santourlidis, Youssef Haikel, Mohamed Hassan, February 2015, Corrigendum to “Bortezomib/proteasome inhibitor triggers both apoptosis and autophagy-dependent pathways in melanoma cells”.

Cellular Signalling, 2015 Feb; doi: 10.1016/j.cellsig.2015.02.002.

[1] Equal contributor

Zusammenfassung

Das metastasierte Melanom gehört zu den am aggressivsten wachsenden und sehr chemotherapie-resistenten Tumorarten.
Die heutzutage verfügbaren therapeutischen Optionen für Patienten mit metastasiertem Melanom sind beschränkt und häufig mit starken Nebenwirkungen assoziiert.
Für anti-neoplastische Substanzen sind im Allgemeinen sowohl endoplasmatischer-Retikulum (ER)-Stress als auch mitochondriale Dysregulation potentielle therapeutische Ziele. Die anti-neoplastische Substanz Bortezomib ist ein kleines Molekül das selektiv und speziell Proteasomen inhibiert, und somit zur Induktion sowohl von pro- als auch anti-apoptotischen Proteinen wie Noxa und Mcl-1, führt. Dies erklärt sowohl die erwünschten als auch unerwünschten Effekte, die bei therapierten Patienten zu verzeichnen sind.
Daher ist es von besonderer Bedeutung, durch funktionelle Analysen von anti-neoplastischen Substanzen, und deren in Melanomzellen hervorgerufenen Effekten die etablierten heutigen Therapien zu verbessern, um besonders in Fällen von metastasierten Melanomen die therapeutische Effizienz zu erhöhen.
Das Ziel dieser Arbeit war es, die Wirkung von anti-neoplastischen Substanzen auf das Zellwachstum von Melanomzellen abzuschätzen, und die molekularen Mechanismen, durch die Bortezomib Apoptose in Melanomzellen auslöst, ausführlich zu charakterisieren.
In der vorliegenden Arbeit zeigte sich, dass die Behandlung von Melanomzellen mit Bortezomib, Carmustine, und Dacarbazine zum Zelltod führt. Die funktionelle Analyse von Bortezomib ergab, dass durch die Behandlung der Melanomzellen mit Bortezomib eine Induktion der Apoptose ausgelöst wurde. Auch eine Hochregulierung von den Proteinen: Noxa, Mcl-1 und HSP70 sowie die Spaltung von LC3 mit Bildung von Autophagosomen konnte nachgewiesen werden. Bortezomib induzierte ER-Stress, welcher anhand von intrazellulärer Ca^{2+} Freisetzung nachgewiesen werden konnte. Des Weiteren führte Bortezomib zu einer gesteigerten Phosphorylierung von IRE1α, ASK1, JNK, p38 als auch zu einer Aktivierung von den Transkriptionsfaktoren AP-1, ATF-2, Ets-1, und HSF1.
Die durch Bortezomib ausgelöste mitochondriale Dysregulation konnte sowohl mit Hilfe der Anhäufung von reaktiven Sauerstoff-Spezies (ROS), Freisetzung von AIF und Cytochrome c, die Aktivierung von caspase-9 und caspase-3 als auch durch die Spaltung von PARP nachgewiesen werden. Es stellte sich heraus, dass eine Vorbehandlung der Melanomzellen mit einem caspase-3 Inhibitor (Z-DEVD-FMK) zu einer verminderten Bortezomib-induzierten Apoptose führte, die letztendlich eine vermehrte Autophagie bewirkte. Einen gegenteiligen Effekt zeigte eine Blockierung von ASK1, so dass es zu einer verminderten Autophagosomen-Bildung, jedoch vermehrter Apoptose kam.
Eine Inhibition von JNK oder HSP70 führte ebenfalls zu einer vermehrten Apoptose, jedoch ohne Auswirkungen auf die Bildung von Autophagosomen zu zeigen. Die auf den Inhibitions-Test basierenden Ergebnisse zeigen, dass eine Behandlung von Melanomzellen mit Bortezomib beide Signalwege aktiviert, zum einen den ER-Stress assoziierten Signalweg, als auch den, durch mitochondriale Dysfunktion vermittelten Signalweg
Im Rahmen dieser Arbeit wurden zum ersten Mal die molekularen Mechanismen demonstriert, die es Bortezomib ermöglichen sowohl eine Apoptose, als auch Autophagie in Melanomzellen herbeizuführen.

Abstract

Metastatic melanoma is known as one of the biologically most aggressive and chemo resistant cancers known.
The available therapeutic approaches for patients with metastatic melanoma are of limited benefit and commonly associated with numerous adverse effects. Generally, both endoplasmic reticulum (ER) stress and mitochondrial dysregulation are potential therapeutic targets of anticancer agents including bortezomib. Bortezomib is a small molecule that can specifically and selectively inhibit proteasomes, leading to the induction of both pro- and anti-apoptotic proteins, including Noxa and Mcl-1, and thereby leads to the enhancement of desired as well as non-desired effects in treated patients. Therefore, the functional analysis of anticancer agents-induced effects in melanoma cells may help to improve their therapeutic efficiency for the treatment of metastatic melanoma.
The aim of the present study was to assess the inhibitory effect of anticancer agents on cell growth of melanoma cells and to characterize, in detail the molecular mechanisms whereby bortezomib triggers apoptosis in melanoma cells.
The treatment of melanoma with bortezomib, carmustine, dacarbazine was found to induce apoptosis in melanoma cells. However, the functional analysis of bortezomib in detail was found to induce apoptosis of melanoma cells together with the upregulation of Noxa, Mcl-1, and HSP70 proteins, and the cleavage of LC3 and autophagosome formation. Bortezomib induced ER-stress, as evidenced by the increase of intracellular Ca^{2+} release and enhanced the phosphorylation of IRE1α, ASK1, JNK and p38, as well as, the activation of the transcription factors AP-1, ATF-2, Ets-1, and HSF1. Bortezomib-induced mitochondrial dysregulation was associated with the accumulation of reactive oxygen species (ROS), the release of both apoptosis inducing factor (AIF) and Cytochrome c, the activation of caspase-9 and caspase-3, and cleavage of Poly (ADP-ribose) polymerase (PARP). Furthermore, the pretreatment of melanoma cells with the inhibitor of caspase-3 (Z-DEVD-FMK) was found to block bortezomib-induced apoptosis leading subsequently to increased autophagosome formation. In contrast, the inhibition of ASK1 abrogated bortezomib-induced autophagosome formation and increased induced apoptosis. As a beneficial side effect, the inhibition of JNK, of HSP70 increased also induced apoptosis without influencing bortezomib-induced autophagosome formation. Thus, based on inhibitory experiments, the exposure of melanoma cells to bortezomib triggers the activation of both ER-stress-associated pathways, in particular IRE1α-ASK1-p38-ATF-2/ets-1-Mcl-1, and IRE1α-ASK1-JNK-AP-1/HSF1-HSP70 as well as mitochondrial dysregulation-associated pathways, namely ROS-ASK1-JNK-AP-1/HSF1-70, and AIF-caspase-3-PARP and Cyt.c-caspase-9-caspase-3-PARP.
Altogether, we demonstrate for the first time the molecular mechanisms, whereby bortezomib triggers both apoptosis and autophagosome formation in melanoma cells.

Abbreviation

%	Percentage
°C	Degree Celsius
^{32}P	Phosphorus-isotope (mass number 32)
A	Ampere
aa	Amino acid
ABVD	Adriamycin, Bleomycin, Vinblastine, Dacarbazine
AGT	O6-alkylguanine DNA alkyltransferase
AIF	Apoptosis Inducing Factor
AP-1	Activator Protein-1
Apaf-1	Apoptotic Protease Activating Factor-1
Apo2L or TRAIL	TNF Related Apoptosis Inducing Ligand
Apo3L/DR 3	Member of the TNF receptor family
APR-1	Apoptosis Related Protein-1
APR-2	Apoptosis Related Protein-2
ASK 1	Apoptosis signal regulating kinase
ATCC	American Type Culture Collection
ATF2	Activating transcription factor 2
ATP	Adenosine triphosphate
Bad	Bcl-2 Antagonist of Cell Death
BAK	Bcl-2 Homologous Antagonist / Killer
BAX	Bcl-2 Associated X Protein
Bcl-2	B Cell Lymphoma/Leukemia-2
Bcl-XL	Bcl-X (long form)
BCNU	1,3-Bis(2-chloroethyl)-1-nitrosourea
BH3	Bcl-2 homology domain 3
BID	BH3 Interacting Domain Death Agonist
BIK	Bcl-2 Interacting Killer
BIM	Bcl-2 Interacting Mediator of Cell Death
BSA	Bovine Serum Albumin
CA	California
Ca^{2+}	Calcium
CAD	Caspase-activated DNase
c-FLIP	Cellular FLICE- inhibitory protein
cm^2	Square centimetre
CO_2	Carbon dioxide
conc.	Concentration
CTCL	Cutaneous T-Cell Lymphoma
Cyt. c	Cytochrome c
DD	Death Domain
DHR 123	Dihydrorhodamine 123
DIABLO	Direct IAP Binding Protein with Low pI
DIC	Differential Interference Contrast
DISC	Death Inducing Signaling complex
DMEM	Dulbecco`s modified Eagle Medium
DMSO	Dimethyl sulfoxide
DNA	Deoxyribonucleic acid
dNTP	Deoxy ribonucleotide triphosphate
Dox	Doxycycline
DPBS	Dulbecco's Phosphate buffered Saline
DR	Death Receptor

DTIC	(Dimethyltriazeno) Imidazol Carboxamide (Dacarbazine)
ECL	Enhanced chemiluminescence
EDTA	Ethylenediamine tetraacetic acid
ELISA	Enzyme-linked-immuno-sorbent-assay
ELK-1	ETS-like transcription factor
EMSA	Electrophoretic Mobility Shift Assay
ER	Endoplasmic reticulum
ERK	Extracellular signal regulated kinase
et al.	Et alia
ETS-1	V-ets avian erythroblastosis virus E26 oncogene homolog 1
FACS	Fluorescence activated cell sorting
FADD	Fas-associated protein with death domain
FBS	Fetal bovine serum
Fig.	Figure
FITC	Fluorescein isothuocyanate
FLICE	Fas-associated death domain-like interleukin-1-converting enzyme
FLUO 3/AM	1-[2-Amino-5-(2,7-dichloro-6-hydroxy-3-oxo-3H-xanthen-9-yl)]-2-(2′-amino-5′-methylphenoxy)ethane-N,N,N′,N′-tetraacetic Acid Pentaacetoxymethyl Ester (Calcium indicator)
g	Gram
h	Hour
H_2O	Water
HEPES	N-[2-Hydroxyethyl]piperazin-N´-[2-ethansulfonsäure]
hrs	Hours
HSP 70	70 kilodalton heat shock proteins
HtrA2 / Omi	HtrA serine peptidase 2
HUVEC	Human umbilical vein Endothelial Cell
IAP	Inhibitor of Apoptosis Protein
ICAD	Inhibitor of caspase-activated DNase
Inc.	Incorporated
IRE1	Inositol requiring protein 1
JC-1	5,5',6,6'-tetrachloro-1,1',3,3' tetraethylbenzimidazolylcarbocyanine iodide
JNK	C-Jun-N-terminal Kinase
kb	Kilo base pair
l	Litre
LC-3	Microtuble-associated protein light chain 3
MA	Massachusetts
MAP Kinase	Mitogen-activated protein kinase
MBP	Myelin Basic Protein
MCL	Mantle cell lymphoma
Mcl 1	Myeloid Cell Leukemia Sequence
MEF	Mouse embryonic fibroblast
Mg^{2+}	Magnesium
min	Minute
Mito. fraction	Mitochondrial fraction
ml	Millilitre
mM	Milli mol/l
MM	Multiple myeloma
MOMP	Mitochondrial outer membrane permeabilization

MS	Minishaker
MTT-Assay	3-(4,5-Dimethylthiazol-2-yl)-2,5-diphenyltetrazolium bromide
NF-κB	Nuclear factor kappa-light-chain-enhancer of activated B cells
ng	Nano gram
nm	Nano meter
nM	Nano molar
Noxa	Adult T cell leukemia-derived PMA-responsive
p38	p38 mitogen-activated protein kinases
PARP	Poly ADP-Ribose Polymerase
PBS	Phosphate Buffered Saline
pH	Power of hydrogen
PI	Propidium iodide
Pi	Proteasome inhibitor
pmol	Pico moles
Puma	p53 upregulated modulator of apoptosis
PVDF	Polyvinylidene diflouride
RNA	Ribonucleic acid
ROS	Reactive oxygen species
rpm	Rounds per minute
S	Sulphur
SD	Semidry
SDS	Natriumdodecylsulfat
SDS-PAGE	Sodium dodecyl sulfate polyacrylamide gel electrophoresis
sec	Second
siRNA	Small interference Ribonucleic acid
Smac	Second Mitochondria-Derived Activator of Caspase
TAE	Tris-Acetat-EDTA-Puffer
TBE	Tris Borate EDTA buffer
TBS	Tris Buffered Saline
TBST	Tris Buffered Saline and Tween 20
TCA	Trichloroacetic
T-cell	T lymphocytes
Tet	Tetracycline
TMD	Transmembrane Domain
TNF	Tumor Necrosis Factor
TNFα	Tumor Necrosis Factor α
TRADD	TNF receptor-associated protein with death domain
TRE	Tetracycline responsive element
Tris	2-Amino-2-(hydroxymethyl)-propan-1,3-diol
U	Units
USA	United States of America
UV	ultraviolet light
V	Volt
WHO	World Health Organisation
X-ray	Roentgen radiation
Z-DEVD-FMK	Benzyloxycarbonyl-Asp(OMe)-Glu(OMe) -Val-Asp(OMe)-fluoromethylketone
Δψm	Mitochondrial membrane potential
ΔΨm	Mitochondrial membrane potential
µg	Microgram
µM	Micro molar

Content

1. Introduction

1.1 Melanoma

Malignant Melanoma is one of the most aggressive types of cancer, besides being the most aggressive form of skin cancer. The incidence of malign melanoma shows a steady increase within the last two decades, especially in Western cultures (Gray-Schopfer et al., 2007). The chances for healing and complete remission are best, if the tumour is small and grows exclusively in the epidermis without vertical penetration into deeper skin and tissue layers (Eikenberry et al., 2009). Studies have shown that the basal membrane has a barrier function that prevents blood and lymphatic metastases. Once the basal membrane is penetrated by the cancer cells, the access of cancer cells to the dermis facilitates their dissemination into blood vessels and the lymphatic system, leading to rapid spread of cancer cells throughout the entire organism (Uong and Zon, 2010). It has been shown that the occurrence of lymph node metastases results from lymphatic vessel infiltration, whereas the penetration of blood vessels enables the cancer cells to disseminate to other organs. The most common sites of metastases have been shown to be lung, liver, bone and brain, which implies some kind of affinity of the melanoma cells for these organs and tissues (Nguyen et al., 2009).

The survival rate in patients with advanced diseases, based on the cases with confirmed lymph node metastases or organ metastases, is reported to be no better than a 5-year survival rate of <5% (Elder et al., 2005; Gray-Schopfer et al., 2007). This poor prognosis is attributed to the cancer's inherently high potential to form local and distant metastases, aggressive local growth and the development of resistance to most available therapies, including immuno-, radio- or chemotherapy (Whalen and Sharif, 1992; Röckmann and Schadendorf, 2003).

The current available therapy strategies for melanoma treatment include surgical removal of the tumour, which can only benefit patients with early stages of the disease. Melanoma treatment with chemotherapy and radiotherapy, particularly combinations of these different therapeutic approaches have been found to improve the overall poor prognosis of melanoma treatment, whereas unidirectional approaches show only minor or temporary successes (Spagnolo and Queirolo, 2012). The high resistance of melanoma to cytotoxic drugs result from inherent and also acquired defects in cell death

machinery. Studies show a distinct dysregulation on multiple levels of the main apoptotic pathways in combination with other mechanism, ranging from heightened activity of DNA repair systems to increased activity of drug detoxification (Grossman and Altieri, 2001; Soengas and Lowe, 2003; Roos et al., 2011; Zwielly et al., 2011). It is expected, that the above mentioned intracellular alterations on multiple levels, explain the insufficiency of the cell death machinery to compel spontaneous apoptosis *in vivo,* when compared directly to other cancer cells. This may explain the possible mechanism regulating melanoma resistance to cytotoxic drugs, as shown in numerous *in vitro* apoptosis assays (Soengas and Lowe, 2003). Melanoma cells use DNA damage repair systems and drug detoxification systems to avoid induction of apoptosis and thus render a number of highly potent cytotoxic drugs less effective (Soengas and Lowe, 2003). This enormous resistance to apoptosis renders the alternative therapeutic modalities equally less potent, although they may effect cell damage by other means. Overcoming this tremendous inherent resistance of the cancer cells is seen as a possible key to a much more effective and successful treatment of malign melanoma cases (Soengas and Lowe, 2003; Gray-Schopfer et al., 2007).

Currently, there are a number of different substances with therapeutic potential for the treatment of malignant melanoma. These include the chemotherapeutic agents such as dacarbazine, temozolomide, as well as the recently approved targeted drugs, including nivolumab, a monoclonal antibody (Jönsson et al., 1980; Devito et al., 2011; Spain and Larkin, 2016). In advanced cases of metastasized melanoma, the treatment with Interferon alpha and Interleukin-2 has shown a significant potential to modulate the immune system response to cancer cells. Interferon alpha and Interleukin-2 are also used post-surgical as an adjuvant therapy (North and Mully, 2011; Noor et al., 2012). Based on the infamous drug resistance of melanoma cells, and the failure of systemic therapy regiment to achieve complete remission in advanced metastasized cases, it is important to understand the resistance mechanism of melanoma cells, to currently available conventional therapies. Understanding these resistance mechanisms may help to develop reliable therapeutic protocols for the treatment of malign melanoma.

The new German guidelines for melanoma reflect that the participation in clinical studies is most promising for advanced melanoma cases which have already metastasized to internal organs (stage IV) (Garbe et al., 2008).

1.2 Apoptosis

Apoptosis describes an energy dependent active process that leads to a controlled cell death of a single cell or cell group and is of vital importance to the governance of cell groups and during organ development in multicellular organism (Kerr et al., 1972; Portt et al., 2011). It can regulate a cell population with near surgical precision without damaging surrounding tissue, in contrast to another form of cell death, known as necrosis (Grimm, 2003). Apoptosis can be triggered by a multitude of different factors, categorised into internal and external ones (Elmore, 2007). To the group of internal factors belong noxious substances and events that deal extensive damage to the cell's genetic information, external factors can be immune cells which can effect apoptosis by interacting with certain receptors, called "death receptors" (DR) of the tumor necrosis factor (TNF) subfamily (Elmore, 2007).

The mechanisms by which apoptosis is regulated seems to be intricate, energy dependent and tightly controlled, to ensure that no sudden and undesired apoptosis commences (El-Khattouti et al., 2013). There are two main apoptotic pathways that are categorised into an extrinsic pathway that translates an external trigger for apoptosis into an intracellular signal *via* death receptors (Locksley et al., 2001). On the other hand, there is the internal or intrinsic pathway that depends on the cell's mitochondria to function (Danial and Korsmeyer, 2004). These two pathways act not completely separated from each other, in their molecular action, and have the ability to influence each other, as described by newer studies which found extensive inter-linkage between both pathways (Igney and Krammer, 2002a).

In addition to the above mentioned two major pathways there is evidence for at least a third pathway that is mediated *via* T-cells of the host organism. The interaction of cytotoxic T lymphocytes and natural killer cells with a cell that is selected for apoptosis leads to an activation of the perforin/granzyme pathway (Martinvalet et al., 2005). Perforin enables the uptake of the proteases granzyme B or granzyme A into the cell, which in turn can induce cell death by promoting apoptosis (Bots and Medema, 2006). In contrast to the two major pathways, which induce DNA fragmentation, studies show that the granzyme A pathway uses a caspase-independent cell death pathway that effects exclusively single stranded DNA damage, whereas the dominant pathways induce double stranded DNA damage (Lieberman and Fan, 2003; Martinvalet et al., 2005).

All three pathways lead to a central pathway that is commenced by the cleavage and thus activation of caspase-3, which is seen as a sort of “key” for the downstream following apoptosis (Igney and Krammer, 2002b). The activation of caspase 3 leads to a rapid degradation of a large number of proteins that are essential for cell repair mechanisms, cell signaling or homoeostasis, thus further advancing the cell’s march towards death and phagocytosis (Porter and Jänicke, 1999). Most animal cells synthesize proenzyme caspases, which are basically inert preforms, until they are activated, depending on the caspase, by different means (Li and Yuan, 2008). When an apoptotic trigger is received it leads to a dimerization and thus activation of hydrolytic initiator caspases which in turn activate, in a snowball effect-like fashion, other inert initiator caspases as well as the effector caspases (Rastogi et al., 2009). Caspases can be categorized broadly into three groups based on their function, whereas only the first two groups are of central importance for apoptosis. The first group are the initiator caspases (caspase-2, -8, -9, -10), which are activated by dimerization and then proceed to cleave the inert executioner caspases hydrolytically, thereby activate them (Allen and Clarke, 2009; Kurokawa and Kornbluth, 2009; McIlwain et al., 2013). The second group is comprised of the executioner caspases (caspase-3, -6, -7), which in turn cleave a multitude of intracellular substances proteolytically at aspartic acid residues and thus lead to the demise of the cell (Fischer et al., 2003; Kumar, 2006). The third group consists of the inflammatory caspases (caspases--1, -4, -5), which cannot be counted as either initiator or executioner and do not seem to play a central role in apoptosis (Allen and Clarke, 2009; Kurokawa and Kornbluth, 2009).

Once the cell has begun the way towards cell death it expresses surface markers that facilitate recognition and phagocytosis by macrophages and other phagocytes without damaging the surrounding tissue, which sets apoptosis apart from necrosis (Fadok and Chimini, 2001). This feat is managed by a translocation of negative charged phosphatidylserine into the outer layer of the cell’s lipid bilayer. The exposure of the negative charges in the outer layer serves a beacon for phagocytic cells, because an otherwise intact cell would not expose negative charges in the outer layer of the lipid bilayer and thus leads to selective phagocytosis (Bratton et al., 1997). Alongside phosphatidylserine, there are other proteins and membrane lipids that are translocated to the outer layer. Annexin I is also found in the outer layer of apoptotic cells and has been shown to be a recombinant phosphatidylserine-binding protein. Annexin V has shown

to interact specifically with phosphatidylserine and is used today as a marker to detect apoptosis in assays (van Engeland et al., 1998; Arur et al., 2003).

Typical of apoptotic cells is also that cell integrity is largely unimpaired until phagocytosis has taken place, which is in part achieved by the activation of tissue transglutaminases which create Ca^{2+}-dependent protein crosslinks between proteins that act like a scaffold and appear to be the reason for the found cell integrity (Nemes et al., 1996; Nicholas et al., 2003).

Another typical trait of apoptotic cells is, that the genetic information is processed by endonucleases that lead to the typical DNA fragmentation and chromatin condensation. Both are signs of extensive damage to the genetic information and can be visualized in special assays or using an electron microscope (Sun et al., 1994; Bortner et al., 1995).

1.3 Intrinsic Pathway

The hallmarks of the intrinsic pathway are that it is receptor-independent but necessarily mitochondria-dependent. Without mitochondrial activation it cannot be activated (Cui et al., 2012). The triggers of the intrinsic pathway can influence the pathway in a positive or negative way, meaning they can lead a cell towards apoptosis or even prevent it (Chipuk et al., 2008;). In a functional cell there is a fine balance between pro-apoptotic and anti-apoptotic factors. The group of anti-apoptotic factors consists of signals that promote cell survival or cell proliferation through several cell-stimulating hormones or growth factors (Elmore, 2007). Opposed is a group of factors, the pro-apoptotic-factors that promote cell death *via* a multitude of different ways. Cell-damaging substances and influences like radiation, cell toxins, infections, hypoxia or simply the lack of anti-apoptotic factors promote cell death and thus apoptosis (Chipuk et al., 2010; Anvekar et al., 2011). All the pro-apoptotic influences have in common, that they lead to a loss of mitochondrial membrane potential, which in turn increases mitochondrial permeability (Anvekar et al., 2011; Selimovic et al., 2013). The increase in mitochondrial permeability allows pro-apoptotic proteins outside of the mitochondria where they lead to an activation of the caspase-dependent mitochondrial pathway. Some of the proteins that gain access to the cytosol have been identified as Cytochrome c, Smac/DIABLO and HtrA2/Omi (Du et al., 2000; Garrido and Kroemer, 2004; Elmore, 2007). Their pro-apoptotic function is derived from a structure known as apoptosome, which consists of Apaf-1, Cytochrome c and procaspase-9 (Hill et al., 2004; Anvekar et al., 2011). Recent

studies show that Smac/DIABLO and HtrA2/Omi inhibit inhibitors of apoptosis proteins (IAP) activity irreversibly and thus lead to increased apoptosis (van Loo et al., 2002; Yang et al., 2003; Hegde et al., 2003; Schimmer, 2004). Other pro-apoptotic proteins are permitted into the cytosol from within the mitochondria at a later point, when the process of apoptosis is already under way (Li et al., 2001). The second group of proteins consists of endonuclease G, Caspase-Activated-DNase (CAD) and Apoptosis-inducing factor (AIF). The latter proteins have in common that they lead to DNA fragmentation and nuclear condensation, signs which are also typical for apoptotic cells (Susin et al., 2000; Joza et al., 2001; Li et al., 2001). Endonuclease G and AIF do not require prior activation by a caspase whereas CAD is activated after being cleaved by caspase-3, which has been shown to be one of the key proteins in apoptosis (Enari et al., 1998; Susin et al., 2000; Cao et al., 2001).

The extensive Bcl-2 protein-family, among them members that have pro-apoptotic and others with anti-apoptotic properties, could be described as the stewards of mitochondrial permeability and thus control downstream whether the cell commits to apoptosis or not (Cory and Adams, 2002; Yip and Reed, 2008). It is known that the tumour suppressor protein p53 plays a vital role in governing the mitochondrial membrane permeability by interacting with a multitude of Bcl-2 family proteins (Schuler and Green, 2001; Ha et al., 2013). Among the Bcl-2 family there are the proteins BID and BIM, which are known to activate the proteins BAK and BAX. (Korsmeyer et al., 2000; Letai et al., 2002; Kuwana et al., 2002; 2005). Studies show that the BAK and BAX proteins are chiefly responsible for the regulation of the "mitochondrial outer membrane permeabilization" (MOMP) and can create pores in the outer mitochondrial membrane through which Cytochrome c can be released into the cytosol (Lindsten et al., 2000; Wei et al., 2001; Anvekar et al., 2011). Two further anti-apoptotic proteins are Bcl-Xl and Bcl-2 and their known function is to inhibit the release of Cytochrome c from within the mitochondria, but this anti-apoptotic function can be modulated by formation of heterodimers with Bad, also of the Bcl-2 family, which renders the anti-apoptotic function of Bcl-Xl and Bcl-2 inoperable and thus promotes apoptosis (Yang et al., 1995; Newmeyer et al., 2000; Chipuk et al., 2010). The important Bcl-2 family proteins Puma and Noxa show a p53-dependent heightened expression and are able to trigger apoptosis in certain melanoma cell lines (Elmore, 2007; Hassan et al., 2008). *In vitro* studies show that an increasing expression of Puma leads to an increase in BAX expression, which in turn influences downstream apoptosis

by regulating the release of pro-apoptotic factors by modulating the mitochondrial membrane potential (Liu et al., 2003; Gallenne et al., 2009). Interestingly the protein Noxa is located within mitochondria as well as in the cells endoplasmic reticulum and can interact with other Bcl-2 family members and lead to an increase in caspase-9 activity, which is one of the initiator caspases and as such able to activate capase-3 (Oda et al., 2000; Hassan et al., 2008).

There are a multitude of other proteins, that are known to interact with p53 and Bcl-2 family members and thus are able to influence the cell, either by pushing it further along towards apoptosis or arresting the move towards apoptosis. In all probability, we have only just begun to understand the different pathways and their interactions.

1.4 Extrinsic Pathway

The second dominant apoptosis pathway is characterised by an external stimulus that is translated *via* receptors, the so called death receptors (DR), into an intracellular signal that can promote cell death. Among these receptors are members of the tumour necrosis factor (TNF) receptor superfamily (Locksley et al., 2001; Portt et al., 2011).

A common trait of these TNF receptors is a cytoplasmic domain called “death domain” (DD) which consists of ~80 amino acids and is vital for the translation of the extracellular signal into an intracellular signal and apoptosis induction (Ashkenazi and Dixit, 1998; Guicciardi and Gores, 2009). There are several known death receptors, whereas the receptors that are closely associated with apoptosis upon activation are Fas, TNF-related apoptosis-inducing ligand receptor 1 (TRAIL-R1) and TNF-related apoptosis-inducing ligand receptor 2 (TRAIL-R2) (Guicciardi and Gores, 2009).

When a ligand, also termed “death ligand”, binds to a corresponding receptor, the cytoplasmic death domain performs a conformational change, which acts as a beacon for different receptor-specific adapter proteins exhibiting a matching death domain. In the case of a TNF-receptor the recruited protein is called TNF receptor-associated protein with death domain (TRADD), or in the case of a Fas-receptor it is called Fas-associated protein with death domain (FADD) (Guicciardi and Gores, 2009). Upon binding of the adapter protein with the activated death domain of the receptor, the adapter proteins may activate specific death effector domains, that are deemed essential for the binding and activation of initiator caspase-8 and caspase-10. The entity consisting of the activated adapter protein (FADD or TRADD) and the procaspases is

called death-inducing signalling complex (DISC) (Kim et al., 2000; Guicciardi and Gores, 2009). Upon formation of the DISC, a dimerization of the adapter protein with procaspase-8 is effected, which in turn is auto activated and can launch the execution phase which leads ultimately to apoptosis (Kischkel et al., 1995; Shirley et al., 2011). At this point it has to be noted that there are intracellular proteins that can modulate or even inhibit apoptosis triggered by a death receptor ligand. One such protein, called c-FLIP, can intervene and modulate the signal cascade at the DISC by binding to FADD, caspase-8 and caspase-10, thus leading to a deactivation of these proteins. (Kataoka et al., 1998; Scaffidi, 1999; Safa et al., 2008; Guicciardi and Gores, 2009).

1.5 Execution Phase

The execution phase is characterised by the irreversible activation of the effector or executioner caspases (caspase-3, -6, -7) and is the endpoint of both dominant apoptotic pathways (Elmore, 2007; Lutz et al., 2014). The activated effector caspases begin to proteolytically cleave a wide range of substrates, ranging from DNA repair enzymes like Poly ADP-ribose polymerase (PARP), structural proteins like gelsolin or vimentin to regulatory proteins like p21-activated kinase 2 (PAK-2) and many others (Porter and Jänicke, 1999; Slee et al., 2001; Elmore, 2007). Caspase-3 plays a central role in the proteolytic process and studies show that it can be activated by any of the initiator caspases, but has also the ability to process and thus activate pro-caspases (pro-caspases-2, -6, -7, -9) furthering its image as a vital component along the way towards apoptosis (Porter and Jänicke, 1999; Hassan et al., 2009; Lin et al., 2015). Another most important property of activated caspase-3 is that it can cleave Inhibitor of caspase-activated DNase (ICAD), thus activating the caspase-activated DNase, which in turn translocates to the nuclei to fragment the genetic material within, leading to chromatin condensation, considered as one earmark of apoptosis (Sakahira et al., 1998; Porter and Jänicke, 1999). Studies, using a cell-free system, showed that caspase-3 seems to have the broadest spectrum of substrates it can cleave and is considered the most important executioner caspase, whereas the caspase-6 and caspase-7 are thought to play a more sophisticated and regulatory role upstream and cannot substitute caspase-3 (Slee et al., 2001). Since the late 1990s it has been shown that a Fas stimulation, *in vivo*, leads to gelsolin-cleavage effected by activated caspase-3 and caspase-7 (Kothakota et al., 1997; Martin et al., 2010). Gelsolin belongs to the group of actin-binding proteins that interact

with the actin cytoskeleton in numerous ways (Sun et al., 1999). The cytoskeleton itself is responsible for numerous cellular functions ranging from cell motility and migration to signal transduction. Gelsolin upregulation has been associated with increased cell motility in different human cancer cells (Deng et al., 2015). Astonishing was, that the caspase-3-cleaved gelsolin-product severed actin filaments in a way that did not require Ca^{2+} in order to function. The cells confronted with the cleaved gelsolin product showed nuclear fragmentation and rounding up, both typical signs of apoptosis (Kothakota et al., 1997). All the above shows that an activation of caspase-3 leads to a destruction and impairment of many vital cell functions by affecting multiple structures that regulate different cell functions simultaneously and thus cannot be seen as one solitary damaging "strike" launched at one specific site (Kothakota et al., 1997; Elmore, 2007).

After the cell has been rendered beyond repair by the caspase-activity and is well on its way towards cell death, the last phase of apoptosis sets in, meaning the removal of the dying cell *via* phagocytosis (Erwig and Henson, 2008). As described before, we know of radical changes within the cell and its lipid bilayer during apoptosis (Orlando and Pittman, 2006). A normal and functional cell is characterised by an asymmetrical distribution of phospholipids within its lipid bilayer, meaning some phospholipids are situated primarily within the outer layer, like sphingomyelin, whereas aminophospholipids are mostly sequestered within the inner layer (Fadok et al., 1998). It is known, that phosphatidylserine belongs exclusively within the inner layer of a functional cell's lipid bilayer, but translocates, as described before, to the outer layer during apoptosis and serves as a beacon for phagocytes (Verhoven et al., 1995). Two proteins are deemed important for this change in the lipid bilayer. One protein is called aminophospholipid translocase, which seems to transport phosphatidylserine to the inner layer and does so in a Mg^{2+}-dependent fashion that can be impaired by a heightened Ca^{2+} concentrations (Fadok et al., 1998; Verhoven et al., 1999). The second protein is called scramblase and is believed to speed the process of phosphatidylserine externalisation in an ATP-independent way. It has to be noted that the scramblase-activity is upregulated *via* a heightened intracellular Ca^{2+} concentration, meaning that Ca^{2+} leads to an inhibition of the aminophospholipid translocase while activation the scramblase (Fadok et al., 1998; Verhoven et al., 1999; Sahu et al., 2007). Studies using erythrocytes have shown that aged or oxidatively stressed erythrocytes display an active caspase-3, which in turn is responsible for the downregulation of the afore mentioned aminophospholipid translocase and finally phosphatidylserine externalisation (Mandal

et al., 2005). These erythrocytes displayed, that a Fas-pathway activation leads to an increase in active caspase-8, activation of caspase-3, downregulation of aminophospholipid translocase, phosphatidylserine externalisation and eventually apoptosis (Mandal et al., 2005). In addition to these findings, there are also indications that phosphatidylserine externalisation can also be achieved in a caspase-independent way, as shown in experiments using primary T-lymphocytes. It is hypothesized that this effect could be triggered by the apoptosis-inducing factor (AIF), which is able to effect phosphatidylserine exposure upon direct injection into the cell's cytoplasm, even during caspase-inhibition (Ferraro-Peyret et al., 2002; Elmore, 2007).

The signal-function of phosphatidylserine exposure leads to the rapid attraction of phagocytic cells, like macrophages. These phagocytic cells seem to have specific phosphatidylserine-receptors that facilitate phagocytosis of the apoptotic cell (Fadok et al., 1998). As described before, apoptosis leads to a cell death that does not lead to an inflammatory response and thus prevents damage to surrounding tissue (Verhoven et al., 1995). It is believed that phosphatidylserine receptors are accountable for the lack of inflammatory responses by leading to an active induction of anti-inflammatory mediators which allow this "silent" cell death *via* apoptosis and phagocytosis (Penberthy and Ravichandran, 2016).

2. The aim of this study

Currently, the available therapies of advanced cases of metastasised melanoma are limited and unreliable. Therefore, the functional analysis of conventional anti-cancer agents based on their molecular action may help to improve their therapeutic efficiency in patients with advanced diseases.
This work does focus on the following subjects:

1. The assessment of the killing efficiency of anti-cancer agents (e.g. bortezomib, dacarbazine and carmustine) in melanoma cell lines, using MTT assay and Comet Assay.

1. Functional analysis of anti-cancer agent induced apoptosis using embryonic fibroblast knockout cell lines.

2. Determination of molecular mechanisms whereby anti-cancer agent bortezomib triggers both apoptosis and autophagosome formation in melanoma cell lines.

3. Materials and Methods

3.1 Materials

Cell lines

Melanoma cell lines BLM, A375 were obtained from ATCC, American type culture collection. The cells were maintained in Dulbecco's Modified Eagle Medium (DMEM-F12) supplemented with 10% heat-inactivated Fetal Bovine Serum (FBS), 2 mM glutamine and 1% antibiotic solution (100 U/ml penicillin and 100 µg/ml streptomycin) at 37°C in a humidified atmosphere of 5% CO2.

Media for cell culture

DMEM/F12 (1:1)-medium: Serva (Heidelberg, Germany)

Dulbecco's Phosphate buffered Saline (DPBS): Sigma (Deisenhofen, Germany)

Doxycycline: Clontech (Palo Alto, USA)

Dulbecco's Modified Egale Medium (DMEM): Gibco BRL (Eggenstein, Germany)

Fetal Bovine Serum (FBS): Gibco BRL (Eggenstein, Germany)

Genticin: Gibco BRL (Eggenstein, Germany)

Penicillin Streptomycin Tetracycline: Clontech (Palo Alto, USA)

Trypsin/EDTA solution: Seromed/Biochem (Berlin, Germany)

Chemicals, enzymes, and antibodies

All antibodies, chemicals and enzymes were obtained by the following companies: Serva (Heidelberg, Germany), Biometra (Göttingen, Germany), Promega (Mannheim, Germany), Peqlab (Erlangen, Germany), Amersham Buchler (Braunschweig, Germany), Perkin Elmer (New Jersey, USA), Roche, Molecular Biochemicals (Mannheim, Germany), Upstate Biotechnology (Eching, Germany), GeneCraft (Münster, Germany), Sigma-Aldrich (Deisenhofen, Germany), Biolabs (Schwalbach, Germany), Qiagen (Hilden, Germany), Chemicon (Hofheim, Germany), Santa Cruz (Santa Cruz, USA), Calbiochem (Bad Soden, Germany), Gibco BRL (Eggenstein, Germany), Boehringer-Ingelheim (Heidelberg, Germany), Merck (Darmstadt, Germany), Bio-Rad (München, Germany), Pharmacia Biotech (Uppsala, Sweden), Invitrogen (NV Leek, Netherlands) and Clontech (Palo Alto, California, USA). If not declared in detail, we received the material in best quality and highest grade of purity.

Chemicals:

The chemicals are listed in alphabetic order

[γ-^{32}P] ATP (Hartmann Analytika, Munich, Germany)

Adenosine Triphosphate (ATP): Sigma (St.Louis, USA)

Agar: Difco Laboratories (Detroit, USA)

Ampicillin: Gibco BRL (Eggenstein, Germany)

AMV Reverse Transcriptase: Boehringer Mannheim (Mannheim, Germany)

Cell proliferation Kit (MTT): Boehringer Mannheim (Mannheim, Germany)

Didesoxynucleotide (dNTP): Sigma (St.Louis, USA)

Enzymes for RT-PCR: (Genecraft, Germany)

Glutathione-Sepharose: Pharmacia (Freiburg, Germany)

MBP (Biomol, Germany)

NaCL: Difco Laboratories (Detroit, USA)

OxiSelect™ Comet Agarose (Cell Biolabs Inc, San Diego, USA)

OxiSelect™ Comet Slide (Cell Biolabs Inc, San Diego, CA, USA)

Poly T-oligonucleotide: Birsner/Grob (Denzlingen, Germany) Boehringer, Mannheim

Protease-inhibitor (Tablette): Boehringer Mannheim (Mannheim, Germany)

Protein A agarose conjugate (Santa Cruz, USA)

Proteinase K: Sigma (St.Louis, USA)

Restriction enzymes: Genecraft (Münster; Germany)

RNAse A: Boehringer Mannheim (Mannheim, Germany)

RNAse-inhibitor: Boehringer Mannheim (Mannheim, Germany

Salmon sperm -DNA: Stratagene (Heidelberg, Germany

T4 polynucleotide kinase (Genecraft, Munster, Germany)

T4-Ligase: Boehringer Mannheim (Mannheim, Germany)

Trypton: Difco Laboratories (Detroit, USA)

3.2 Antibodies

A. Primary antibodies

Immunoblot analysis was performed according to standard procedures using the following antibodies and dilutions:

Santa Cruz Biotechnology Inc., Santa Cruz, CA, USA:

Anti-ASK1 (SC-7931), 1:1000

Anti-ERK (SC-271270, 1:1000

Anti-HSP 70 (SC-66048) 1:2000

Anti-IRE1a (SC-100772), 1:1000

Anti-JNK (SC-474), 1:1000

Anti-LC 3ß (SC-376404), 1:1000

Anti-Mcl-1 (SC-20679) 1:500

Anti-Noxa (SC-2697) 1:1000

Anti-p38 (SC-535), 1:1000

Anti-p-ASK1 (SC-01633), 1:1000

Anti-p-JNK (SC-6254), 1:1000

Anti-p-p38 (SC- 7973), 1:500

Anti-β-actin (SC-1615) 1:5000

Cell Signaling Technology, Inc., Danvers, MA, USA:

Anti-AIF (#4642), 1:1000

Anti-caspase 3 (#7190), 1: 1000

Anti-caspase 9 (#9501), 1: 1000

Anti-PARP (#9542), 1: 1000

Abcam, Cambridge, MA, USA:

Anti-Cytochrome c (ab1357-100) 1:1000

B. Secondary antibodies
Santa Cruz Biotechnology Inc., Santa Cruz, CA, USA:

Alkaline phosphatase anti-mouse: Santa Cruz (Santa Cruz, USA)

Alkaline phosphatase anti-rabbit: Santa Cruz (Santa Cruz, USA)

Alkaline phosphatase anti-goat: Santa Cruz (Santa Cruz, USA)

C. Gel shift oligonucleotides:

Santa Cruz Biotechnology Inc., Santa Cruz, CA, USA:

AP-1 binding site

ATF-2 binding site

ELK-1 binding site

Ets-1 binding site

HSF-1 binding site

D. Protease inhibitors:

Prepare as 25x stock solution; store at -20°C; and add fresh to the lysis buffer.

ASK1 inhibitor (thioredoxin) (MERCK, Darmstadt, Germany)

Caspase-3 inhibitor (zVAD-fmk) (R&D systems, Minneapolis, USA)

JNK inhibitor SP600125 (Biomol, Loerach, Germany)

p38 inhibitor (SB-203580) (Biomol, Loerach, Germany)

E. siRNA:

Santa Cruz Biotechnology Inc., Santa Cruz, CA, USA:

Ets-1 siRNA

HSP 70 siRNA

Mcl-1 siRNA

F. Dyes and indicator substances:

Santa Cruz Biotechnology Inc., Santa Cruz, CA, USA:

JC 1

Invitrogen, Karlsruhe, Germany:

Annexin V

FLUO 3/AM

Propidium iodide

Sigma-Aldrich Corporation, Germany:

Dihydrorhodamine 123

Cell Biolabs Inc, San Diego, USA:

Vista Green DNA Dye

MP Biomedicals, Eschwege, Germany:

DEVD-AMC for caspase-3

LEHD-AMC for caspase-9

Kits for molecular biology:

Bio-Rad protein Assay kit (Bio-Rad, Germany)

Qiagen plasmid isolation kits (Qiagen, Germany)

X-ray films

Hyperfilm ECL: Amersham Biosciences (Buckinghamshire, UK)

3.3 Buffers and solutions

Buffers and solutions for DNA electrophoresis:

0.5x TBE buffer (Tris-borate-EDTA)

0.045 M Tris-borate

0.001 M EDTA

1x TAE buffer (Tris-acetate-EDTA)

0.04 M Tris-acetat

0.001 M EDTA

6x loading buffer

0.25% Bromophenol blue

0.25% Xylenecyanol FF

30% Glycerol in water, mix well and store at 4°C.

Buffers for the preparation of nuclear - and whole cell extracts

RIPA buffer

50 mM Tris (pH 8.0)

150 mM NaCl

1.0% NP-40

0.5% DOC

0.1% SDS

Modified RIPA buffer

50 mM Tris (pH 7.4)

150 mM NaCl

1 mM EDTA

1 mM $Na3VO_4$

1 mM NaF

1.0% NP-40

0.25% DOC

NP-40 Lysis buffer

50 mM Tris (pH 8.0)

150 mM NaCl

1.0% NP-40

High salt lysis buffer

50 mM Tris (pH 8.0)

500 mM NaCl

1.0% NP-40

Low salt lysis buffer

50 mM Tris (pH 8.0)

1.0% NP-40

Buffer A

20 mM HEPES; pH 7.9.

10 mM NaCl

0.2 mM EDTA

2 mM DTT

Store at 4°C until use. Before use add the protease inhibitor to buffer A (1 volume protease stock solution: 24 volumes buffer A).

Buffer C

20 mM HEPES; pH 7.9

0.75 mM spermidin

0.15 mM spermin

420 mM NaCl

0.2 mM EDTA

2 mM DTT

25% Glycero

Store at 4°C until use. Before use add the protease inhibitor to buffer C (1 volume protease stock solution: 24 volumes buffer C).

Buffers and solutions for protein electrophoresis and Western blot

30% acrylamide stock solution

30g acrylamide: bisacrylamide (19:1)

Adjust the volume to 100 ml with deionized H_2O. Store at 4°C.

4x Resolving buffer

181.7 g Tris base

40 ml 10% SDS

Adjust the pH to 8.8 and add deionized H_2O to final volume of 1l.

Store at room temperature.

4x Stacking buffer

60.6 g Tris-base

40 ml 10% SDS

Adjust the pH to 6.8 and add deionized H_2O to final volume of 1l.

Store at room temperature.

5x running buffer stock

15g Tris-base

72g glycine

Adjust the volume to 1l with deionized H_2O. Store at room temperature.

1x running buffer

200 ml 5x running buffer stock

0.1% SDS

Adjust the volume to 1l with deionized H_2O.

Staining solution

25% Isopropanol

10% Glacial acetic acid

0.25% Coomassie brilliant (R250)

Adjust the volume to 800ml with H_2O

Destaining solution:

7% glacial acetic acid

2x loading buffer

15 g Tris-base

72 g Glycine

0.25 mg Bromophenol blue

2.0 ml Glycerol

0.5 ml ß-mercaptoethanol

2.0 ml 10% SDS

2.5 ml 4x stacking gel buffer

Adjust the volume to 10 ml with deionized H_2O. Store at room temperature.

Transfer buffer

14.41 g Glycine

3.025 g Tris-base

200 ml Methanol

Adjust the pH to 8.3 and made up to 1l.

10x TBS buffer

100 mM Tris-base

1.5 M NaCl

Adjust the volume to 1l with H_2O and the pH to 8.3.

Blot solution A

5% BSA

100 ml 10x TBS

Adjust the volume to 1l with deionized H_2O.

Blot solution B

5% BSA

100 ml 10x TBS

0.10% Triton X-100

0.05% Tween 20

Adjust the volume to 1l with deionized H_2O.

Washing solution

0.10% Triton X-100

0.05% Tween 20

100 ml 10x TBS

Adjust the volume to 1l with deionized H_2O.

3.4 Equipment and applications

Centrifuges:

Biofuge 28 RS (Heraeus, Sepatech, Germany)

Centrifuge 5414 R (Eppendorf, Hamburg, Germany)

Centrifuge 5415 D (Eppendorf, Hamburg, Germany)

EBA 20 (Hettig, Germany)

DNA gel electrophoresis apparatus:

Electrophoresis chamber (Cell Biolabs, Inc, Heidelberg)

Wide mini and mini cells for DNA agarose electrophoresis and power supplies (Bio-Rad)

Other equipment:

CCD camera (Nikon, Japan)

Comet image analyzing system (Kinetic Imaging, UK)

FACSCalibur (Becton Dickinson Biosciences, Heidelberg, Germany)
JEOL 1200 EX transmission electron microscope (JEOL Ltd., Japan)
Lambda Fluro 320 Plus fluorometer (Biotek)
Leica Confocal microscopy (Leica, Wetzlar, Germany)
MS1 Minishaker (Ika)
Polymax 1040 shaker (Heidolph)
Spectrophotometer ultraspec 3000 (Pharmacia Biotech)
Thermomixer 5437 (Eppendorf)
Trans-Blot SD Semi-Dry Tranfer cell
UV-chamber (Bio-Rad)
UV-Transilluminators: Wavelength 302 nm and UVT-20M (Herolab)

3.5 Methods

Assessment of cell survival using MTT assay

To assess the percentage of surviving cells, a 3-(4,5-dimethylthiazol-2-yl)-2,5-diphenyltetrazolium bromide (MTT) assay was utilized as described (Hassan et al., 2004; 2005a; 2005b; 2008) was utilized. The cells were plated at recommended density in 96 well microtiter plates and incubated for 24 h in a moist atmosphere at 37°C and 5% CO2. After 24 h of incubation, the medium was removed from some of the wells in order to be replaced by cytotoxic substances (e.g. bortezomib, dacarbazine). The plate was incubated for another 24 h – 72 h, until visible effects could be detected using light-microscope (400x magnification) (Zeiss, Germany). 120 min before the end of incubation, 20 µl of MTT solution (5mg/ml) was added to each of the 96 cell containing wells. After further 180 min in a CO_2 incubator at 37°C, the medium was removed and 100 µl of DMSO was added to each well. To dissolve the crystals, the plate was shaken slowly at RT for additional 15 min. The plate was transferred to an ELISA reader to measure the absorbance at 550 nm.

Assessment of cytotoxic-substance-induced cell death following pretreatment with kinase inhibitors using MTT assay

To assess the percentage of surviving cells, a 3-(4,5-dimethylthiazol-2-yl)-2,5-diphenyltetrazolium bromide (MTT) assay was utilized as described (Hassan et al., 2004; 2005a; 2005b; 2008) was utilized. The cells were plated at recommended density

in 96 well microtiter plates and incubated for 24 h in a moist atmosphere at 37°C and 5% CO2. After 24 h of incubation, the medium was removed from some of the wells in order to be treated with kinase inhibitors (e.g. z-VAD-fmk). Plates were left to incubate for another 30 min before removal of medium and kinase inhibitors from some of the wells in order to be replaced by cytotoxic substances (e.g. bortezomib, dacarbazine). The plates were incubated for another 24 h – 72 h, until visible effects could be detected using light-microscope (400x magnification) (Zeiss, Germany). 120 min before the end of incubation, 20 µl of MTT solution (5mg/ml) was added to each of the 96 cell containing wells. After further 180 min in a CO_2 incubator at 37°C, the medium was removed and 100 µl of DMSO was added to each well. To dissolve the crystals, the plate was shaken slowly at RT for additional 15 min. The plates were transferred to an ELISA reader to measure the absorbance at 550 nm.

Preparation of cell lysates

After one washing with ice-cold PBS, A375, BLM cells were lysed in petri dishes on ice *via* 500 µL of RL lysis buffer and scraped off the petri dishes with a plastic scraper. The cells were centrifuged at 12.000 rpm for 3 min. The resulting cell debris-pellet was extracted *via* pipette. Lysates were stored frozen at –20°C until analysis by SDS-PAGE and Western blotting.

Western blot analysis

Prefabricated 10 to 15% polyacrylamide gels were prepared according to the manufacturers' instructions. A Full Range Rainbow molecular weight marker (Amersham Biosciences) was loaded onto the gels for accurate molecular weight determination. Samples were mixed with 5 x SDS sample buffer and heated for 5 min at 95°C. After short centrifugation, the samples were loaded onto SDS-PAGE gels, which were run at 100 V in a Mini-Protean II electrophoresis cell (Bio-Rad).
Transfer of protein from SDS-PAGE (Biorad, Munich, Germany) was accomplished in a Biometra unit by using a single transfer buffer for 7 h at 5V (0.8 A per cm^2 of gel). Protan (PVDF, 0.45µm, Amersham, Braunschweig, Germany) transfer membranes were pre-incubated with methanol. The Western blots were blocked in Blot solution A overnight at 4°C with constant agitation. The blots were washed three times for 15 min at RT in western blot washing buffer. The washed blots were incubated with the primary antibody diluted in blot solution B (monoclonal antibody 1:5000 and polyclonal

antibody 1:1000) with constant agitation overnight at 4°C. The blots were washed three times at RT in TBST, 15 min each. The western blots were allowed to incubate for 60 min at RT with the secondary antibody diluted in blot solution B (1:2000). Again the western blots were washed three times, 15 min each, in Washing Buffer A. The specific signal was detected using ECL western blotting detection reagents (Amersham Pharmacia biotech, Braunschweig, Germany).
Bound antibody was removed from Western blots by washing repeatedly with Washing Buffer A overnight under constant agitation. After washing the Western blots three times for 10 min with TBS-T, Western blots were ready for another immunodetection of protein.

Evaluation of cellular DNA damage *via* Comet Assay

To assess bortezomib and dacarbazine-induced apoptosis of melanoma cell, the cells were treated with bortezomib (10nM) or dacarbazine (100µg/ml) for the indicated time period. At the end of incubation with bortezomib or dacarbazine the melanoma cells A375 and BLM were scraped off from petri dishes with a plastic scraper and washed repeatedly with ice-cold PBS. Cells were centrifuged at 1000 rpm for 2 min, the supernatant discarded and the cells were resuspended in ice-cold PBS. Buffer, Alkaline Solution, Electrophoresis Running Solution and Vista Green DNA dye were prepared and thoroughly chilled at 4°C. OxiSelect™ Comet Agarose (Cell Biolabs Inc, San Diego, USA) bottle was heated in a water bath until adequate agarose liquification. Cell samples were combined with Comet Agarose at 1:10 ratio, mixed and immediately loaded onto OxiSelect™ Comet Slide (75 µL/well).
Slides were prepared for the assay after washing in pre-chilled Lysis Buffer, Alkaline Solution and finally in TBE Electrophoresis Solution in the dark. Slides were transferred to the electrophoresis chamber (Cell Biolabs, Inc, Heidelberg) and voltage was applied for 60 min at 1 volt/cm (35 volts). After electrophoresis the slides were washed with pre chilled DI H20 and 70 % Ethanol, before ice-chilled Vista Green DNA Dye was applied to the slides (100µL/well), followed by a 30 min incubation period. Finally, the slides were viewed and evaluated using an epifluorescence microscope using a FITC filter. Lysis Buffer, Alkaline Solution, Electrophoresis Running Solution and Vista Green DNA dye were prepared and thoroughly chilled at 4°C. OxiSelect™ Comet agarose (Cell Biolabs Inc, San Diego, USA) bottle was heated in a water bath at 95°C for 20 min, until agarose liquification. The agarose bottle was then heated in a

water bath at 37°C for at least 20 min. After washings with ice-cold PBS, A375 and BLM cells were scraped off from petri dishes with a plastic scraper. Cells were washed again with ice-cold PBS, centrifuged at 1000 rpm for 2 min and the supernatant discarded. Finally, the cells were resuspended at 1x 10^5 cells/mL in ice-cold PBS. Cell samples were combined with Comet Agarose at 1:10 ratio, mixed, and immediately loaded onto OxiSelect™ Comet Slide (Cell Biolabs Inc, San Diego, USA) (75 µL/well). Slides were kept horizontally in the dark at 4°C for 15 min. The slides were treated with pre-chilled Lysis Buffer in the dark at 4°C for 60 min. The Lysis Buffer was replaced by pre-chilled Alkaline Solution and again stored in the dark at 4°C for 30 min. Alkaline Solution was aspirated and replaced with pre-chilled TBE Electrophoresis Solution. Slides were transferred horizontally to the electrophoresis chamber and voltage was applied for 60 min at 1 volt/cm (35 volts). After electrophoresis the slides were immersed three times in pre-chilled DI H2O, two minutes each time. Water was replaced with cold 70% Ethanol for 5 min, and then the slides were allowed to air dry. Pre-prepared ice-chilled Vista Green DNA Dye was applied to the slides (100µL/well), followed by a 30 min incubation period. Finally, the slides were evaluated by using an epifluorescence microscope using a FITC filter. The taking of the microscopic pictures as well as cell-counting was performed by Dr. Abdelouahid El-Khattouti (Institute of Haemostasis and Transfusion Medicine, UKD, Düsseldorf, Germany).

Preparation of nuclear extracts

Nuclear extracts were prepared from treated and untreated cells as described (Hassan et al., 2004; 2005a; 2007; 2008). Unless indicated otherwise, all procedures were performed at 4°C. Cells were briefly washed with ice-cold PBS and harvested by adding 500 µl of buffer A (20 mM HEPES, pH 7.9; 10 mM NaCl, 0.2 mM EDTA; and 2 mM DTT) containing protease inhibitor and incubated on ice for 10 min. Cells were scraped off the petri dishes and transferred to centrifuge tubes (Eppendorf, Hamburg, Germany). The supernatant was discarded after centrifugation at 1.000 rpm for 5 min. The pellet was resuspended in 50 µl of buffer C (20 mM HEPES, pH 7.9, 0,75 mM Spermidin, 0,15 mM spermin, 420 mM NaCl, 0,2 EDTA; 2 mM DTT, 25% glycerol, and 1 mM proteinase inhibitor) and incubated for 30 min at 4°C and then centrifuged at 1.000 rpm for 5 min. The supernatant was collected without disturbing the pellet, transferred into a microfuge tube and stored at -80°C until use.

Electrophoretic mobility shift assay (EMSA)

The gel shift or electrophoretic mobility shift assay (EMSA) provides a simple and a rapid method for detecting DNA-binding proteins (Hassan et al., 2009; Selimovic et al., 2011; 2012). The assay is based on the observation that free DNA fragments or double-stranded oligonucleotides migrate faster through a native polyacrylamide gel than complexes of protein and DNA. The double stranded, transcription factor binding site carrying synthetic oligonucleotides were end-labeled with [γ-^{32}P] ATP (Hartmann Analytika, Munich, Germany) in the presence of T4 polynucleotide kinase (Genecraft, Munster, Germany). For binding, 4 µg nuclear extract was allowed to bind to a labeled probe in a total volume of 30 µl for 30 min. in binding buffer (10 mM Tris, pH 7.5; 50 mM NaCl, 1mM EDTA; 1 mM MgCl2; 0.5 mM DTT and 4 % glycerol) at room temperature. The competition assay was performed in the same manner, with the exception of unlabeled probes containing the sequence of the binding site of interest were allowed to incubate with nuclear extracts for 20 min. at room temperature before being added to the labeled probes. Electrophoresis was performed for 3 h at 100 V in 0.5 X Tris-borate-EDTA running buffer at room temperature. The dried gel was visualized *via* exposure to high performance autoradiography film. As a safety precaution handling of radioactive substances, the transfer of the radioactive probes to the gel and the visualization of the dried gel was performed only by the lab supervisor Dr. Mohamed Hassan (Heinrich Heine University of Düsseldorf, Düsseldorf, Germany).

Staining of intracellular calcium

The intracellular Ca^{2+} staining was performed as described (Hassan et al., 2008, Selimovic et al., 2011).

A375 and BLM cells were treated with bortezomib (10 nM) for 24h, the medium was replaced completely by medium without phenol red and incubated for further 2h before adding the calcium sensitive dye Flou3-AM (1,5 µM) (Invitrogen). The cells were stored for 30 minutes at room temperature and life pictures were taken under standard cell culture conditions by a LeicaTCS SP2 AOBS with a 40 X oil immersion magnification using Leica Confocal microscopy (Leica, Wetzlar, Germany). The taking of the microscopic pictures was performed by Dr. Abdelouahid El-Khattouti (Institute of Haemostasis and Transfusion Medicine, UKD, Düsseldorf, Germany).

Detection of ROS

The measurement of ROS accumulation was performed as described (Hassan et al., 2008). The melanoma cells were pretreated with bortezomib (10 nM) prior to incubation with 0,5 µM DHR 123 (dihydrorhodamine 123) (Sigma) for 30 min at 37 °C. After the incubation period, the cells were collected from culture tissues using trypsin. The collected cells were washed three times with PBS and resuspended in 500 µl PBS before the measurement of reactive oxygen species using fluorescence-activated cell sorting (FACS). Handling of the FACSCalibur- apparatus was performed by members of the Institute of Dermatology, UKD Düsseldorf, Germany.

Measurement of mitochondrial membrane potential (ΔΨm) using JC-1

The loss of mitochondrial membrane potential (Δψm) was assessed by flow cytometric analysis using JC-1 staining as described (Hassan et al., 2009; Cetindere et al., 2010). The melanoma cells A375 and BLM were either treated with bortezomib or left untreated. After 24h, the cells were collected from culture tissue using trypsin and washed twice in ice-cold PBS (PBS; Biotrend, Cologne, Germany) and resuspended in PBS. The cells were stained with 10 µM JC-1 for 30 min in the dark at room temperature. The intensities of green fluorescence at 520–530 nm and of red fluorescence at 550 nm were analysed on a FACSCalibur (Becton Dickinson Biosciences, Heidelberg, Germany) for 50.000 individual cells. Handling of the FACSCalibur- apparatus was performed by members of the Institute of Dermatology, UKD Düsseldorf, Germany.

Flow cytometric analysis of apoptosis by annexin V/PI staining

The detection of apoptosis was performed as described (Hassan et al., 2008; Cetindere et al., 2010). Briefly, before the exposure of bortezomib (10 nM) for 24h the cell lines A375 and BLM were allowed to grow for 24h under the recommended conditions. The cells were stained with 5 µl of annexin V (Vybrant; Invitrogen, Karlsruhe, Germany) and 1µl propidium iodide (100 µg/ml) for 15 min at room temperature as recommended by the manufacturer's protocol. Cells being annexin V-FITC positive and PI negative were considered as apoptotic. The percentage of apoptotic cells being annexin V positive/PI negative was quantified using a FACSCalibur (Becton Dickinson Biosciences, Heidelberg, Germany). Handling of the FACSCalibur- apparatus was performed by members of the Institute of Dermatology, UKD Düsseldorf, Germany.

Transmission electron microscopy

Treated and non-treated melanoma (A375 and BLM) cells were fixed in 2.5% glutaraldehyde in 0.1M sodium cacodylate buffer (pH 7.4) for 1 h at room temperature and then washed 3 times in cacodylate buffer. Cells were postfixed in 1% osmium tetroxide in 0.1M cacodylate buffer for 1 h at room temperature. Thereafter 70 nm sections were cut on a 'Reichert Ultracut S' ultramicrotome. The sections were subsequently post-stained with 4% uranyl acetate for 10 min and Reynald's lead citrate for 1.5 min. Sections were imaged at 80 kV, with a resulting maginification factor of 8000, on a JEOL 1200 EX transmission electron microscope (JEOL Ltd., Japan). The microscopy and subsequent picture generation was performed by Dr. K. Zanger (Institute of Anatomy and brain research, head of the electron microscopy, UKD, Düsseldorf, Germany).

RNA interference

Melanoma cell lines A375 and BLM were grown in 6-well plates and transfected with an Ets-1-specific small interfering RNA oligonucleotide; Mcl-1 siRNA (5'-CGCCGAAUUCAUUAAUUUATT-3'; Qiagen); Ets-1 siRNA (# sc-29309; 150 pmol; Santa Cruz) or scrambled oligonucleotides (si-scrambled; Cat no:sc-37007; 150 pmol; Santa Cruz); HSP70 siRNA (5' -UGC ACC UUG GGC UUG UCU CCG UCG U-3') and Control siRNA (5'-UGC GUC GUC GAU CGCUUA CUC UCG U-3') using Lipofectamine TM 2000 (Invitrogen, USA) for 72h according to the manufacturer's instructions. The cells were subjected to either MTT assay or harvested to prepare nuclear protein extractions for EMSA or total protein lysates for Western blot analysis.

Assessment of caspase activity

Briefly, lysates -from both control and bortezomib treated melanoma cells were supplemented with 50 mM of the fluorogenic substrates DEVD-AMC for caspase-3 and LEHD-AMC for caspase-9 (MP Biomedicals, Eschwege, Germany), respectively. The release of aminomethylcoumarin was measured fluorometrically over 5 h at 37 °C using a Lambda Fluro 320 Plus fluorometer (Biotek, Bad Friedrichsall, Germany; excitation: 360 nm, emission: 475 nm). The catalytic activities are expressed as fluorogenic units (FU/min). The caspase inhibitor zVAD-fmk was purchased from MP Biomedicals and used at a concentration of 50 mM. The results were statistically evaluated in

cooperation with Mrs. Geraldine König (Institut National de la Santé et de la Recherché Médicale, U977, University of Strasbourg, Strasbourg, France).

4. Results

In this study, various anticancer agents including bortezomib, dacarbazine and carmustine were examined *in vitro* for their reliability in the treatment of melanoma cells. Bortezomib belongs to a novel kind of anticancer agents, the proteasome inhibitors which mediate effects *via* an inhibition of the proteasome pathway. Based on its successful clinical application in the treatment of different tumor types including multiple myeloma and mantle cell lymphoma it was interesting to determine the molecular mechanisms whereby bortezomib triggers melanoma cell death. Therefore, understanding of the underlying molecular pathways could help to enhance existing therapeutic protocols for the treatment of metastatic melanoma with bortezomib.

4.1 Effect of anticancer agents on the viability of melanoma cell lines

The effect of bortezomib on the cell viability of both melanoma cell lines A375 and BLM was assessed using cell viability assay. To assess the killing efficiency of the anticancer agents bortezomib, dacarbazine and carmustine on the cell viability of melanoma cells, the cells were allowed to grow under normal condition for 24h to become physiologically active and to reach recommended cell density before the exposure to bortezomib (10 nM), carmustine (25 μM), and dacarbazine (100 μg/ml). Based on data obtained from pilot studies (concentration and time dependent) the melanoma cell lines were allowed to grow for 24h in the presence and absence of tested anticancer agent until cell morphology changes could be detected using a light-microscope and cell viability was determined using MTT assay. Data obtained from MTT assay (Fig. 1) demonstrated the reduction of cell viability in both melanoma cell lines in response to the treatment with bortezomib (Fig. 1A), carmustine (Fig. 1B) and dacarbazine (Fig. 1C). The reduction of the cell viability noted in A375 treated with bortezomib, carmustine, or dacarbazine was 60, 22 and 19%, respectively. Also, the exposure of BLM treated to bortezomib (Fig. 1A), carmustine (Fig. 1B) and dacarbazine (Fig. 1C), reduced the cell viability in response to the treatment with bortezomib, carmustine, and dacarbazine to 55, 20, 76%, respectively. Taken together, these data confirm the killing efficiency of bortezomib, dacarbazine and carmustine in melanoma cells.

Fig. 1A

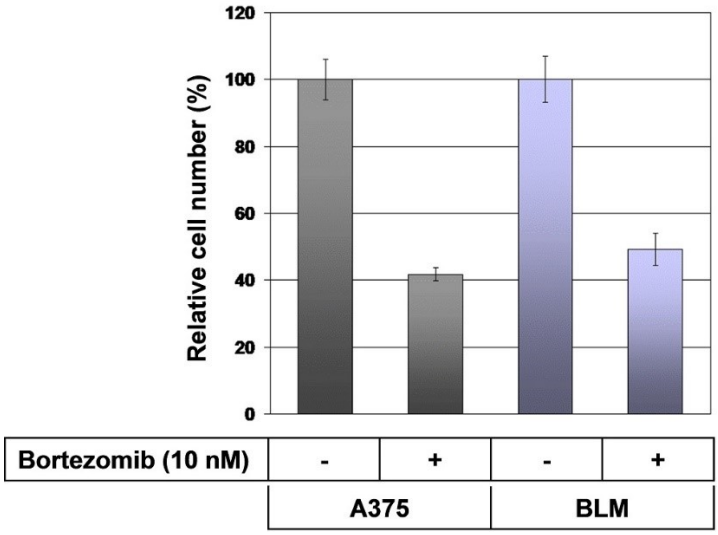

Fig. 1A. MTT assay demonstrates the reduction of cell viability in melanoma cell lines in response to the exposure to bortezomib. Data are mean ± S.D of three experiments performed in 6 replicates.

Fig. 1B

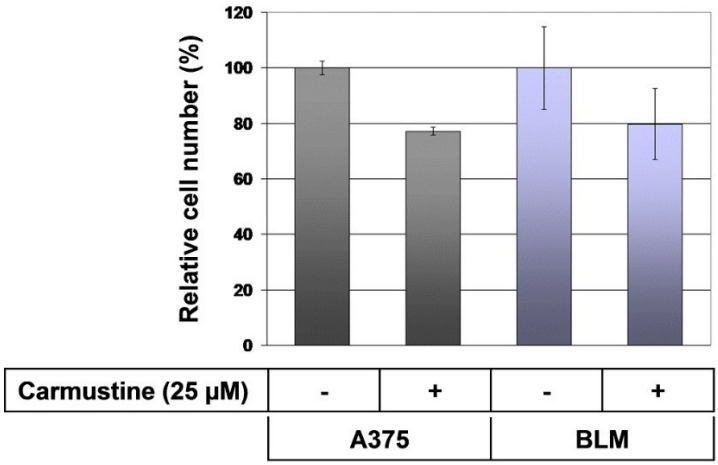

Fig. 1B. MTT assay demonstrates the reduction of cell viability in melanoma cell lines in response to the exposure to carmustine. Data are mean ± S.D of three experiments performed in 6 replicates.

Fig. 1C

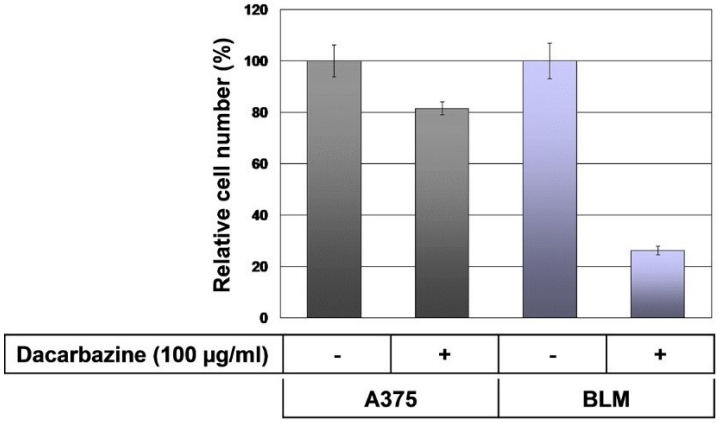

Fig. 1C. MTT assay demonstrates the reduction of cell viability in melanoma cell lines in response to the exposure to dacarbazine. Data are mean ± S.D of three experiments performed in 6 replicates.

4.2 Screening of anticancer agents-induced effects in double knockout mouse embryonic fibroblasts

To identify the signal pathways, which are involved in the regulation of anticancer agents-induced cell growth inhibition, the wild type and double knock out mouse embryonic fibroblasts (MEFs) including, MEF $p53^{-/-}$, $ASK1^{-/-}$, $IRE1^{-/-}$ were treated with bortezomib, dacarbazine and carmustine. Twenty-four hours later, the cell viability was assessed using MTT assay. Data obtained from MTT assay (Fig. 2A) demonstrated the knockout of p53 protect, in part bortezomib-induced cell death in MEF cells, when compared to wild type MEF cells, suggesting a partial role for p53 in the modulation of bortezomib-induced death of MEF cells.

Fig. 2A

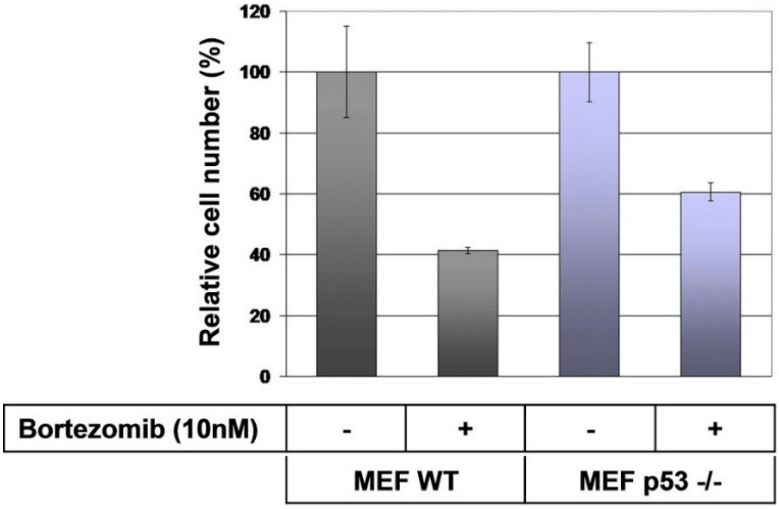

Fig. 2A. MTT assay demonstrates the reduction of cell viability in mouse embryonic fibroblasts wild type (MEF WT) and double knockout p53 (MEF p53-/-) cell lines in response to the exposure to bortezomib. Data are mean ± S.D of three experiments performed in 6 replicates.

On the other hand, MTT assays using ASK1 double knock out mouse embryonic fibroblasts and IRE1 double knock out mouse embryonic fibroblasts demonstrated the inhibition of bortezomib-induced cell death of MEF cells by the knockout of either ASK1 or IRE, suggesting a partial role for both ASK1 and IRE in the modulation of bortezomib-induced cell death of MEF cells (Fig. 2B and 2C).

Fig. 2B

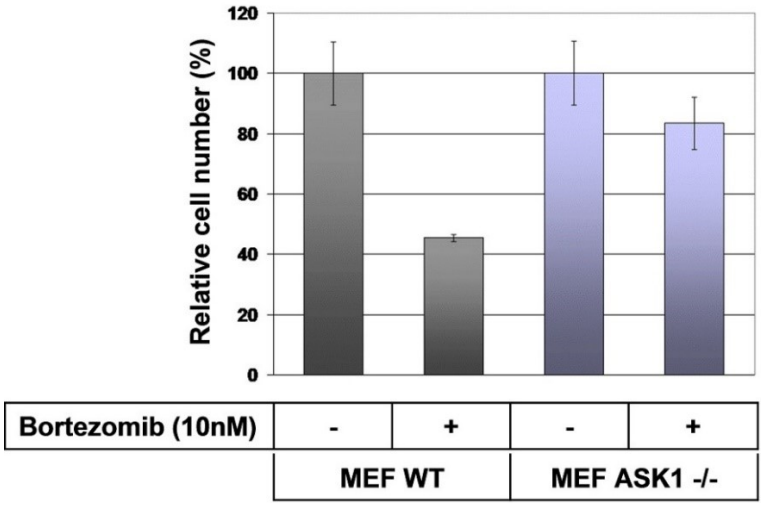

Fig. 2B. MTT assay demonstrates the reduction of cell viability in mouse embryonic fibroblasts wild type (MEF WT) and double knockout apoptosis signal regulating kinase 1 (ASK1) (MEF ASK1-/-) cell lines in response to the exposure to bortezomib. Data are mean ± S.D of three experiments performed in 6 replicates.

Fig. 2C

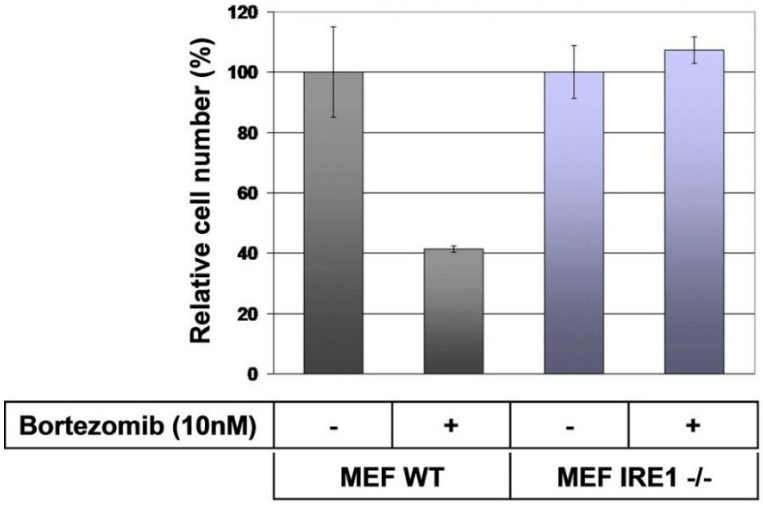

Fig. 2C. MTT assay demonstrates the reduction of cell viability in mouse embryonic fibroblasts wild type (MEF WT) and double knockout inositol requiring enzymes α (IRE1α) (MEF IRE1$^{-/-}$) cell lines in response to the exposure to bortezomib. Data are mean ± S.D of three experiments performed in 6 replicates.

Taken together, these data demonstrate the importance of the p53, ASK, and IRE pathways in the modulation of bortezomib-induced effects.

Dacarbazine treatment of double knock out MEF cells showed similar effects to those induced by bortezomib. Dacarbazine-induced inhibition of cell growth of MEFs were found to be abrogated in response to the knockout of p53 or ASK1 (Fig. 3A and 3B).

Fig. 3A

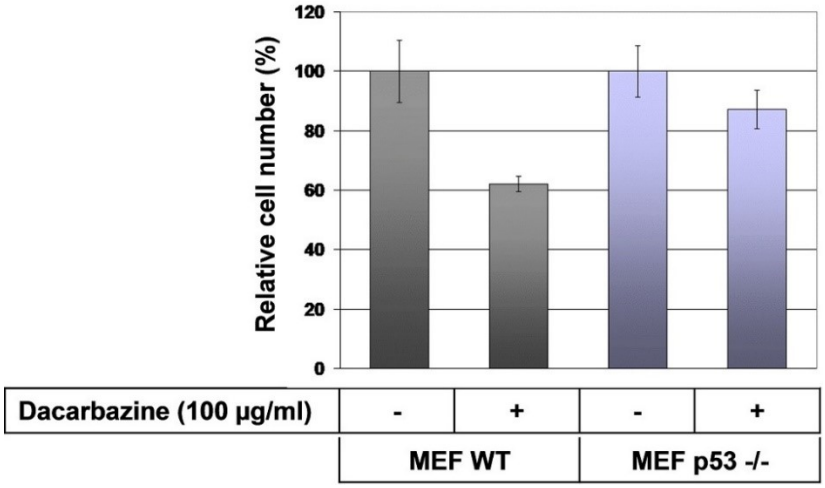

Fig. 3A. MTT assay demonstrates the reduction of cell viability in mouse embryonic fibroblasts wild type (MEF WT) and double knockout p53 (MEF $p53^{-/-}$) cell lines in response to the exposure to dacarbazine. Data are mean ± S.D of three experiments performed in 6 replicates.

Fig. 3B

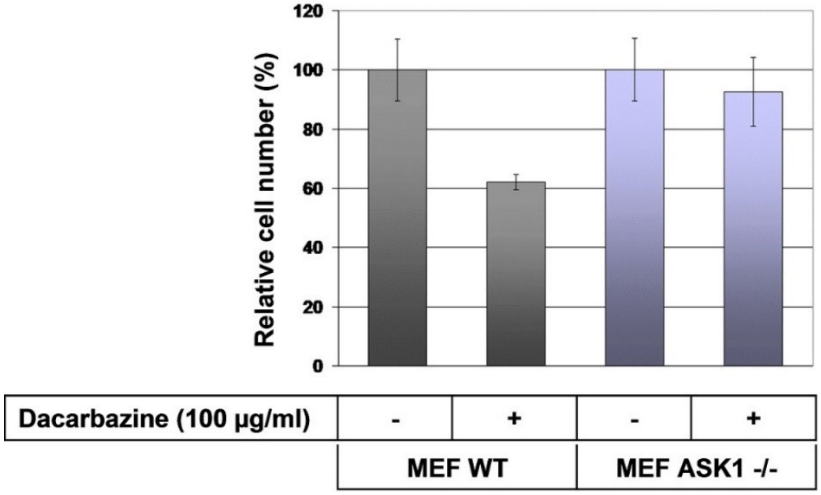

Fig. 3B. MTT assay demonstrates the reduction of cell viability in mouse embryonic fibroblasts wild type (MEF WT) and double knockout apoptosis signal regulating kinase (ASK1) (MEF $ASK1^{-/-}$) cell lines in response to the exposure to dacarbazine. Data are mean ± S.D of three experiments performed in 6 replicates.

Dacarbazine-induced inhibition of cell growth of MEFs was not found to be abrogated in response to the knockout of IRE1 (Fig. 3C).

Fig. 3C

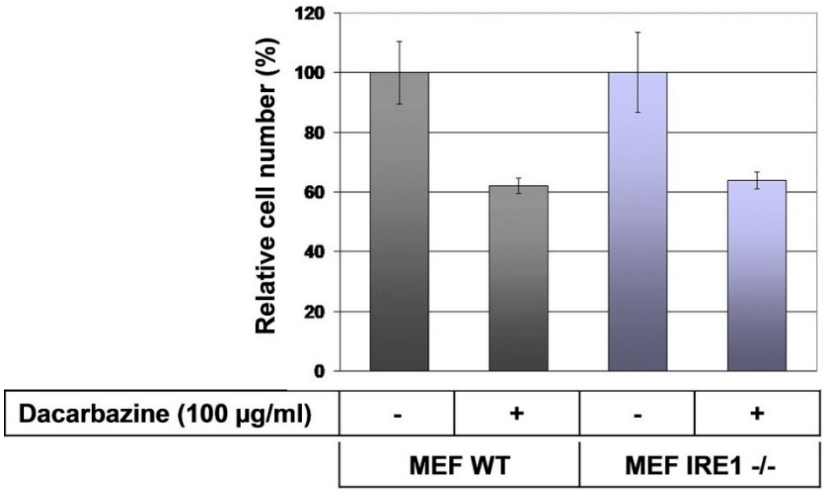

Fig. 3C. MTT assay demonstrates the reduction of cell viability in mouse embryonic fibroblasts wild type (MEF WT) and double knockout inositol requiring enzymes α (IRE1α) (MEF IRE1$^{-/-}$) cell lines in response to the exposure to dacarbazine. Data are mean ± S.D of three experiments performed in 6 replicates.

This suggests an involvement of both p53 and ASK1, but not IRE1 in the modulation of dacarbazine-induced cell death in MEF cells.

In contrast to dacarbazine the knockout of p53, ASK1 or IRE1 was found to block carmustine-induced death of MEF p53$^{-/-}$, ASK1$^{-/-}$ and IRE1$^{-/-}$ cells (Fig. 4A, B and C)

Fig. 4A

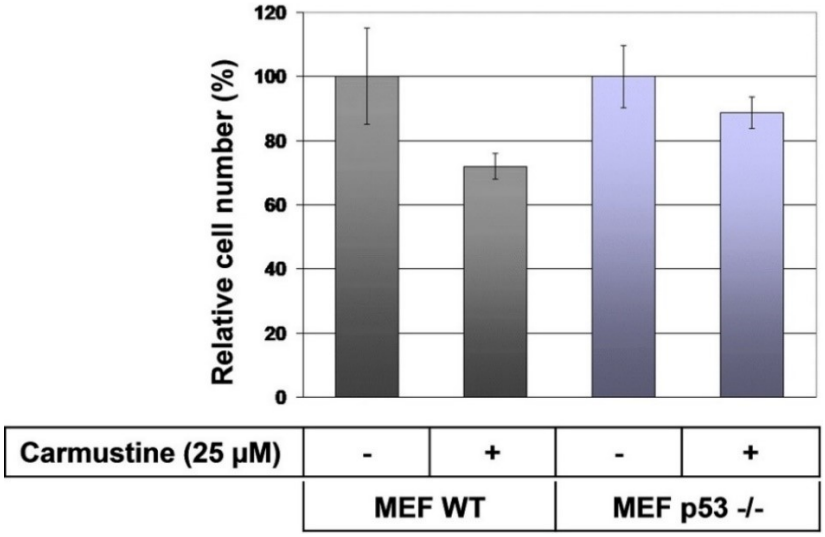

Fig. 4A. MTT assay demonstrates the reduction of cell viability in mouse embryonic fibroblasts wild type (MEF WT) and double knockout p53 (MEF p53$^{-/-}$) cell lines in response to the exposure to carmustine. Data are mean ± S.D of three experiments performed in 6 replicates.

Fig. 4B

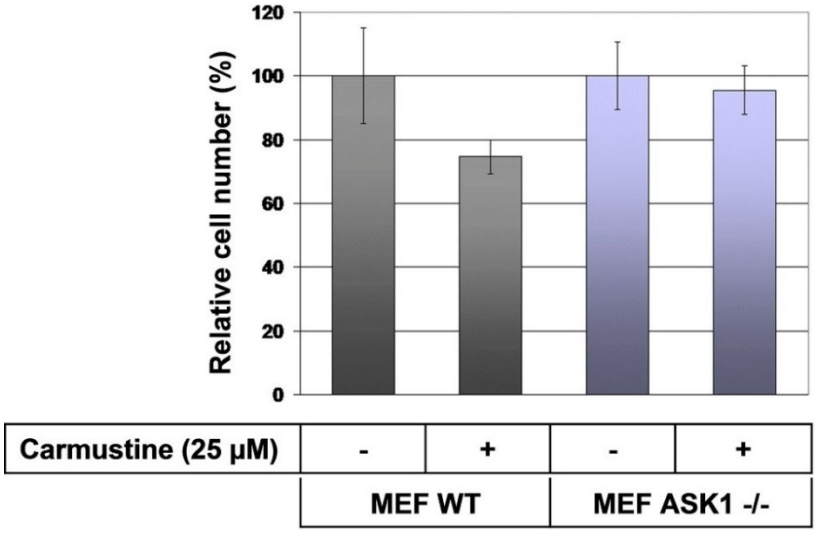

Fig. 4B. MTT assay demonstrates the reduction of cell viability in mouse embryonic fibroblasts wild type (MEF WT) and double knockout apoptosis signal regulating kinase (ASK1) (MEF ASK1$^{-/-}$) cell lines in response to the exposure to carmustine. Data are mean ± S.D of three experiments performed in 6 replicates.

Fig. 4C

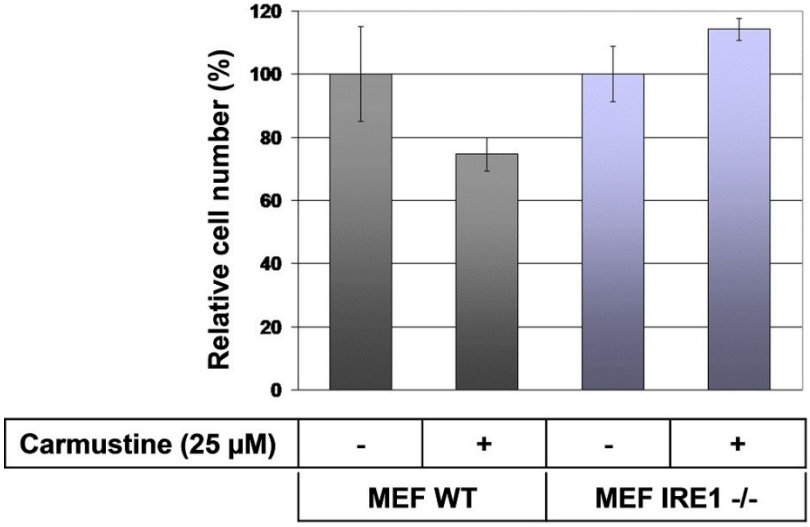

Fig. 4C. MTT assay demonstrates the reduction of cell viability in mouse embryonic fibroblasts wild type (MEF WT) and double knockout inositol requiring enzymes α (IRE1α) (MEF IRE1$^{-/-}$) cell lines in response to the exposure to carmustine. Data are mean ± S.D of three experiments performed in 6 replicates.

In comparison to wild type MEFs this suggests that p53, ASK1, and IRE1 are involved in the modulation of carmustine-induced death of MEF cells.

4.3 Bortezomib induces both apoptosis and autophagy in melanoma cells

In addition to its ability to trigger apoptosis, the impact of bortezomib on autophagy was examined in melanoma cell lines A375 and BLM. First, the level of bortezomib-induced apoptosis in melanoma cells was assessed following the exposure of bortezomib (10 nM) for 24h. Data obtained from comet assay confirmed the ability of bortezomib to trigger apoptosis in melanoma cell lines A375 and BLM (Fig. 5A, Fig. 5B).

Fig. 5A

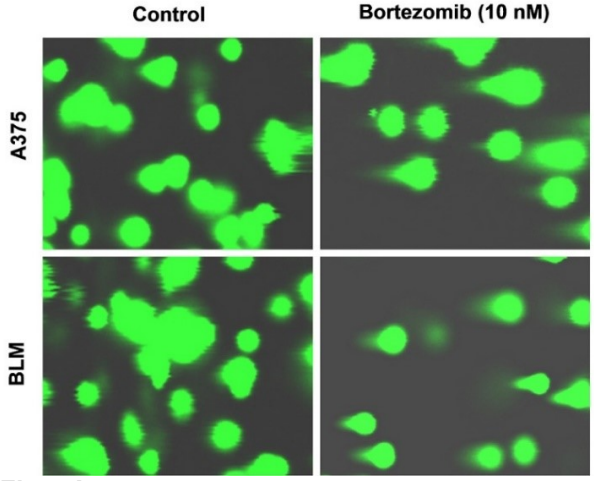

Fig. 5A. DNA fragmentation assessed by comet assay in bortezomib treated and untreated melanoma cell lines, the pictures were taken with a microscope using a FITC filter and 10× objective lens (magnification factor 400).

Fig. 5B

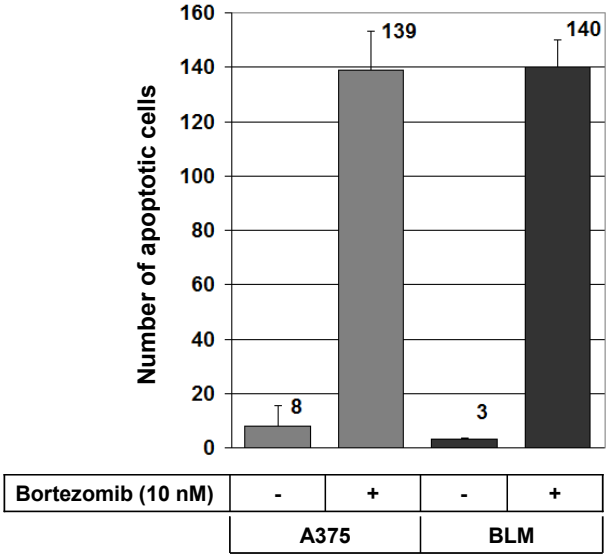

Fig. 5B. DNA fragmentation assessed by comet assay in bortezomib treated and untreated melanoma cell lines. The extent of DNA damage measured as the number of DNA tails in the comet assay in both A375

and BLM cells before and after the treatment with bortezomib. Treated cells were significantly different from the untreated controls, as calculated by paired t-test.

Bortezomib-induced apoptosis in melanoma cells is mediated by an apoptotic mechanism that is characterized by the release of both Cytochrome c (Cyt. c) and apoptosis inducing factor (AIF) and PARP cleavage (Fig.5C).

Fig. 5C

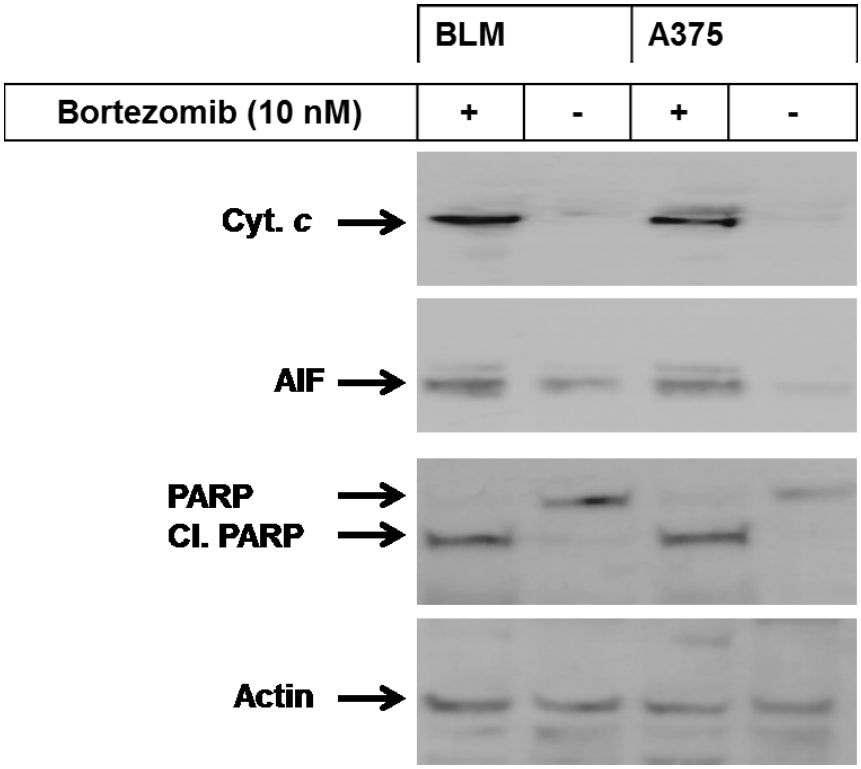

Fig. 5C. Western blot analysis demonstrates the release of Cytochrome c (Cyt. c), apoptosis inducing factor (AIF), and PARP cleavage. β-actin was used as internal control for loading and transfer.

In addition, we assessed the activity of both caspase-9 and caspase-3 using a fluorometric cleavage assay in bortezomib-treated melanoma cells (Fig.5D). We found, as expected a drastic increase in caspase-9 and caspase-3 activity in bortezomib-treated cells.

Fig. 5D

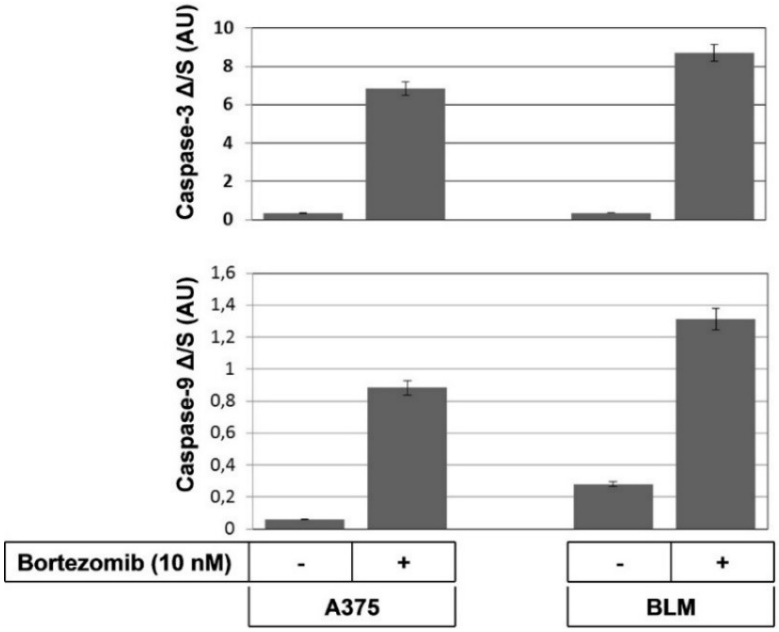

Fig. 5D. The activity of caspase-3 and caspase-9 was determined in control and bortezomib-treated melanoma cell lines A375 and BLM using fluorogenic substrates DEVD-AMC and LEHD-AMC, respectively. Results (Extinctions/s in arbitrary units) are expressed as the mean±s.d. of three separate experiments.

The induction of the expression of Noxa, Mcl-1 and HSP70 proteins, as well as the cleavage of LC3 was noted in melanoma cells following the exposure to bortezomib, as evidenced by Western blot analysis (Fig. 5E).

Fig. 5E

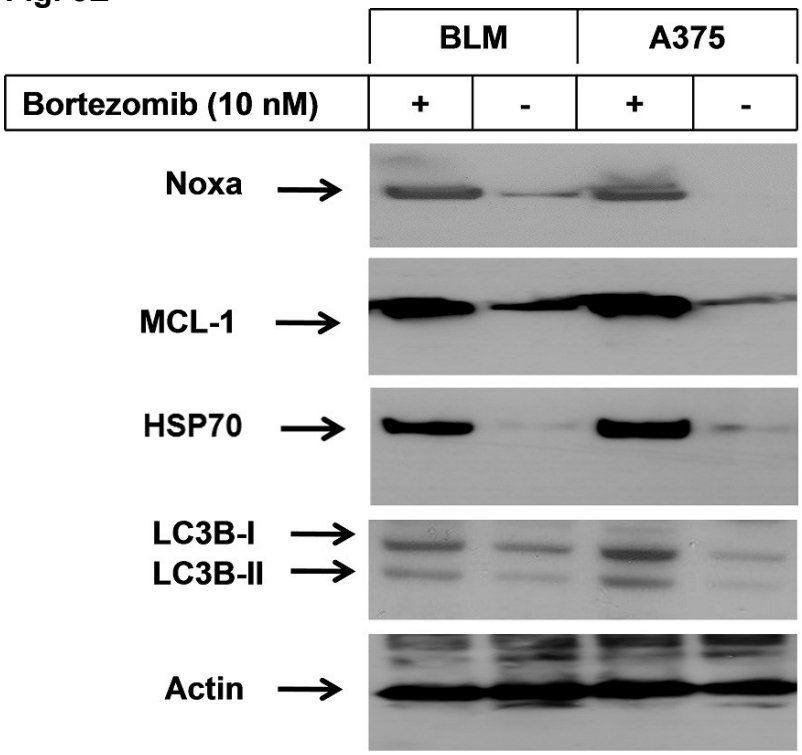

Fig. 5E. Western blot demonstrates bortezomib induced expression of Noxa, Mcl-1, HSP70 proteins and cleavage of LC3II in melanoma cells. β-actin was used as internal control for loading and transfer.

To investigate whether bortezomib-induced cleavage of LC3 is associated with autophagy, the melanoma cell lines A375 and BLM were analysed for autophagosome formation by electron transmission microscopy. Interestingly, the treatment of melanoma cells with bortezomib led to the formation of autophagosomes, an evidence for the impact of bortezomib on the regulation of autophagosome formation in melanoma cells (Fig.5F). Taken together, these data demonstrate for the first time the ability of bortezomib to trigger both apoptosis and autophagosome formation in melanoma cells.

Fig. 5F

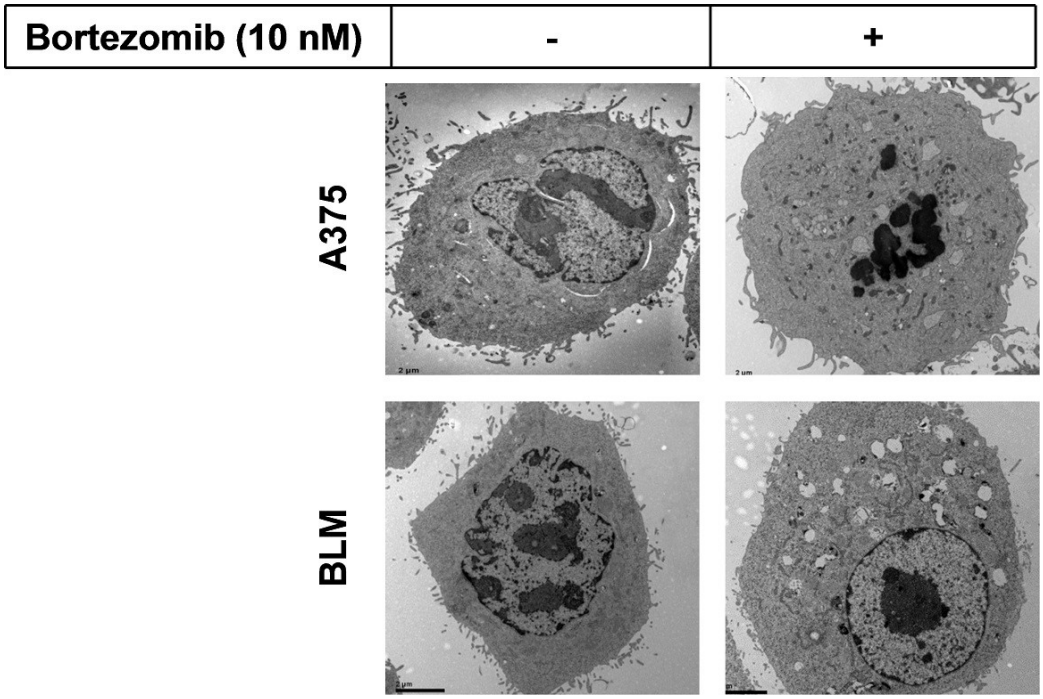

Fig. 5F. Melanoma cell lines (A375 and BLM) treated with bortezomib (10 nM) for 12h were harvested, fixed in 2.5% glutaraldehyde and postfixed in 1% osmium tetroxide. Ultra-microtome sections were post-stained and imaged on a JEOL 1200 EX transmission electron microscope at 80 kV (magnification factor 8000).

4.4 Bortezomib triggers the loss of mitochondrial membrane potential and endoplasmic reticulum stress in melanoma cells

Based on the fact that the overexpression of Noxa is associated with both mitochondrial dysregulation and ER stress (Hassan et al., 2008), the effect of bortezomib-induced expression of Noxa on the mitochondrial membrane potential (ΔΨm) and endoplasmic reticulum stress was examined in melanoma cells. As expected the treatment of melanoma cell lines A375 and BLM with bortezomib for 24h was found to trigger both the loss of ΔΨm and ER stress. Data obtained from flow cytometry analysis of JC-1-stained cells demonstrated the increased loss of ΔΨm as evidenced by the shifted increase of green fluorescence stained cells and the decrease of red fluorescence stained cells compared to control cells (Fig. 6A).

Fig. 6A

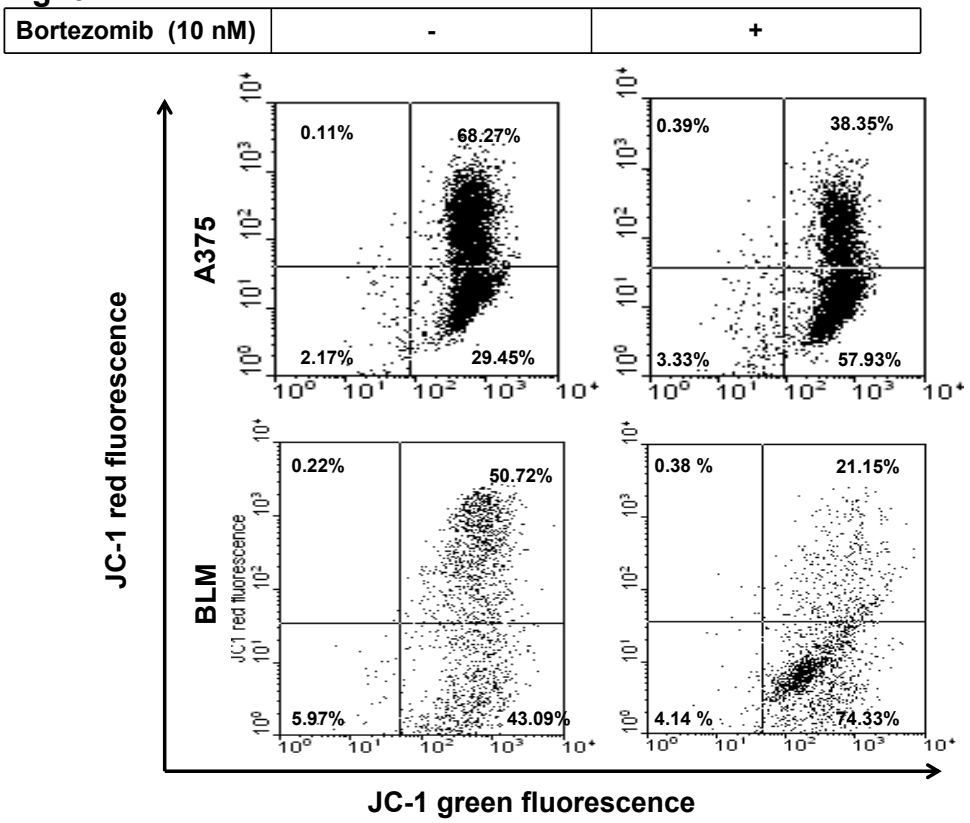

Fig. 6A. Loss of mitochondrial membrane potential in response to the exposure of melanoma cells to bortezomib. Flow cytometry analysis, using JC-1 staining, shows the loss of ΔΨm in response to the treatment with bortezomib. Cells with intact mitochondria displayed high red and low green fluorescence and appear in the upper right quadrant of the scatterplots. In contrast, cells that had lost their ΔΨm displayed high green and low red fluorescence and appear in the lower right quadrant.

This is an evidence for the loss of ΔΨm in response to bortezomib-induced expression of Noxa protein. Also, the analysis of intracellular Ca^{2+} in both bortezomib-treated and untreated cells using fluorescence microscopy following cell staining Fluo3-AM (Fig. 6B) revealed the increase of intracellular Ca^{2+} release in response to bortezomib-induced expression of Noxa in both melanoma cells, an evidence for the induction of ER stress in response to the treatment with bortezomib (Fig. 6B). Altogether, these data provide evidence for the involvement of both mitochondrial and ER-associated pathways in the modulation of bortezomib-induced effects in melanoma cells.

Fig. 6B

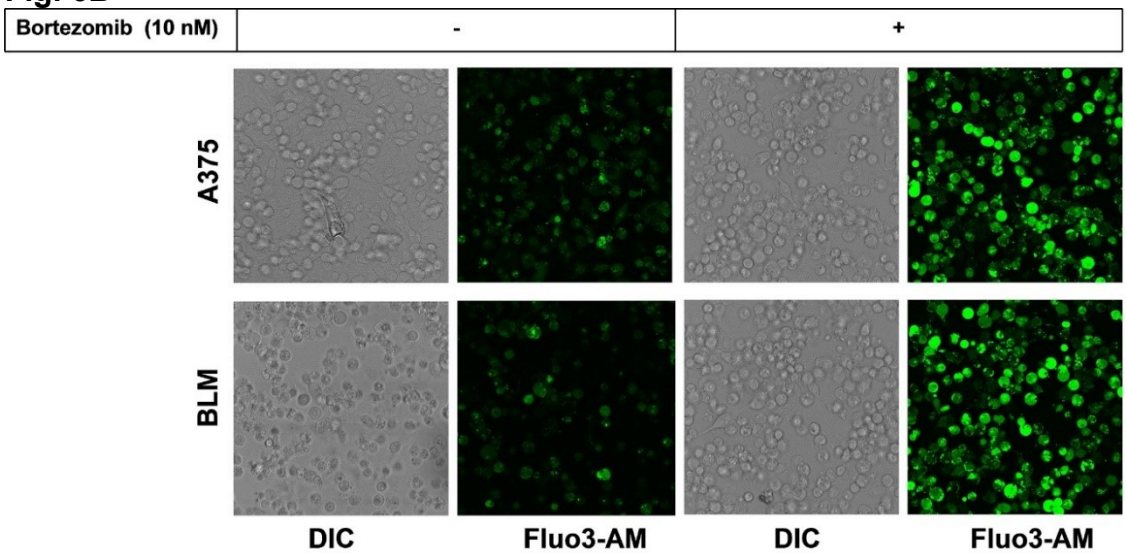

Fig. 6B. Increase of intracellular Ca^{2+} release in response to the exposure of melanoma cells to bortezomib. Intracellular Ca^{2+} levels in response to the treatment of melanoma cells (A375 and BLM) with bortezomib as assessed by staining with Ca^{2+} -sensitive dye Fluo3-AM. Differential interference contrast images (DIC) are shown. Pictures were taken using a LeicaTCS SP2 AOBS with a 40 X oil immersion magnification using Leica Confocal microscopy. Data are representative of three independent experiments.

4.5 Enhancement of ROS accumulation and the activation of IRE1α and MAP kinase pathways by the exposure of melanoma cells to bortezomib

Next, to examine whether the exposure of melanoma cells to bortezomib influences the level of reactive oxygen species (ROS), IRE1α or MAP kinase pathways, the melanoma cell lines A375 and BLM were treated with bortezomib for 24h, and subsequently subjected either to flow cytometry analysis for assessment of ROS level or to Western blot analysis for the analysis of IRE1α and MAP kinase pathways. Data obtained from flow cytometry analysis demonstrated an increased accumulation of ROS in response to the exposure to bortezomib (Fig.7A).

Fig. 7A

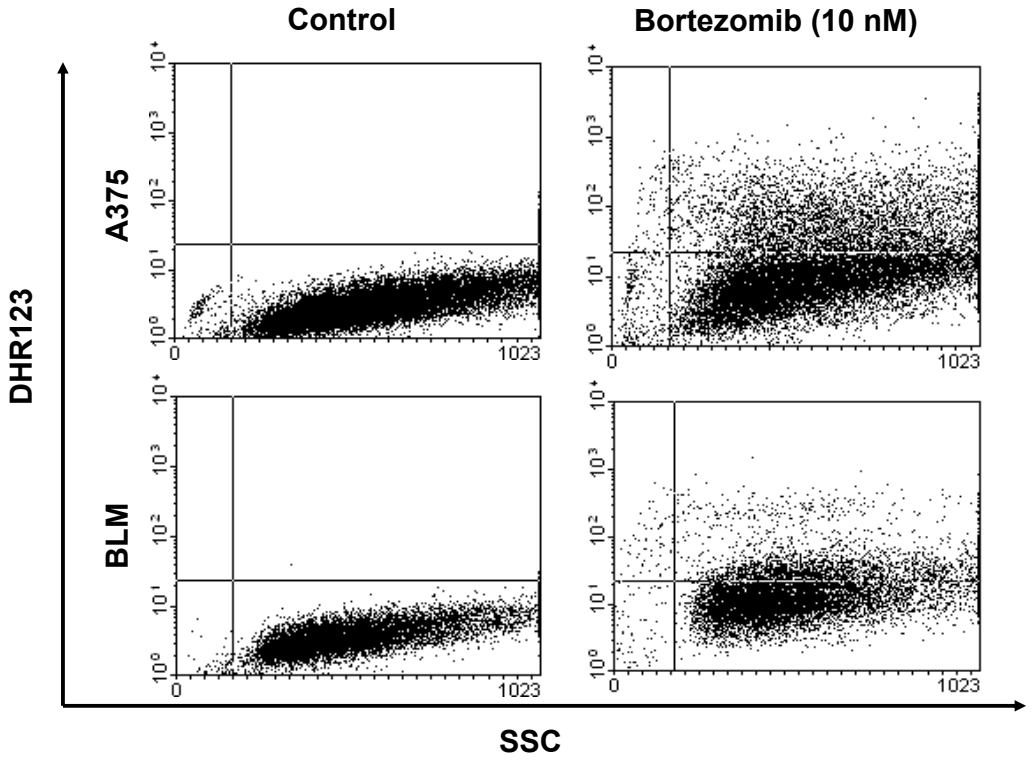

Fig. 7A. Assessment of the level of reactive oxygen species (ROS) following the treatment of both melanoma cell lines A375 and BLM with bortezomib. ROS generation was measured by flow cytometry using dihydrorhodamine (DHR 123).

Although no alteration was noted on the total expression of IRE1α, ASK1, JNK and p38, the exposure of melanoma cell was found to trigger the phosphorylation of IRE1α, ASK1, JNK and p38 protein when compared to control cells (Fig. 7B). These results suggest an IRE1α, ASK1, JNK and p38 dependent modulation of bortezomib-induced effects in melanoma cells.

Fig. 7B

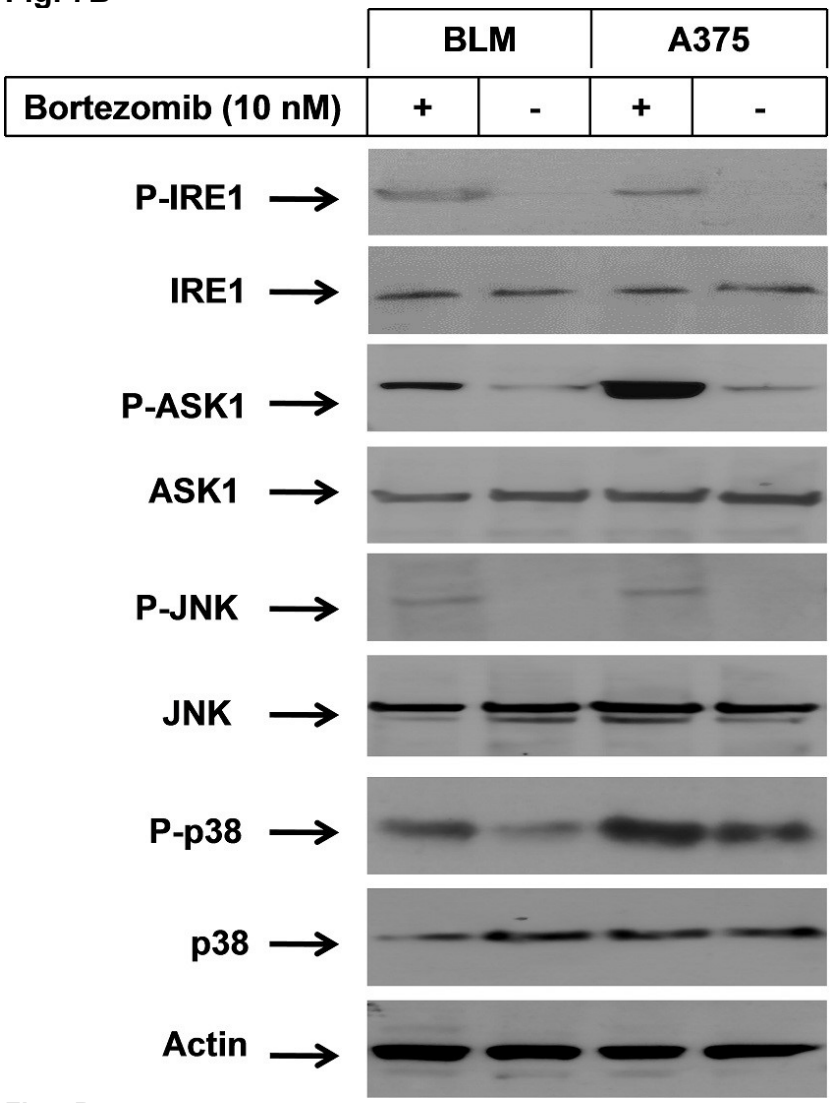

Fig. 7B. Western blot analysis demonstrates the total expression and the phosphorylation levels of IRE1α, ASK1, JNK, and p38 in response to the exposure of melanoma cells to bortezomib. β-actin was used as internal control for loading and transfer. Data are representative of three independent experiments.

4.6 Bortezomib-induced ASK1 is involved in the regulation of both JNK and p38 pathways

To demonstrate whether bortezomib-induced ASK1 is involved in the regulation of both JNK and p38 pathways, the melanoma cell lines were pre-treated with the inhibitor of ASK1 (thioredoxin) before exposure to bortezomib. Twenty-four hours later, the cells were harvested and total cell lysates were prepared. Data obtained from Western blot analysis (Fig. 7C) demonstrated the inhibition of bortezomib-induced phosphorylation of both JNK and p38 in response to the inhibition of ASK1, suggesting the involvement of bortezomib-induced ASK1 activation in the regulation of both JNK and p38 pathways.

Fig. 7C

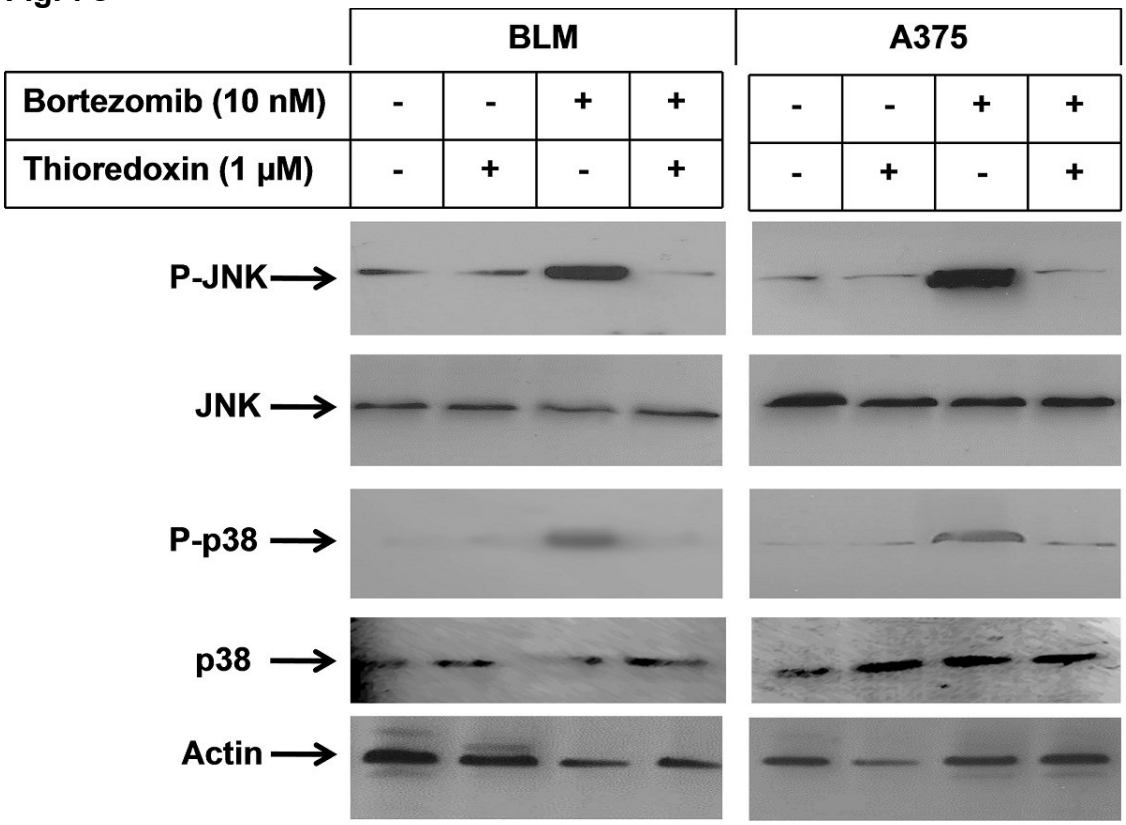

Fig. 7C. Western blot analysis demonstrates the inhibition of bortezomib-induced phosphorylation of JNK and p38 in response to the treatment of melanoma cells with the inhibitor of ASK1 (thioredoxin). β-actin was used as internal control for loading and transfer. Data are representative of three independent experiments.

4.7 The exposure of melanoma cells to bortezomib enhances the DNA-binding activities of the transcription factors AP-1, ATF-2, Ets-1, and HSF1

To identify, which transcription factors are influenced by the exposure of melanoma cells to bortezomib, the melanoma cells lines were treated with bortezomib for 24h and nuclear extracts were prepared. Using EMSA, it could be shown that the exposure of melanoma cells to bortezomib enhances the DNA-binding activities of the transcription factors AP-1 (Fig. 8A), ATF-2 (Fig. 8B), Ets-1 (Fig. 8C), and HSF1 (Fig.8D), suggesting a role for these transcription factors in the modulation of bortezomb-induced effects in melanoma cells.

Fig. 8A

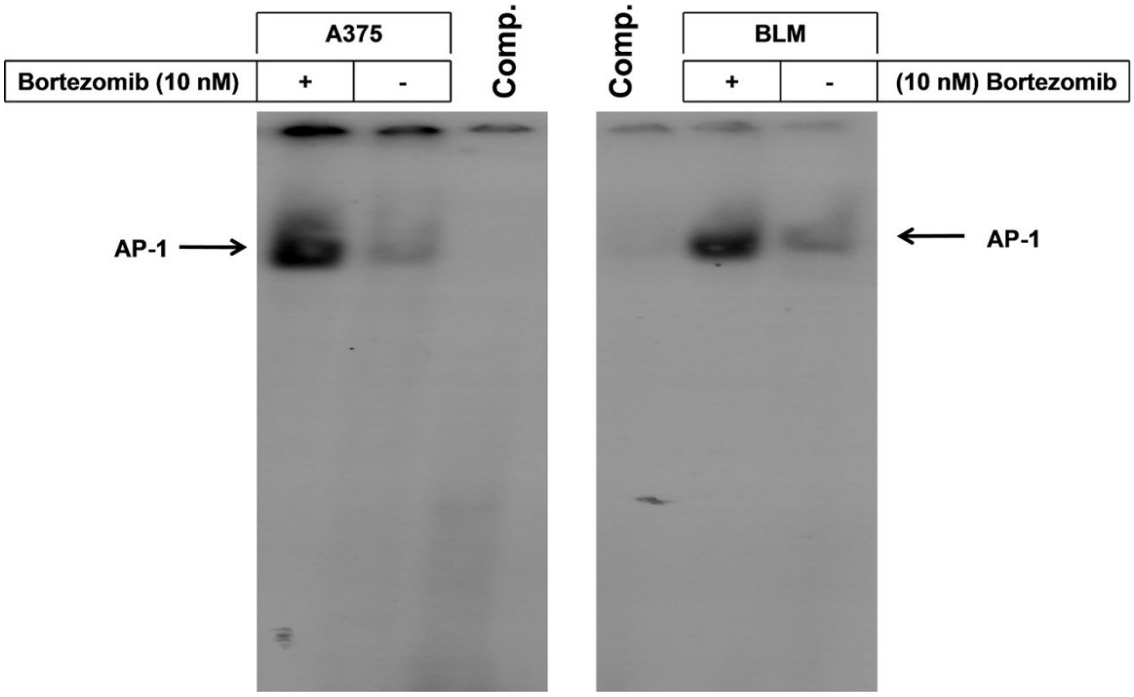

Fig. 8A. Electrophoretic mobility shift assay (EMSA) demonstrates the enhancement of DNA-binding activity of the transcription factors AP-1 in response to exposure of melanoma cells to bortezomib. Data are representative of three independent experiments.

Fig. 8B

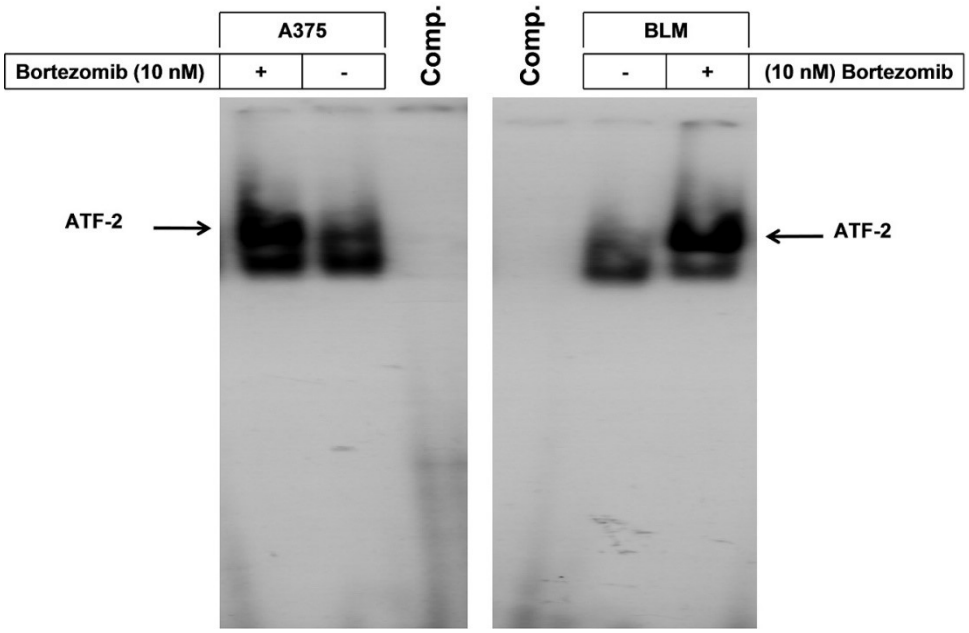

Fig. 8B. Electrophoretic mobility shift assay (EMSA) demonstrates the enhancement of DNA-binding activity of the transcription factors ATF-2 in response to exposure of melanoma cells to bortezomib. Data are representative of three independent experiments.

Fig. 8C

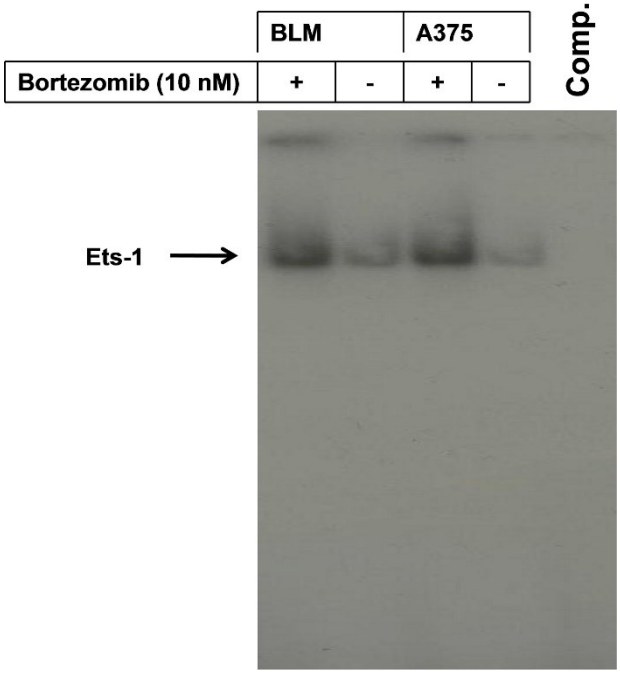

Fig. 8C. Electrophoretic mobility shift assay (EMSA) demonstrates the enhancement of DNA-binding activity of the transcription factors Ets-1 in response to exposure of melanoma cells to bortezomib. Data are representative of three independent experiments.

Fig. 8D

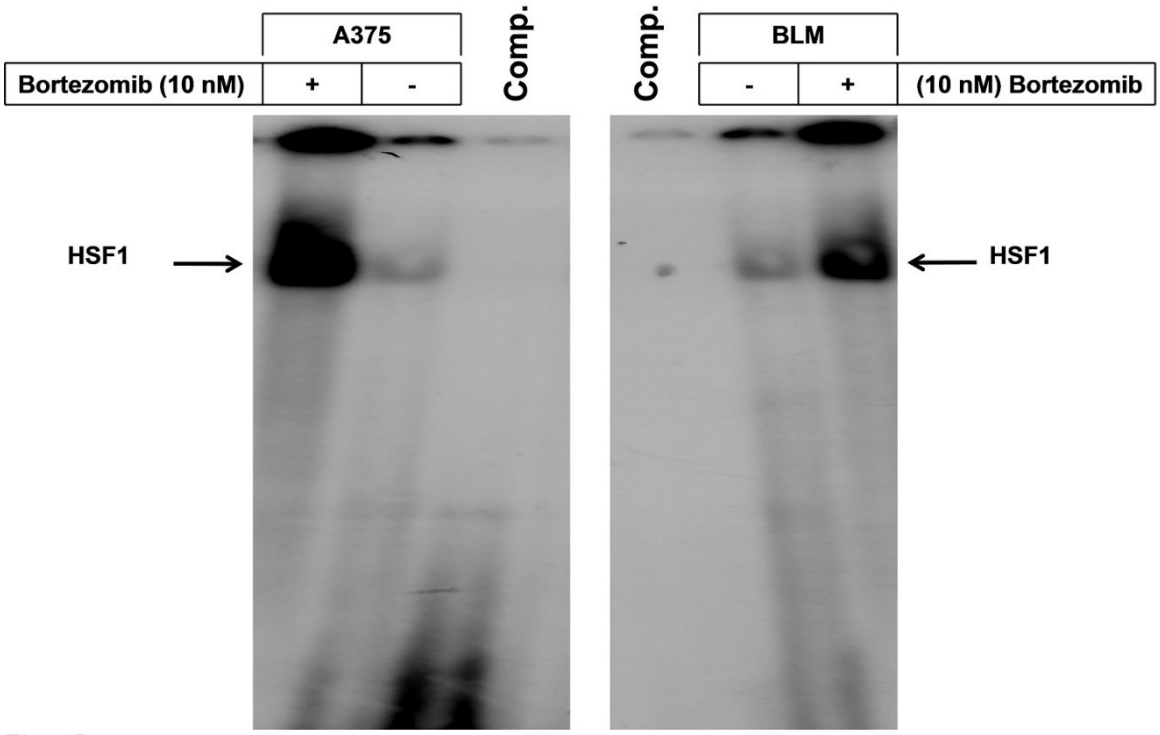

Fig. 8D. Electrophoretic mobility shift assay (EMSA) demonstrates the enhancement of DNA-binding activity of the transcription factors HSF1 in response to exposure of melanoma cells to bortezomib. Data are representative of three independent experiments.

Next, the signal pathways, which are involved in the regulation of Ets-1 and HSF1, were determined following to exposure of melanoma cells to bortezomib. Prior to the treatment with bortezomib, the melanoma cells were pre-treated with either the inhibitor of JNK (SP600125) or with the inhibitor of p38 (SB203580). Twenty-four hours later, the nuclear extracts were prepared from treated and control cells and were prepared for EMSA assay. Data obtained from EMSA (Fig. 9A and 9B) demonstrated the inhibition of bortezomib-induced DNA-binding activity of Ets-1 in response to the pre-treatment of melanoma cell lines A375 (Fig. 9A) and BLM (Fig. 9B) with the inhibitor of p38, suggesting the involvement of p38 pathway in the regulation of Ets-1. Whereas, the pre-treatment of the same melanoma cells with the inhibitor of JNK (SP600125) was found to abrogate bortezomib-induced DNA-binding activity of HSF1 in both melanoma cell lines A375 (Fig. 9A) and BLM (Fig. 9B), suggesting the involvement of JNK in the regulation of bortezomib-induced activation of HSF1.

Fig. 9A

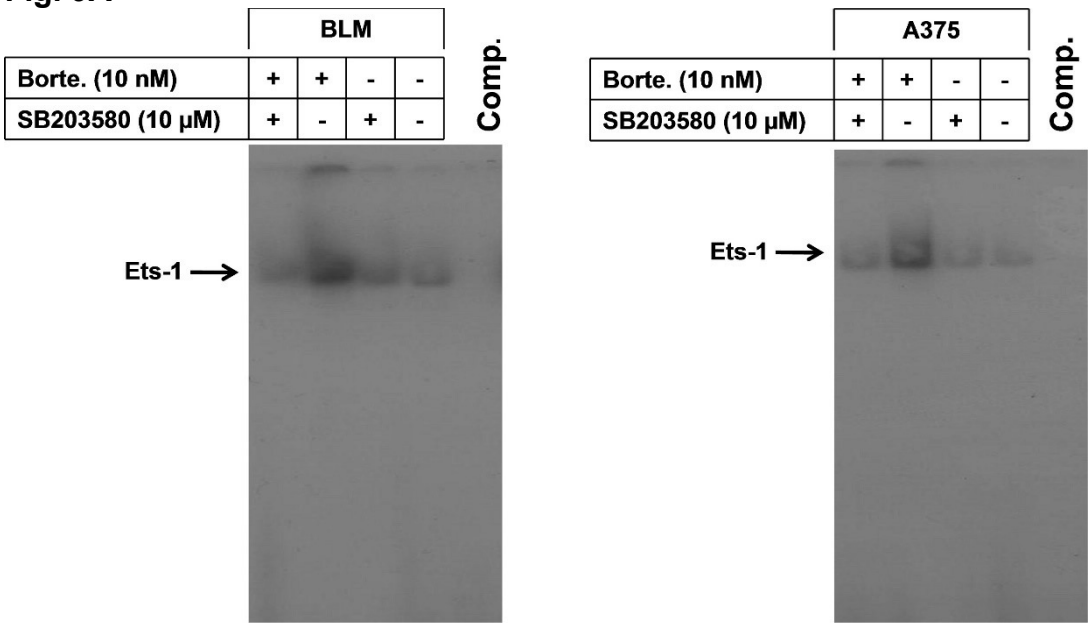

Fig. 9A. Electrophoretic mobility shift assay (EMSA) demonstrates the inhibition of bortezomib-induced activation of the transcription factors Ets-1 in response to the treatment of melanoma cells with the inhibitor of p38 (SB203580). Data are representative of three independent experiments.

Fig. 9B

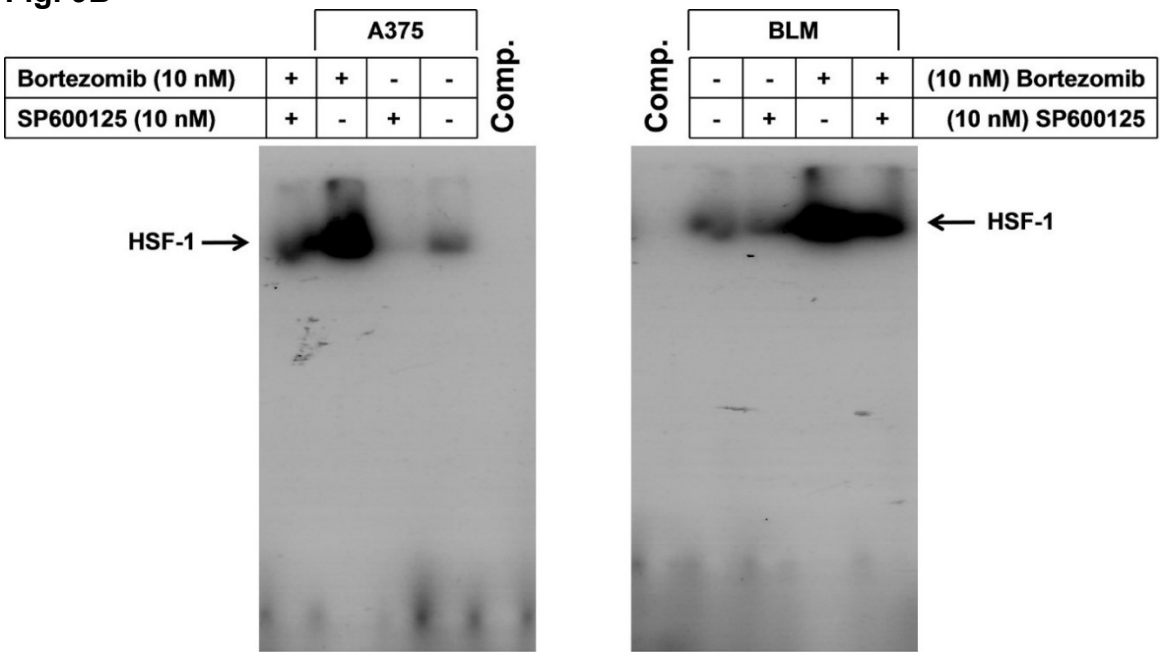

Fig. 9B. Electrophoretic mobility shift assay (EMSA) demonstrates the inhibition of bortezomib-induced activation of the transcription factors HSF1 in response to the treatment of melanoma cells with the inhibitor of JNK pathway (SP600125). Data are representative of three independent experiments.

4.8 Bortezomib-induced autophagosome formation in melanoma cells is an ASK1-dependent mechanism and positively regulated by inhibition of apoptosis

To investigate the mechanisms, which are involved in the regulation of bortezomib-induced autophagy, the melanoma cells were pre-treated with either the inhibitors of ASK1 (thioredoxin) or caspase-3 (zVAD-fmk) before the exposure to bortezomib. Twenty-four hours later, treated and control cells were analysed for autophagosome formation using Western blot analysis and transmission electron microscopy. As expected, the inhibition of ASK1 was found to increase induced apoptosis, as evidenced by chromatin condensation, and to abrogate bortezomib-induced autophagosome formation (Fig. 10A).

Fig. 10A

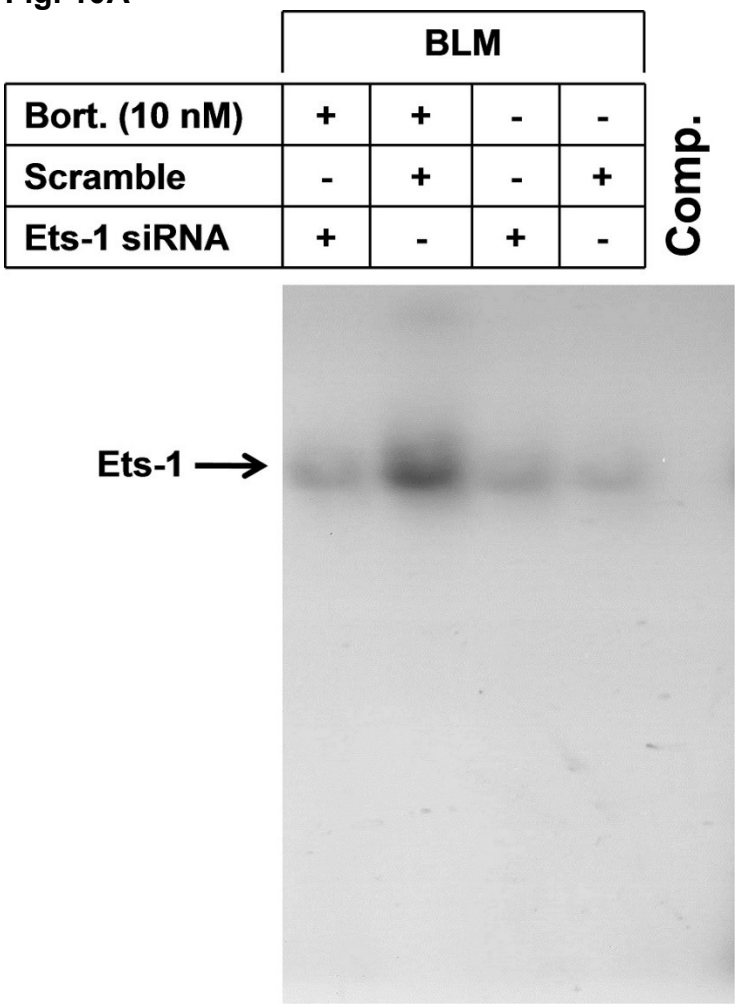

Fig. 10A. EMSA demonstrates the inhibition of bortezomib-induced activation of the transcription factor Ets-1 by its specific siRNA in melanoma cell line BLM. Data are representative of three independent experiments.

In addition, data obtained from Western blot (Fig.10B) confirmed that the inhibition of ASK pathway is associated with the abrogation of bortezomib-induced LC3 cleavage and the inhibition of apoptosis with caspase-3 inhibitor leads to the enhancement of bortezomib-induced LC3 cleavage, suggesting that bortezomib-induced autophagosome formation in melanoma cells is mediated by ASK1 pathway and that the inhibition of apoptosis positively influences bortezomib-induced autophagosome formation in melanoma cells.

Fig. 10B

	BLM					
Bort. (10 nm)	-	+	+	+	+	+
Scramble	-	-	-	+	-	-
Ets-1 siRNA	-	+	-	-	-	-
MCl-1 siRNA	-	-	+	-	-	-
Casp.3 Inhi. (50 nM)	-	-	-	-	+	-
Thioredoxin (1 nM)	+	-	-	-	-	-

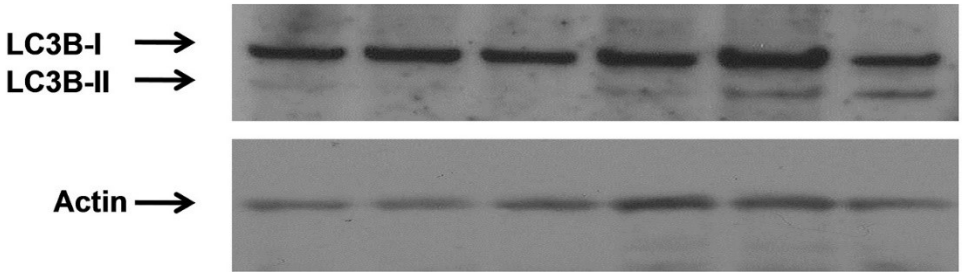

Fig. 10B. Western blot analysis demonstrates the inhibition of bortezomib-induced cleavage of LC3, or by inhibition of ASK1 in response to the knockdown of Ets-1, Mcl-1 by their specific siRNA, or through the inhibition of ASK1 by its specific inhibitor (thioredoxin), and the increase of bortezomib-induced cleavage of LC3 in response to the treatment of melanoma cells by the inhibitor of caspase-3 (zVAD-fmk). β-actin was used as internal control for loading and transfer.

4.9 Bortezomib-induced autophagosome formation in melanoma cells is mediated by both ER stress and mitochondrial dysregulation-dependent pathways

To address the molecular mechanisms, which are responsible for the regulation of bortezomib-induced autophagosome formation in melanoma cells, the melanoma cells were treated with the inhibitors of caspase-3 (zVAD-fmk), ASK1(thioredoxin), JNK

(SP600125), or with the specific siRNAs of ets-1, Mcl-1 or HSP70 before exposure to bortezomib. Twenty four hours later, the cells were either harvested for isolation of nuclear cell extracts, total cell lysates or prepared for transmission electron microscopy. Data obtained from EMSA (Fig. 10A) demonstrated the efficiency of Ets-1-specific siRNA to knockdown its cognate gene. Next, data obtained from Western blot (Fig. 10B) demonstrated the abrogation of bortezomib-induced cleavage of LC3 in response to the knockdown of Ets-1 or Mcl-1 by their specific siRNAs or in response to the pre-treatment with ASK1 inhibitor. In contrast, the pre-treatment of melanoma cells with the inhibitor of caspase-3 was found to enhance bortezomib-induced cleavage of LC3 (Fig. 10B), suggesting that the inhibition of apoptosis positively influences bortezomib-induced autophagosome formation in melanoma cells. In addition to the ability of Mcl-1-specific siRNA to knockout its cognate gene, the data obtained from Western blot analysis (Fig. 10C) demonstrated the inhibition of bortezomib-induced expression of Mcl-1 in response to the knockdown of Ets-1 by its specific siRNA, suggesting the involvement of bortezomib-induced activation of Ets-1 in the regulation of bortezomib-induced expression of Mcl-1.

Fig. 10C

	BLM							
Bort. (10 nm)	-	-	-	-	+	+	+	+
Scramble	+	-	+	-	+	-	+	-
Ets-1(siRNA)	-	-	-	+	-	-	-	+
MCl-1 (siRNA)	-	+	-	-	-	+	-	-

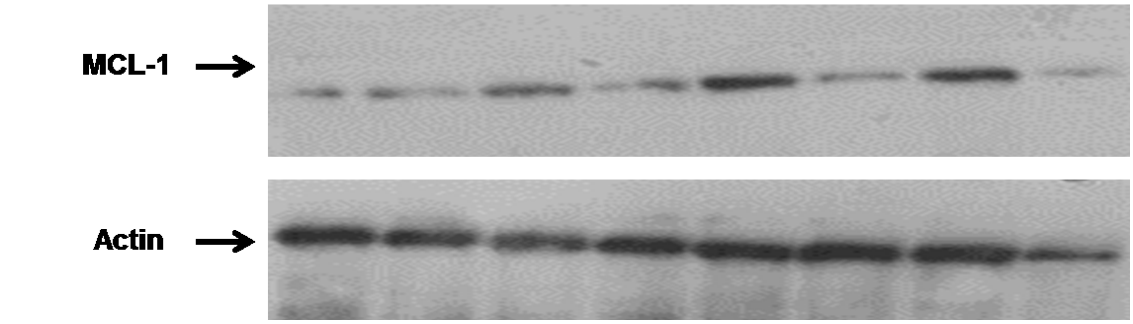

Fig. 10C. Western blot analysis demonstrated the inhibition of bortezomib-induced expression of Mcl-1 in response to the knockdown of either Ets-1 or Mcl-1-specific siRNA in melanoma cells. β-actin was used as internal control for loading and transfer.

Next, the mechanisms of bortezomib-induced expression of HSP70 were determined in melanoma cells. The melanoma cells were pre-treated with inhibitor of ASK1, JNK or with HSP70-specific siRNA prior to exposure of melanoma cells to bortezomib for 24h. Besides the knockdown of bortezomib-induced HSP70 by its specific siRNA, data obtained from Western blot analysis demonstrated the inhibition of bortezomib-induced HSP70 in response to the inhibition of ASK1 or JNK, an evidence for the involvement of ASK1/JNK pathways in the regulation of bortezomib-induced expression of HSP70 in melanoma cells (Fig. 10D).

Fig. 10D

	BLM							
Bort. (10 nm)	-	+	-	+	-	+	+	+
SP600125 (10 nM)	+	-	+	-	+	+	-	-
Thioredoxin (1 nM)	+	-	-	+	-	-	-	-
Scramble	+	-	-	-	-	-	+	-
HSP70 siRNA	+	-	-	-	-	-	-	+

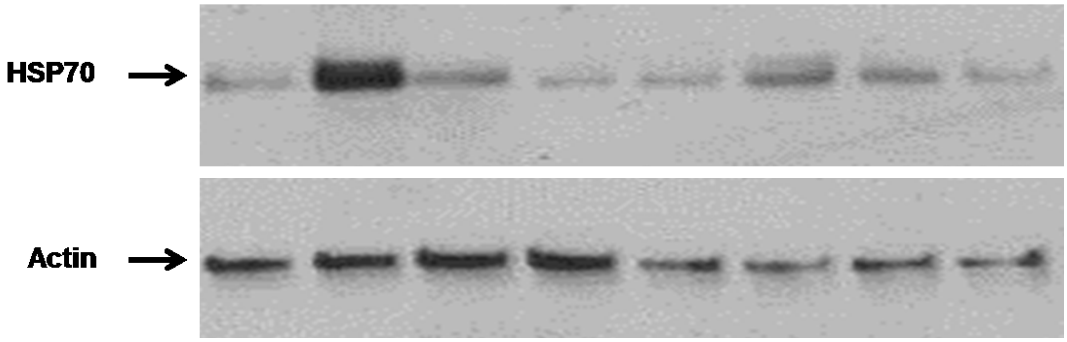

Fig. 10D. Western blot analysis demonstrates the inhibition of bortezomib-induced expression of HSP70 in response to the inhibition of ASK1 or JNK by their inhibitors or through the knockdown of HSP70 by its specific siRNA. β-actin was used as internal control for loading and transfer.

Furthermore, data obtained from transmission electron microscopy (Fig. 10E) demonstrated the enhancement of bortezomib-induced autophagosome formation in response to the inhibition of apoptosis. Although the abrogation of bortezomib-induced autophagosome formation in response to the pre-treatment of melanoma cells with ASK1 inhibitor was detected, the knockdown of HSP70 by its specific siRNA does not seem to influence bortezomib-induced autophagosome formation (Fig. 10E). The collected data provides an insight concerning the involvement of ASK/p38/Ets-1/Mcl-1 in the regulation of bortezomib-induced autophagosome formation, and the involvement

of ASK1/JNK/HSF-1pathway in the regulation of bortezomib-induced expression of HSP70.

Fig. 10E

Bort. (10 nM)	-	+	+	+	-
zVAD-fmk (50 nM)	-	-	+	-	-
Thior. (1 nM)	-	-	-	+	-
Scramble	+	-	-	-	-
HSP70 siRNA	-	-	-	-	+

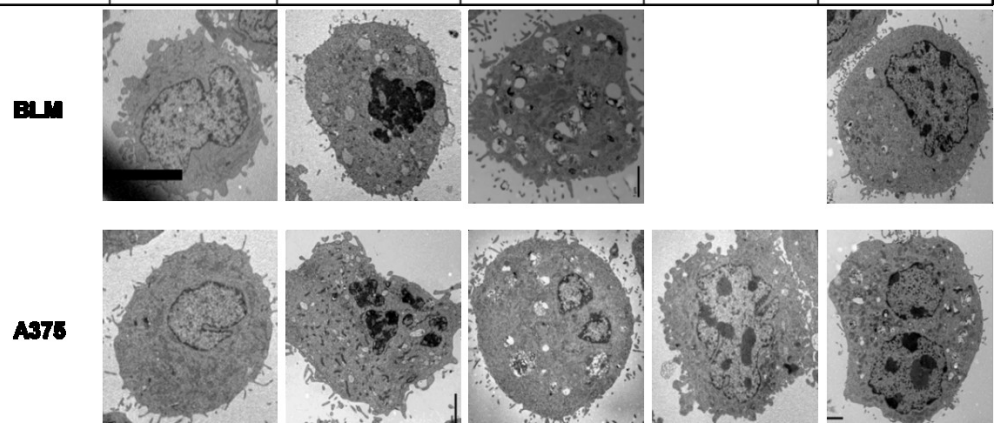

Fig. 10E. Transmission electron microscopy (magnification factor 8000) showing the inhibition of bortezomib-induced autophagy by the inhibitor of ASK1, whereas the knockdown of HSP70 did not influence bortezomib-induced autophagosome formation. In contrast, the inhibition of bortezomib-induced apoptosis in response to pre-treatment of melanoma cells with caspase-3 inhibitor (zVAD-fmk) potentiates induced autophagy. Data are representative of three independent experiments.

4.10 Bortezomib-induced apoptosis in melanoma cells is mediated by a mitochondrial dysregulation-dependent pathway

To determine the molecular mechanism of bortezomib-induced apoptosis in melanoma cells, the melanoma cell lines were pre-treated with the inhibitors of caspase-3, JNK, p38, ASK1, as well as Ets-1, Mcl-1, HSP70-specific siRNAs before the exposure to bortezomib. Twenty-four hours later, the cells were subjected for the assessment of the cell viability using MTT assay. Data obtained from Western blot analysis (Fig. 11A) also demonstrated the inhibition of bortezomib-induced expression of HSP70 in response to the pre-treatment of melanoma cells with the inhibitor of JNK.

Fig. 11A

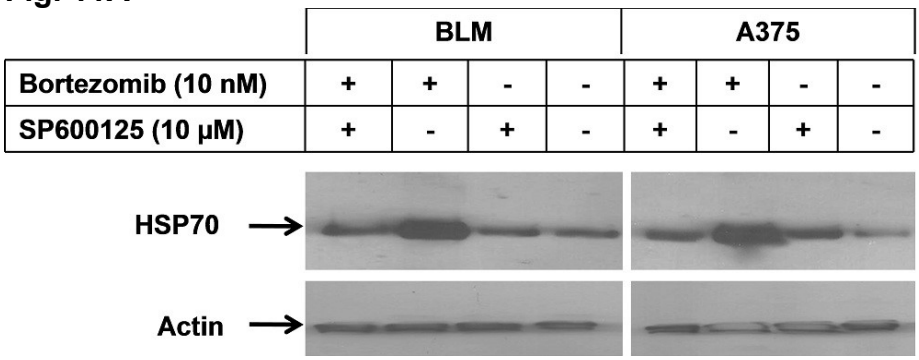

Fig.11A. Western blot demonstrates the inhibition of bortezomib-induced expression of HSP70 in response to pre-treatment of melanoma cells with the inhibitor of JNK pathway. β-actin was used as internal control for loading and transfer.

The inhibition of caspase-3 showed a remarkable inhibition of bortezomib-induced cell death of both melanoma cells A375 (Fig. 11B) and BLM (Fig.11B), whereas the pre-treatment of the same cells with the inhibitors of ASK, JNK, p38 or with the siRNAs of Ets-1, Mcl-1, and HSP70 was found to enhance bortezomib-induced cell death of melanoma cells.

Fig. 11B

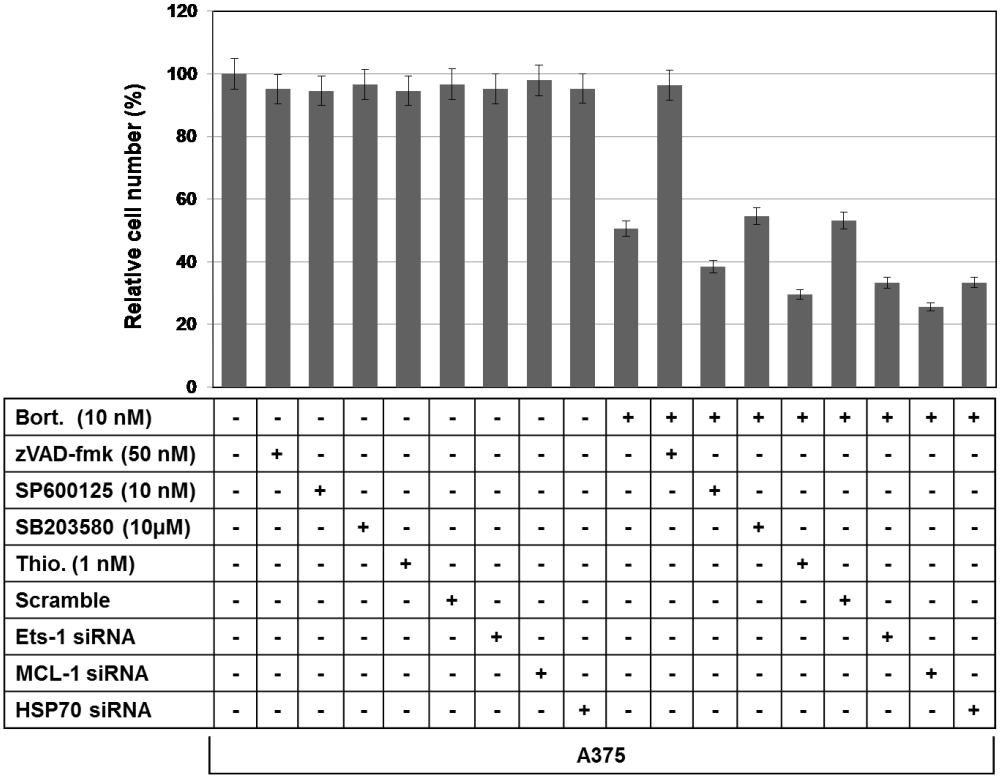

Fig. 11B. MTT assay demonstrates the inhibition of bortezomib-induced cell death in response to pre-treatment of melanoma cell line A375 with inhibitor of caspase-3 (zVAD-fmk), whereas the inhibition ASK1, JNK, p38 or knockdown of Ets-1, Mcl-1 or HSP70 enhanced bortezomib-induced cell death.

Fig. 11C

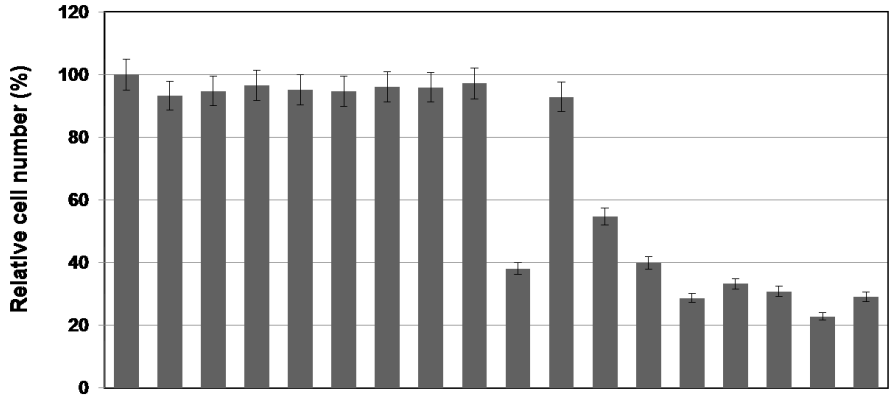

Bort. (10 nM)	-	-	-	-	-	-	-	-	-	+	+	+	+	+	+	+	+	+
zVAD-fmk (50 nM)	-	+	-	-	-	-	-	-	-	-	+	-	-	-	-	-	-	-
SP600125 (10 nM)	-	-	+	-	-	-	-	-	-	-	-	+	-	-	-	-	-	-
SB203580 (10μM)	-	-	-	+	-	-	-	-	-	-	-	-	+	-	-	-	-	-
Thio. (1 nM)	-	-	-	-	+	-	-	-	-	-	-	-	-	+	-	-	-	-
Scramble	-	-	-	-	-	+	-	-	-	-	-	-	-	-	+	-	-	-
Ets-1 siRNA	-	-	-	-	-	-	+	-	-	-	-	-	-	-	-	+	-	-
MCL-1 siRNA	-	-	-	-	-	-	-	+	-	-	-	-	-	-	-	-	+	-
HSP70 siRNA	-	-	-	-	-	-	-	-	+	-	-	-	-	-	-	-	-	+
	BLM																	

Fig. 11C. MTT assay demonstrates the inhibition of bortezomib-induced cell death in response to pre-treatment of melanoma cell line BLM with zVAD-fmk, whereas the inhibition of ASK1, JNK, p38 or knockdown of Ets-1, Mcl-1 or HSP70 enhanced bortezomib-induced cell death.

However, the enhancement of bortezomib-induced cell death was more pronounced in response to the knockdown of HSP70 protein (Fig. 11B and 11C).

Taken together, these data provide evidence for the involvement of mitochondrial-dependent mechanisms in the regulation of bortezomib-induced apoptosis of melanoma cells.

5. Discussion

In the present study, the anticancer agents bortezomib, carmustine and dacarbazine were examined for their killing efficiency, in an *in vitro* model, using established melanoma derived cell lines. Although the anticancer agents show a variable killing efficiency in melanoma cells, their application in melanoma treatment is of great interest. Also, the analysis of these anticancer agents in double knockout mouse embryonic fibroblasts provides evidence for the involvement of different signaling pathways in the regulation of their cytotoxic effects. The most thoroughly analyzed anticancer agent in this study was bortezomib. It is an approved anticancer agent that belongs to the group of Proteasome inhibitors (Pis) (Adams et al, 1999). It is an especially effective anticancer agent, with proven clinical success in the treatment of hematological cancers, like relapsed and/or refractory multiple myeloma (MM) and mantle cell lymphoma (MCL), even if it shows less promise in the therapy of solid tumors (Vink et al, 2006; Berenson et al., 2007, Berkers et al., 2012). A prolonged treatment with bortezomib is associated with the appearance of undesired side effects, as well as the development of drug-resistance and toxicity, which is a common side effect and problem with cytotoxic drugs (Berkers et al., 2012). Bortezomib has shown to be more effective when combined with other anti-cancer drugs or inhibitors (Vink et al, 2006).

Bortezomib (Velcade®, PS-341) is a dipeptide boronic acid analogue which inhibits the proteasome pathway reversibly by binding to the β-5 subunit of the 26S proteasome-complex. (Adams et al., 1998 and 1999; Frankel et al., 2000). Proteasomes are accepted as crucial regulators of cellular processes associated with different functions. Accordingly, *in vitro* trials show that an exposure to bortezomib leads to the stabilization and accumulation of several intracellular proteins that are usually targets for the ubiquitin system. These proteins include cyclin-dependent kinase inhibitors (e.g. p21) and pro-apoptotic Bik/NBK, whose stabilization promotes cell cycle arrest in the G2-M phase, and subsequently apoptosis (Zhu et al., 2005; Vink et al, 2006; Hong et al., 2012, Yerlikaya et al., 2012).

Proteasome inhibitors mediate their effects through the inhibition of protein degradation, particularly proteins that are crucial to cancer development and progression. The validity of proteasome inhibitors as anti-cancer agents relies on their efficiency to disturbs the balance between pro-apoptotic and anti-apoptotic proteins

within a cell, tipping the scales towards the pro-apoptotic side and thus leading to enhanced apoptosis (Adams, 2002b). Beside triggering apoptosis through indirect means as explained above, there are studies that show that proteasome inhibitors can trigger apoptosis through interaction with specific proteins like inhibitory protein Iκ. Proteasome inhibitors prevent the degradation of inhibitory protein Iκ, which remains bound to nuclear factor κB, preventing its nuclear translocation and consecutively the transcription of survival-associated genes (Wang et al., 1996, Vink et al, 2006). The nuclear transcription factor NF- κB is an essential factor that is associated with the promotion of cell survival and proliferation, as well as with tumor resistance to chemotherapy *via* the suppression of the inhibitor of apoptosis XIAP. It has also been shown that the nuclear factor κB pathway is frequently overactive in different cancer cells and thus keeps the cells from submitting to chemotherapy or otherwise induced apoptosis (Vink et al., 2006). Thus, the downregulation, or inhibition of the components of factor NF- κB pathway may promote apoptosis in many common cancer cells, when bortezomib is used in concert with other chemotherapeutic agents or radiotherapy (Cusack et al., 2001; Russo et al., 2001). Studies using head and neck squamous cell carcinoma show that bortezomib can induce apoptosis by leading to autophagosome formation, but requires the existence and function of certain key proteins to be effective (Li and Johnson, 2012). JNK is such a key protein. Bortezomib induced apoptosis in head and neck squamous cell carcinoma relies on the phosphorylation of JNK enzymes and JNK-dependent phosphorylation of Bcl-2. A deactivation or impairment of the JNK enzymes causes a direct impairment of bortezomib induced apoptosis *via* autophagosome formation, because it is assumed that the JNK enzymes are crucial for the regulation of autophagosome formation (Li and Johnson, 2011).

Like with many cytotoxic agents, the most frequent adverse effects that are associated with bortezomib treatment are plentiful and are of neurological, hematologic and gastrointestinal nature. Also, severe adverse effects, such as a fatal liver failure has been reported (Cornelis et al., 2012). The neuropathy presents with painful sensory sensations of the distal extremities, hypoesthesia or numbness (Corthals et al., 2011; Beijiers et al., 2012). Autonomic dysfunctions are suffered by ~10% of the treated patients, whereas motoric impairments are not a common side effect of bortezomib treatments. In up to 75% of patients receiving bortezomib symptoms are completely reversible within a median follow-up of six months (Beijiers et al., 2012). The

bortezomib induced peripheral neuropathy is considered a dose-limiting side effect, is hard to treat and has a direct impact on the patient's quality of life (Corthals et al., 2011). Most symptoms show to be completely reversibly but require a discontinuation of treatment or dose reduction, which is a major concern in treatment of malign diseases (Corthals et al., 2011). Recent studies explore further ways to reduce bortezomib induces neuropathy by modifying treatment schemes, or by adding neuroprotective substances (Beijiers et al., 2012).

Carmustine, (1,3-Bis(2-chloroethyl)-1-nitrosourea), is a nitrosurea alkylating agent, and its cytotoxic effect leads to DNA damage, in the form of cytosine-guanine-interstrand-DNA-crosslinks, which force a stop to DNA replication, as well as leading to single- and double-strand-DNA-breaks, which again are in itself strong inducers of apoptosis or necrosis (Gerson, 2002; Li et al., 2015). Studies have shown that certain cancer cell lines have an escape mechanism to carmustine-induced DNA damage in the form of a DNA repair enzyme called O6-alkylguanine-DNA-alkyltransferase (AGT), drastically decreasing carmustine therapy effectiveness (Apisarnthanarax et al., 2012). O6-benzylguanine can increase the effectiveness of carmustine therapy by canceling out the DNA repair mechanism provided by AGT. O6-benzylguanine is an AGT substrate which leads to an irreversible inactivation of AGT. First trials with cutaneous T-Cell Lymphoma (CTCL) documented an increase in therapy effectiveness, in a simultaneous carmustine/O6-benzylguanine therapy (Apisarnthanarax et al., 2012). Carmustine is a part of several therapy regimens, especially in those aimed at lymphoma, malignant melanoma, cerebral metastases and certain brain tumors like astrocytoma WHO IV°, also known as glioblastoma multiforme (Li and McClay, 2002; Parney et al., 2005; Bessell et al., 2004; Li et al., 2015). Carmustine displays a high degree of lipophilia and thus is able to traverse the blood brain barrier, making it especially useful in the treatment of cerebral metastases or primary brain cancers (Li et al., 2015). A locally applied form of carmustine, in the form of carmustine wafers, has proven itself equally effective (Bock et al., 2010). These wafers are implanted surgically into the space previously inhabited by the excised brain tumor. In combination with radiotherapy patients show a meaningful improvement in survival, considering a patient collective with newly diagnosed glioblastoma multiforme or recurrent glioblastoma multiforme (Bock et al., 2010; Chowdhary et al., 2015). Patients treated systemically with carmustine suffer from various adverse effects, ranging from pulmonary infiltrates (especially interstitial infiltrates), veno-occlusive disease of the liver, anemia as a result

of myelotoxicity and general gastrointestinal adverse effects accompanied by nausea and vomiting (van der Wall et al., 1995). Surgical site infections were seen to be the most prominent adverse effect leading to removal of the intracranial located carmustine wafers. Other adverse effects were seizures, haematoma, brain necrosis or development of hydrocephalus (Chowdhary et al., 2015).

Dacarbazine (5-(3,3-Dimethyl-1-triazenyl) imidazole-4-carboxamide) is a United States Food and Drug Administration approved anticancer agent and belongs to the group of alkylating agents (Lev et al., 2003). Dacarbazine is an effective anticancer agent for the treatment of malignant melanoma and Hodgkin Lymphoma, but especially in cases of advanced malign melanoma the response rates are disappointingly low with just up to 25% and often short lived (Canellos et al., 1992; Middleton et al., 2000b; Lev et al., 2003; Mouawad et al., 2010). Dacarbazine is part of the modern treatment regime for Hodgkin's lymphoma called ABVD. The ABVD regime consists of the agents: adriamycin, bleomycin, vinblastine, dacarbazine and is perceived as a standard treatment for Hodgkin's lymphoma (Canellos et al., 1992). This, still viable therapy regime, replaced the previous regime due to reduced adverse effects at equal effectiveness in the low-risk patient population (Canellos et al., 1992). As with bortezomib and carmustine, dacarbazine leads to numerous minor adverse effects like nausea and vomiting which are manageable *via* symptomatic therapy (Middleton et al., 2000a). Dacarbazine can induce a myelodepression, leading to a reduced cell count of all three hematopoietic cell lines, associated with predictable consequences like anemia, bleeding disorder and susceptibility to infections (Middleton et al., 2000a).

Thus, based on the obtained data of this study, the analysis of the anticancer agents in the melanoma model as well as the double knock out mouse embryonic fibroblasts (MEF) may help to develop an optimal management protocol for the treatment of metastatic melanoma.

The studies of recent years have shown the profound involvement of the endoplasmic reticulum (ER) stress and the mitochondrial dysregulation in apoptosis, thus making both pathways prime targets for anticancer agents, to increase therapy efficiency. A targeted activation of ER stress and mitochondrial dysregulation-dependent pathways may offer considerable benefit in the treatment of especially resistant cancer types.

As widely demonstrated, the activation of ER and mitochondrial-associated pathways in response to gene transfer of apoptotic mediators such as Noxa, APR-1, and APR-2 triggers apoptosis in melanoma cell lines (Hassan et al., 2008; Selimovic et al., 2011;

2012). The role of ER stress in the modulation of anticancer agents such as taxol and CH11-induced apoptosis has reported in several studies (Selimovic et al., 2008; Cetindere et al., 2010). Thus, based on the data of this study, the modulation of both ER stress and mitochondrial dysregulation-associated pathways may be a reliable therapeutic target for melanoma treatment. In addition to the emerging evidence, this study suggests an essential role of the mitochondrial pathways in the modulation of anti-cancer-induced apoptosis. The role of ER-stress and mitochondrial pathways in modulation of autophagy has been suggested (Park et al., 2008; Oh and Lim, 2009; Periyasamy-Thandavan et al., 2010). Autophagy has shown, on the one hand to promote cell survival by counteracting the accumulation of unfolded proteins, but on the other hand participates in ER stress-induced cell death (Buytaert et al., 2006; Heath-Engel et al., 2008; Kawaguchi et al., 2011).

To elucidate the mechanism of bortezomib-induced autophagy, part of the study focused on the role of ER stress-associated pathways, which have been shown previously to be activated by proteasome inhibitors (Mozos et al., 2011; Kawaguchi et al., 2011). In addition to the increase of intracellular Ca^{2+} release, the exposure of melanoma cells to bortezomib was associated with phosphorylation/activation of IRE1α enzymes and the expression of ASK1, p38, ATF-2/Ets-1 and Mcl-1 proteins and pathways, which are associated or even resulting from induction of ER stress (Hassan et al., 2008; Selimovic et al., 2011; 2012). The increase of intracellular Ca^{2+}-level is a marker for ER stress and is an important regulator of protein activity as well (Buytaert et al., 2006; Heath-Engel et al., 2008; Kawaguchi et al., 2011). The bortezomib-induced autophagosome formation hast been observed in cervical cancer as well as in head and neck sqamous cell carinoma cells (Li and Johnson, 2011; Laussmann et al., 2011). Autophagy-induced pro-survival has been shown for multiple cancer cells, among them prostate, head and neck squamous cell carcinoma, colon carcinoma cells (Li and Johnson, 2011; Shen and Codogno, 2012; Miranda et al., 2012). Contrary to these findings, there are reports that indicate that autophagy induces cell death in certain other cell types, like mouse embryonic fibroblasts (MEFs), human umbilical vein Endothelial Cells and multiple myeloma cells (Wang et al., 2008; Maclean et al., 2008; Csordas et al., 2011; Li and Johnson, 2011; Michallet et al., 2011; Zeng et al., 2012).

This diametrically opposed effect shows that a treatment with bortezomib can either increase or decrease apoptosis, depending on the cell type, making treatment-projections less reliable.

It hast become apparent that available knowledge about bortezomib-induced effects in cancer cells, especially on a molecular level is not complete. Although the molecular mechanism underlying bortezomib-induced autophagy, so far, is not fully determined, this study described for the first time, the ability of bortezomib to trigger both apoptosis and autophagosome formation in melanoma cells, and addressed the molecular mechanisms, whereby bortezomib triggers both apoptosis and autophagy. Bortezomib-induced apoptosis of melanoma cells is mediated, primarily, by a mitochondrial-dependent pathway. The activation of the mitochondrial pathway results from bortezomib-induced Noxa expression which in turn, triggers the loss of mitochondrial membrane potential ($\Delta\Psi m$). The loss of $\Delta\Psi m$ leads to the accumulation of reactive oxygen species (ROS), as well as to the release of two staunch promoters of apoptosis, namely Cytochrome c (Cyt. c) and apoptosis inducing factor (AIF). The accumulation of Cytochrome c in the cytoplasm leads to an activation of caspase-9. This in turn starts the caspase cascade, leading to the activation of caspase-3 by either caspase-9 and/or AIF, leading to PARP cleavage, an evidence for bortezomib-induced apoptosis in melanoma cells. On the other hand, the accumulation of ROS in response to the loss of $\Delta\Psi m$ seems to be involved in the activation of apoptosis signal regulating kinase 1 (ASK1) that subsequently mediates the activation of both JNK/AP-1/HSF1/HSP70 and p38/Ets-1/ATF-2/Mcl-1, which promote cell survival or autophagy, respectively. Furthermore, the localization of bortezomib-induced Noxa protein at the ER leads to increased intracellular Ca^{2+} release, an evidence for ER stress. Further evidence for ER stress is the enhancement of the phosphorylation of inositol requiring enzyme 1α (IRE1α), which is involved in the activation of ASK1. ASK1 on the other hand, has been shown to potentiate the activation of both afore mentioned pathways: JNK/AP-1/HSF1/HSP70 and p38/Ets-1/ATF-2/Mcl-1.

The functional analysis of bortezomib-induced effects in inhibitory experiments demonstrated that bortezomib-induced ER stress leads to the activation of IRE1α-ASK1-JNK-AP-1/HSF1-HSP70 pathway and subsequently, in part, to the inhibition of bortezomib-induced apoptosis. Additionally, it was shown, that bortezomib-induced activation of the IRE1α-p38-Ets-1/ATF-2-Mcl-1 pathway leads to autophagosome formation in melanoma cells. Unlike the inhibition of bortezomib-induced apoptosis which potentiates bortezomib-induced autophagy, the inhibition of bortezomib-induced activation of both IRE1α-ASK1-JNK-AP-1/HSF1-HSP70 and IRE1α-p38-Ets-1/ATF-2-Mcl-1 pathways enhances bortezomib-induced apoptosis of melanoma cells.

Currently, targeting the autophagy pathway is considered a novel means to augment tumor therapy. Accordingly, our data obtained from inhibitory experiments demonstrated that the inhibition of the IRE1α-p38-Ets-1/ATF-2-Mcl-1 pathway is involved in the modulation of bortezomib-induced autophagosome formation. Autophagy has shown both pro-survival and cyto-protective functions in different cancer cell types in response to ER stress-induced apoptosis (Davids et al., 2009; Wilson et al., 2011). According to several studies revealing the role of bortezomib-induced HSP70 in the inhibition of bortezomib-induced apoptosis, the inhibition of bortezomib-induced anti-apoptotic effects by inhibition of the ASK1/ JNK pathway or by knockdown of HSP70 will potentiate the efficacy of bortezomib in melanoma treatment (Yerlikaya et al., 2010).

Based on the data of the present study it has become clear that the treatment of melanoma cells with bortezomib can be outlined in a proposed model (Fig. 12).

This model demonstrates that bortezomib induces different responses that seem diametrically opposed. One of these responses is a desired response and deals with melanoma cell death and is mediated by both mitochondrial and non-mitochondrial dependent mechanisms. In contrast the other response, an undesired response that leads to cyto-protective effects / cell survival, is also dependent on mitochondrial and non-mitochondrial mechanisms. Additionally, this model addresses the main pathways, which are involved in the regulation of bortezomib induced apoptosis- and autophagosome formation and their divergent and common sites. The combination of autophagosome formation inhibitors or / and heat shock protein inhibitors may enhance the cytotoxic effect of bortezomib and reduce side effects.

The detailed information of the proposed model presents only a part of the mechanisms which may play a central role in the regulation of apoptosis and autophagy. Further study based on the addressed mechanisms may help to identify additional pathways and thus lead to new therapeutic approaches.

Fig. 12

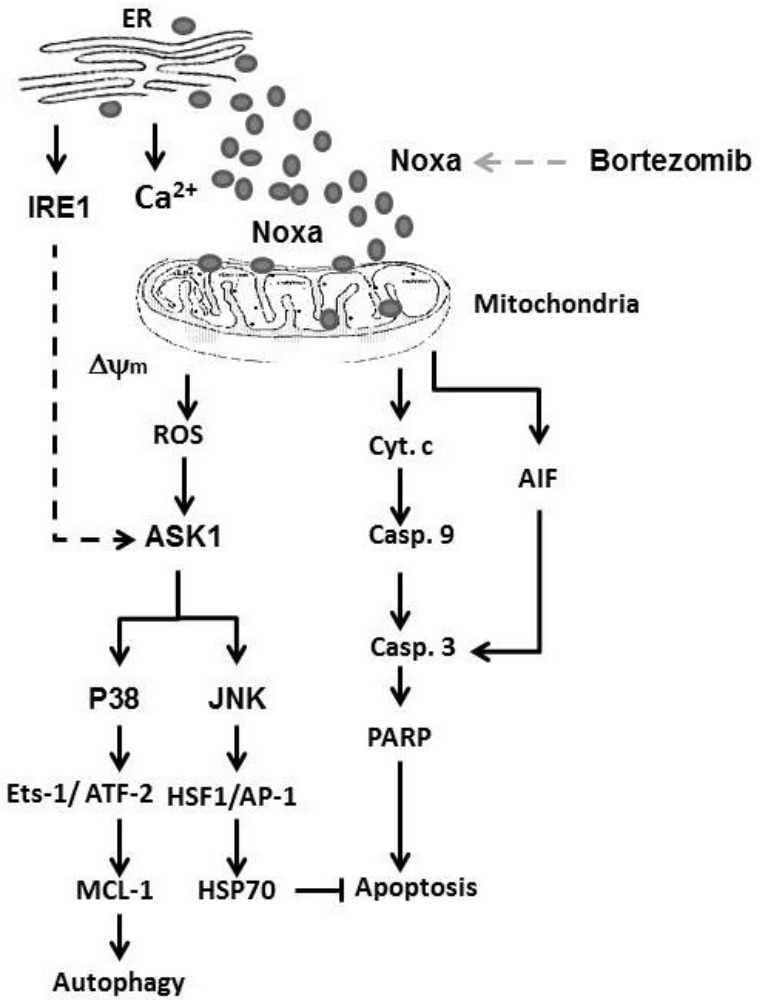

Fig. 12 Proposed model for bortezomib-induced autophagy and apoptosis in melanoma cells. The overexpression of Noxa protein in response to the exposure of melanoma cells to bortezomib. Noxa effects the activation of both ER stress and mitochondrial dysregulation-dependent pathways. The activation of the pathways is associated with the promotion of different cellular mechanisms. One of these pathways, namely Cyto. c-caspase-9/AIF-caspase-3-PARP is a mitochondrial-dependent pathway and is involved in the regulation of bortezomib-induced apoptosis. Whereas, another pathway, namely IRE1α-ASK1-p38-Ets-1/ATF-2-Mcl-1, is an ER-stress-dependent pathway, and is involved in the regulation of bortezomib-induced autophagosome formation. In addition, a second ER-stress-associated pathway, namely IRE1α-ASK1-JNK-AP-1/HSF-1-HSP70, affects the inhibition of bortezomib-induced apoptosis. Two other observed mitochondrial-related pathways, which are activated through mitochondrial dysregulation-associated ROS accumulation, namely ASK1-p38-Ets-1/ATF-2-Mcl-1; and ASK1-JNK-AP-1/HSF-1-HSP70, are involved in the regulation of bortezomib-induced autophagosome formation, and inhibition of bortezomib-induced apoptosis, respectively.

6. Conclusion

Metastatic melanoma is known as one of the biologically most aggressive and chemo resistant cancers known. The treatment of metastatic melanoma is of importance, due to its significantly increasing incidence over the last decades, especially in Western cultures. The emergence of this malignancy results from the accumulation of genetic and/or epigenetic events leading to the activation of various oncogenes giving the altered melanocytes a growth advantage over normal melanocytes. Available therapeutic approaches for patients with metastatic melanoma are of limited benefit and commonly associated with a multitude of adverse effects. Generally, both endoplasmic reticulum (ER) stress and mitochondrial dysregulation are potential and potent therapeutic targets of anticancer agents including bortezomib. Bortezomib is a small molecule that can specifically and selectively inhibit proteasomes, leading to the induction of both pro-and anti-apoptotic proteins including Noxa and Mcl-1 and thereby leads to the enhancement of both desired and undesired effects in treated patients. Therefore, the functional analysis of anticancer agents-induced effects in melanoma cells may help to improve their therapeutic efficiency for the treatment of metastatic melanoma.

The aim of the present study was to assess the inhibitory effect of different anticancer agents on cell growth of melanoma cells and to characterize, in detail, the molecular mechanisms whereby bortezomib triggers apoptosis and autophagosome formation in melanoma cells.

Several cell biological and molecular biological techniques and procedures were used for the analysis of anticancer agents-induced effects in melanoma cells.

In the present study the treatment of melanoma cells with bortezomib, carmustine, dacarbazine was found to induce apoptosis in melanoma cells. However, the in detail function analysis of bortezomib revealed an induction of apoptosis in melanoma cells conjoint with the upregulation of Noxa, Mcl-1, and HSP70 proteins and the cleavage of LC3 and autophagosome formation. In addition, bortezomib induced ER-stress as evidenced by the increase of intracellular Ca^{2+} release. Furthermore, bortezomib enhanced the phosphorylation of inositol-requiring transmembrane kinase and endonuclease 1α (IRE1α), apoptosis signal-regulating kinase 1(ASK1), c-jun-N-terminal kinase (JNK) and p38, as well as the activation of the transcription factors AP-

1, ATF-2, Ets-1, and HSF1. Whereas bortezomib-induced mitochondrial dysregulation was associated with the accumulation of reactive oxygen species (ROS), the release of both apoptosis inducing factor (AIF) and Cytochrome c, the activation of caspase-9 and caspase-3, and cleavage of Poly (ADP-ribose) polymerase (PARP). The pre-treatment of melanoma cells with the inhibitor of caspase-3 (Z-DEVD-FMK) was found to block bortezomib-induced apoptosis that subsequently led to the increase of autophagosome formation. In contrast, the inhibition of ASK1 abrogated bortezomib-induced autophagosome formation and increased inducted apoptosis. The inhibition of JNK, or HSP70 showed an increased induction of apoptosis without influencing bortezomib-induced autophagosome formation. Thus, based on inhibitory experiments, the exposure of melanoma cells to bortezomib triggers the activation of both ER-stress-associated pathways, namely IRE1α-ASK1-p38-ATF-2/ets-1-Mcl-1 and IRE1α-ASK1-JNK-AP-1/HSF1-HSP70 as well as mitochondrial dysregulation-associated pathways, namely ROS-ASK1-JNK-AP-1/HSF1-70 and AIF-caspase-3-PARP and Cyt.c-caspase-9-caspase-3-PARP. This study demonstrates, for the first time, the molecular mechanisms, whereby bortezomib triggers both apoptosis and autophagosome formation in melanoma cells.

In the past years there have been only few revolutionary new anticancer drugs that are highly effective in cases of metastatic melanoma. Therefore, it could be promising to concentrate on enhancing effective existing anticancer agents, by using recent years' research and insight into their molecular mechanisms to increase therapeutic efficiency of existing anticancer agents instead of creating completely new agents, which is an extremely time- and resource-consuming process without guaranteed successful outcome.

The results of this study show that future melanoma therapies may benefit from the above mentioned enhanced drug therapy by combining the proteasome inhibitor bortezomib with an autophagosome inhibitor. This novel therapeutic concept could lead to increase bortezomib-induced apoptosis in melanoma cells and thus increase patient outcome in cases of advanced metastatic melanoma.

Clinical trials are essential to confirm whether the *in vitro* results of this study can be applied to *in vivo* clinical therapy settings.

7. References

Unless stated otherwise, all references were taken from:
http://www.ncbi.nlm.nih.gov/pubmed

1. Adams JM, Cory S. Apoptosomes: engines for caspase activation. Curr Opin Cell Biol. 2002; 14:715-20.

2. Adams J, Behnke M, Chen S, Cruickshank AA, Dick LR, Grenier L, Klunder JM, Ma YT, Plamondon L, Stein RL. Potent and selective inhibitors of the proteasome: dipeptidyl boronic acids. Bioorg Med Chem Lett. 1998; 8:333-8.

3. Adams J, Palombella VJ, Sausville EA, Johnson J, Destree A, Lazarus DD, Maas J, Pien CS, Prakash S, Elliott PJ. Proteasome inhibitors: a novel class of potent and effective antitumor agents. Cancer Res. 1999; 59:2615-22.

4. Adams J. Development of the proteasome inhibitor PS-341. Oncologist. 2002; 7:9-16.

5. Adams J. Proteasome inhibitors as new anticancer drugs. Curr Opin Oncol. 2002; 14:628-34.

6. Anvekar RA, Asciolla JJ, Missert DJ, Chipuk JE. Born to be alive: a role for the BCL-2 family in melanoma tumor cell survival, apoptosis, and treatment. Front Oncol. 2011; 1:1-13.

7. Apisarnthanarax N, Wood GS, Stevens SR, Carlson S, Chan DV, Liu L, Szabo SK, Fu P, Gilliam AC, Gerson SL, Remick SC, Cooper KD. Phase I Clinical Trial of O6-Benzylguanine and Topical Carmustine in the Treatment of Cutaneous T-Cell Lymphoma, Mycosis Fungoides Type. Arch Dermatol. 2012; 148:613-20.

8. Arur S, Uche UE, Rezaul K, Fong M, Scranton V, Cowan AE, Mohler W, Han DK. Annexin I is an endogenous ligand that mediates apoptotic cell engulfment. Dev Cell. 2003; 4:587-98.

9. Ashkenazi A, Dixit VM. Death receptors: signaling and modulation. Science. 1998; 281:1305-8.

10. Beijers AJ, Jongen JL, Vreugdenhil G. Chemotherapy-induced neurotoxicity: the value of neuroprotective strategies. Neth J Med. 2012; 70:18-25.

11. Berenson JR, Matous J, Swift RA, Mapes R, Morrison B, Yeh HS. A phase I/II study of arsenic trioxide/bortezomib/ascorbic acid combination therapy for the treatment of relapsed or refractory multiple myeloma. Clin Cancer Res. 2007; 13:1762-8.

12. Berkers CR, Leestemaker Y, Schuurman KG, Ruggeri B, Jones-Bolin S, Williams M, Ovaa H. Probing the specificity and activity profiles of the proteasome inhibitors bortezomib and delanzomib. Mol Pharm. 2012; 9:1126-35.

13. Bessell EM, Graus F, Lopez-Guillermo A, Lewis SA, Villa S, Verger E, Petit J. Primary non-Hodgkin's lymphoma of the CNS treated with CHOD/BVAM or BVAM chemotherapy before radiotherapy: long-term survival and prognostic factors. Int J Radiat Oncol Biol Phys. 2004; 59:501-8.

14. Bock HC, Puchner MJ, Lohmann F, Schütze M, Koll S, Ketter R, Buchalla R, Rainov N, Kantelhardt SR, Rohde V, Giese A. First-line treatment of malignant glioma with carmustine implants followed by concomitant radiochemotherapy: a multicenter experience. Neurosurg Rev. 2010; 33:441-9.

15. Bortner CD, Oldenburg NB, Cidlowski JA. The role of DNA fragmentation in apoptosis. Trends Cell Biol. 1995; 5:21-6.

16. Bots M, Medema JP. Granzymes at a glance. J Cell Sci. 2006; 119(Pt 24):5011-4.

17. Bratton DL, Fadok VA, Richter DA, Kailey JM, Guthrie LA, Henson PM. Appearance of phosphatidylserine on apoptotic cells requires calcium-mediated nonspecific flip-flop and is enhanced by loss of the aminophospholipid translocase. J Biol Chem. 1997; 272:26159-65.

18. Buytaert E, Callewaert G, Vandenheede JR, Agostinis P. Deficiency in apoptotic effectors Bax and Bak reveals an autophagic cell death pathway initiated by photodamage to the endoplasmic reticulum. Autophagy. 2006; 2:238-40.

19. Canellos GP, Anderson JR, Propert KJ, Nissen N, Cooper MR, Henderson ES, Green MR, Gottlieb A, Peterson BA. Chemotherapy of advanced Hodgkin's disease with MOPP, ABVD, or MOPP alternating with ABVD. N Engl J Med. 1992; 327:1478-84.

20. Cao G, Pei W, Lan J, Stetler RA, Luo Y, Nagayama T, Graham SH, Yin XM, Simon RP, Chen J. Caspase-activated DNase/DNA fragmentation factor 40 mediates apoptotic DNA fragmentation in transient cerebral ischemia and in neuronal cultures. J Neurosci. 2001; 1;21(13):4678-90.

21. Cetindere T, Nambiar S, Santourlidis S, Essmann F, Hassan M. Induction of indoleamine 2, 3-dioxygenase by death receptor activation contributes to apoptosis of melanoma cells via mitochondrial damage-dependent ROS accumulation. Cell Signal. 2010; 22:197-211.

22. Chipuk JE, Fisher JC, Dillon CP, Kriwacki RW, Kuwana T, Green DR. Mechanism of apoptosis induction by inhibition of the anti-apoptotic BCL-2 proteins. Proc Natl Acad Sci U S A. 2008; 105:20327-32.

23. Chipuk JE, Moldoveanu T, Llambi F, Parsons MJ, Green DR. The BCL-2 family reunion. Mol Cell. 2010; 12;37(3):299-310.

24. Chowdhary SA, Ryken T, Newton HB. Survival outcomes and safety of carmustine wafers in the treatment of high-grade gliomas: a meta-analysis. J Neurooncol. 2015; 122(2):367-82.

25. Cornelis T, Beckers EA, Driessen AL, van der Sande FM, Koek GH. Bortezomib-associated fatal liver failure in a haemodialysis patient with multiple myeloma. Clin Toxicol (Phila). 2012; 50:444-5.

26. Corthals SL, Kuiper R, Johnson DC, Sonneveld P, Hajek R, van der Holt B, Magrangeas F, Goldschmidt H, Morgan GJ, Avet-Loiseau H. Genetic factors underlying the risk of bortezomib induced peripheral neuropathy in multiple myeloma patients. Haematologica. 2011; 96:1728-32.

27. Csordas A, Kreutmayer S, Ploner C, Braun PR, Karlas A, Backovic A, Wick G, Bernhard D. Cigarette smoke extract induces prolonged endoplasmic reticulum stress and autophagic cell death in human umbilical vein endothelial cells. Cardiovasc Res. 2011; 92:141-8.

28. Cui Z, Song E, Hu DN, Chen M, Rosen R, McCormick SA. Butein-Induces Apoptosis in Human Uveal Melanoma Cells through Mitochondrial Apoptosis Pathway. Curr Eye Res. 2012; 37:730-9.

29. Cusack JC Jr, Liu R, Houston M, Abendroth K, Elliott PJ, Adams J, Baldwin AS Jr. Enhanced chemosensitivity to CPT-11 with proteasome inhibitor PS-341: implications for systemic nuclear factor-kappaB inhibition. Cancer Res. 2001; 61:3535-40.

30. Danial NN, Korsmeyer SJ. Cell death: critical control points. Cell. 2004; 23;116(2):205-19.

31. Davids LM, Kleemann B, Cooper S, Kidson SH. Melanomas display increased cytoprotection to hypericin-mediated cytotoxicity through the induction of autophagy. Cell Biol Int. 2009; 33:1065-72.

32. Deng R, Hao J, Han W, Ni Y, Huang X, Hu Q. Gelsolin regulates proliferation, apoptosis, migration and invasion in human oral carcinoma cells. Oncol. Lett. 2015; 9(5):2129-2134.

33. Devito N, Yu M, Chen R, Pan E. Retrospective study of patients with brain metastases from melanoma receiving concurrent whole-brain radiation and temozolomide. Anticancer Res. 2011; 31:4537-43.

34. Du C, Fang M, Li Y, Li L, Wang X. Smac, a mitochondrial protein that promotes cytochrome c-dependent caspase activation by eliminating IAP inhibition. Cell. 2000; 102:33-42.

35. Eikenberry S, Thalhauser C, Kuang Y. Tumor-immune interaction, surgical treatment, and cancer recurrence in a mathematical model of melanoma.PLoS Comput Biol. 2009; 5:e1000362.

36. Elder DE, Gimotty PA, Guerry D. Cutaneous melanoma: estimating survival and recurrence risk based on histopathological features. Dermatol Ther. 2005; 15:369-85.

37. El-Khattouti A, Selimovic D, Haikel Y, Hassan M. Crosstalk between apoptosis and autophagy: molecular mechanisms and therapeutic strategies in cancer. J Cell Death. 2013; 18;6:37-55.

38. Elmore S. Apoptosis: a review of programmed cell death. Toxicol Pathol. 2007; 35:495-516.

39. Enari M, Sakahira H, Yokoyama H, Okawa K, Iwamatsu A, Nagata S. A caspase-activated DNase that degrades DNA during apoptosis, and its inhibitor ICAD. Nature. 1998; 391:43-50.

40. Erwig LP, Henson PM. Clearance of apoptotic cells by phagocytes. Cell Death Differ. 2008; 15(2):243-50.

41. Fadok VA, Chimini G. The phagocytosis of apoptotic cells. Semin Immunol. 2001; 13:365-72.

42. Fadok VA, Bratton DL, Frasch SC, Warner ML, Henson PM. The role of phosphatidylserine in recognition of apoptotic cells by phagocytes. Cell Death Differ. 1998; 5(7):551-62.

43. Ferraro-Peyret C, Quemeneur L, Flacher M, Revillard JP, Genestier L. Caspase-independent phosphatidylserine exposure during apoptosis of primary T lymphocytes. J Immunol. 2002; 169:4805-10.

44. Fischer U, Jänicke RU, Schulze-Osthoff K. Many cuts to ruin: a comprehensive update of caspase substrates. Cell Death Differ. 2003; 10:76-100.

45. Frankel A, Man S, Elliott P, Adams J, Kerbel RS. Lack of multicellular drug resistance observed in human ovarian and prostate carcinoma treated with the proteasome inhibitor PS-341. Clin Cancer Res. 2000; 6:3719-28.

46. Gallenne T, Gautier F, Oliver L, Hervouet E, Noël B, Hickman JA, Geneste O, Cartron PF, Vallette FM, Manon S, Juin P. Bax activation by the BH3-only protein Puma promotes cell dependence on antiapoptotic Bcl-2 family members. J Cell Biol. 2009; 20;185(2):279-90.

47. Garbe C, Hauschild A, Volkenandt M, Schadendorf D, Stolz W, Reinhold U, Kortmann RD, Kettelhack C, Frerich B, Keilholz U, Dummer R, Sebastian G,

Tilgen W, Schuler G, Mackensen A, Kaufmann R. Evidence-based and interdisciplinary consensus-based German guidelines: systemic medical treatment of melanoma in the adjuvant and palliative setting. Melanoma Res. 2008; 18:152-60.

48. Garrido C, Kroemer G. Life's smile, death's grin: vital functions of apoptosis-executing proteins. Curr Opin Cell Biol. 2004; 16:639-46.

49. Gerson SL. Clinical relevance of MGMT in the treatment of cancer. J Clin Oncol. 2002; 20:2388-99.

50. Gray-Schopfer VC, Wellbrock C, Marais R. Melanoma biology and new targeted therapy. Nature. 2007; 445:851-7.

51. Gray-Schopfer VC, Karasarides M, Hayward R, Marais R. Tumor necrosis factor-alpha blocks apoptosis in melanoma cells when BRAF signaling is inhibited Cancer Res. 2007; 1;67(1):122-9.

52. Grimm S. Die Apoptose: Programmierter Zelltod. Chemie in unserer Zeit. 2003; 37:172–178. doi: 10.1002/ciuz.200300260 http://onlinelibrary.wiley.com/doi/10.1002/ciuz.200300260/abstract (13.01.2016)

53. Grossman D, Altieri DC. Drug resistance in melanoma: mechanisms, apoptosis, and new potential therapeutic targets. Cancer Metastasis Rev. 2001; 20:3-11.

54. Guicciardi ME, Gores GJ. Life and death by death receptors. FASEB J. 2009; 23(6):1625-37.

55. Ha JH, Shin JS, Yoon MK, Lee MS, He F, Bae KH, Yoon HS, Lee CK, Park SG, Muto Y, Chi SW. Dual-site interactions of p53 protein transactivation domain with anti-apoptotic Bcl-2 family proteins reveal a highly convergent mechanism of divergent p53 pathways. J Biol Chem. 2013; 8;288(10):7387-98.

56. Hassan M, Ghozlan H, Abdel-Kader O. Activation of RB/E2F signaling pathway is required for the modulation of hepatitis C virus core protein-induced cell growth in liver and non-liver cells. Cell Signal. 2004; 16(12):1375-85.

57. Hassan M, Ghozlan H, Abdel-Kader O. Activation of c-Jun NH2-terminal kinase (JNK) signaling pathway is essential for the stimulation of hepatitis C virus (HCV) non-structural protein 3 (NS3)-mediated cell growth. Virology. 2005a; 15;333(2):324-36.

58. Hassan M, Mirmohammadsadegh A, Selimovic D, Nambiar S, Tannapfel A, Hengge UR. Identification of functional genes during Fas-mediated apoptosis using a randomly fragmented cDNA library. Cell Mol Life Sci. 2005b; 62(17):2015-26.

59. Hassan M, Selimovic D, Ghozlan H, Abdel-Kader O. Induction of high-molecular-weight (HMW) tumor necrosis factor(TNF) alpha by hepatitis C virus (HCV) non-structural protein 3 (NS3) in liver cells is AP-1 and NF-kappaB-dependent activation. Cell Signal. 2007; 19(2):301-11.

60. Hassan M, Alaoui A, Feyen O, Mirmohammadsadegh A, Essmann F, Tannapfel A, Gulbins E, Schulze-Osthoff K, Hengge UR. The BH3-only member Noxa causes apoptosis in melanoma cells by multiple pathways. Oncogene. 2008; 27:4557-68. Erratum in Oncogene. 2011; 30:2086.

61. Hassan M, Feyen O, Grinstein E. Fas-induced apoptosis of renal cell carcinoma is mediated by apoptosis signal-regulating kinase 1 via mitochondrial damage-dependent caspase-8 activation. Cell Oncol. 2009; 31:437-56.

62. Heath-Engel HM, Chang NC, Shore GC. The endoplasmic reticulum in apoptosis and autophagy: role of the BCL-2 protein family. Oncogene. 2008; 27:6419-33.

63. Hegde R, Srinivasula SM, Datta P, Madesh M, Wassell R, Zhang Z, Cheong N, Nejmeh J, Fernandes-Alnemri T, Hoshino S, Alnemri ES. The polypeptide chain-releasing factor GSPT1/eRF3 is proteolytically processed into an IAP-binding protein. J Biol Chem. 2003; 3;278(40):38699-706

64. Hill MM, Adrain C, Duriez PJ, Creagh EM, Martin SJ. Analysis of the composition, assembly kinetics and activity of native Apaf-1 apoptosomes. EMBO J. 2004; 23:2134-45.

65. Hong YS, Hong SW, Kim SM, Jin DH, Shin JS, Yoon DH, Kim KP, Lee JL, Heo DS, Lee JS, Kim TW. Bortezomib induces G2-M arrest in human colon cancer cells through ROS-inducible phosphorylation of ATM-CHK1. Int J Oncol. 2012; 41:76-82.

66. Igney FH, Krammer PH. Death and anti-death: tumour resistance to apoptosis. Nat Rev Cancer. 2002a; 2:277-88.

67. Igney FH, Krammer PH. Immune escape of tumors: apoptosis resistance and tumor counterattack. J Leukoc Biol. 2002b; 71:907-20.

68. Jönsson PE, Agrup G, Arnbjörnsson E, Hafström L, Rorsman H.Treatment of malignant melanoma with dacarbazin (DTIC-DOME) with special reference to urinary excretion of 5-S-cysteinyldopa. Cancer. 1980; 45:245-8.

69. Joza N, Susin SA, Daugas E, Stanford WL, Cho SK, Li CY, Sasaki T, Elia AJ, Cheng HY, Ravagnan L, Ferri KF, Zamzami N, Wakeham A, Hakem R, Yoshida H, Kong YY, Mak TW, Zúñiga-Pflücker JC, Kroemer G, Penninger JM. Essential role of the mitochondrial apoptosis-inducing factor in programmed cell death. Nature. 2001; 410:549-54.

70. Kataoka T, Schröter M, Hahne M, Schneider P, Irmler M, Thome M, Froelich CJ, Tschopp J. FLIP prevents apoptosis induced by death receptors but not by perforin/granzyme B, chemotherapeutic drugs, and gamma irradiation. J Immunol. 1998; 161:3936-42.

71. Kawaguchi T, Miyazawa K, Moriya S, Ohtomo T, Che XF, Naito M, Itoh M, Tomoda A. Combined treatment with bortezomib plus bafilomycin A1 enhances the cytocidal effect and induces endoplasmic reticulum stress in U266 myeloma cells: crosstalk among proteasome, autophagy-lysosome and ER stress. Int J Oncol. 2011; 38:643-54.

72. Kerr JF, Wyllie AH, Currie AR. Apoptosis: a basic biological phenomenon with wide-ranging implications in tissue kinetics. Br J Cancer. 1972; 26:239-57.

73. Kim JW, Choi EJ, Joe CO. Activation of death-inducing signaling complex (DISC) by pro-apoptotic C-terminal fragment of RIP. Oncogene. 2000; 14;19(39):4491-9.

74. Kischkel FC, Hellbardt S, Behrmann I, Germer M, Pawlita M, Krammer PH, Peter ME. Cytotoxicity-dependent APO-1 (Fas/CD95)-associated proteins form a death-inducing signaling complex (DISC) with the receptor. EMBO J. 1995; 14:5579-88.

75. Korsmeyer SJ, Wei MC, Saito M, Weiler S, Oh KJ, Schlesinger PH. Pro-apoptotic cascade activates BID, which oligomerizes BAK or BAX into pores that result in the release of cytochrome c. Cell Death Differ. 200; 7:1166-73.

76. Kothakota S, Azuma T, Reinhard C, Klippel A, Tang J, Chu K, McGarry TJ, Kirschner MW, Koths K, Kwiatkowski DJ, Williams LT. Caspase-3-generated fragment of gelsolin: effector of morphological change in apoptosis. Science. 1997; 278:294-8.

77. Kurokawa M, Kornbluth S. Caspases and kinases in a death grip. Cell. 2009; 138:838-54.

78. Kuwana T, Bouchier-Hayes L, Chipuk JE, Bonzon C, Sullivan BA, Green DR, Newmeyer DD. BH3 domains of BH3-only proteins differentially regulate Bax-mediated mitochondrial membrane permeabilization both directly and indirectly. Mol Cell. 2005; 17:525-35.

79. Kuwana T, Mackey MR, Perkins G, Ellisman MH, Latterich M, Schneiter R, Green DR, Newmeyer DD. Bid, Bax, and lipids cooperate to form supramolecular openings in the outer mitochondrial membrane. Cell. 2002; 111:331-42.

80. Laussmann MA, Passante E, Düssmann H, Rauen JA, Würstle ML, Delgado ME, Devocelle M, Prehn JH, Rehm M. Proteasome inhibition can induce an autophagy-dependent apical activation of caspase-8. Cell Death Differ. 2011; 18:1584-97.

81. Letai A, Bassik MC, Walensky LD, Sorcinelli MD, Weiler S, Korsmeyer SJ. Distinct BH3 domains either sensitize or activate mitochondrial apoptosis, serving as prototype cancer therapeutics. Cancer Cell. 2002; 2:183-92.

82. Lev DC, Ruiz M, Mills L, McGary EC, Price JE, Bar-Eli M. Dacarbazine causes transcriptional up-regulation of interleukin 8 and vascular endothelial growth factor in melanoma cells: a possible escape mechanism from chemotherapy. Mol Cancer Ther. 2003; 2:753-63.

83. Li C, Johnson DE. Bortezomib induces autophagy in head and neck squamous cell carcinoma cells via JNK activation. Cancer Lett. 2012; 314:102-7.

84. Li J, Yuan J. Caspases in apoptosis and beyond. Oncogene. 2008; 27:6194-206.

85. Li L, Li S, Sun G, Peng R, Zhao L, Zhong R. Influence of the Expression Level of O6-Alkylguanine-DNA Alkyltransferase on the Formation of DNA Interstrand Crosslinks Induced by Chloroethylnitrosoureas in Cells: A Quantitation Using High-Performance Liquid Chromatography-Mass Spectrometry. PLoS One. 2015; 10(3):e0121225.

86. Li LY, Luo X, Wang X. Endonuclease G is an apoptotic DNase when released from mitochondria. Nature. 2001; 412:95-9.

87. Li Y, McClay EF. Systemic chemotherapy for the treatment of metastatic melanoma. Semin Oncol. 2002; 29:413-26.

88. Lieberman J, Fan Z. Nuclear war: the granzyme A-bomb. Curr Opin Immunol. 2003; 15(5):553-9.

89. Lin MT, Lin CL, Lin TY, Cheng CW, Yang SF, Lin CL, Wu CC, Hsieh YH, Tsai JP. Synergistic effect of fisetin combined with sorafenib in human cervical cancer HeLa cells through activation of death receptor-5 mediated caspase-8/caspase-3 and the mitochondria-dependent apoptotic pathway. Tumour Biol. 2015; Epub ahead of print.

90. Lindsten T, Ross AJ, King A, Zong WX, Rathmell JC, Shiels HA, Ulrich E, Waymire KG, Mahar P, Frauwirth K, Chen Y, Wei M, Eng VM, Adelman DM, Simon MC, Ma A, Golden JA, Evan G, Korsmeyer SJ, MacGregor GR, Thompson CB. The combined functions of proapoptotic Bcl-2 family members bak and bax are essential for normal development of multiple tissues. Mol Cell. 2000; 6:1389-99.

91. Liu FT, Newland AC, Jia L. Bax conformational change is a crucial step for PUMA-mediated apoptosis in human leukemia. Biochem Biophys Res Commun. 2003; 310:956-62.

92. Locksley RM, Killeen N, Lenardo MJ. The TNF and TNF receptor superfamilies: integrating mammalian biology. Cell. 2001; 104:487-501.

93. Lutz A, Sanwald J, Thomas M, Feuer R, Sawodny O, Ederer M, Borner C, Humar M, Merfort I. Interleukin-1β enhances FasL-induced caspase-3/-7 activity without increasing apoptosis in primary mouse hepatocytes. PLoS One. 2014; 31;9(12):e115603.

94. Maclean KH, Dorsey FC, Cleveland JL, Kastan MB. Targeting lysosomal degradation induces p53-dependent cell death and prevents cancer in mouse models of lymphomagenesis. J Clin Invest. 2008; 118:79-88.

95. Mandal D, Mazumder A, Das P, Kundu M, Basu J. Fas-, caspase 8-, and caspase 3-dependent signaling regulates the activity of the aminophospholipid translocase and phosphatidylserine externalization in human erythrocytes. J Biol Chem. 2005; 280:39460-7.

96. Martin P, Pardo J, Schill N, Jöckel L, Berg M, Froelich CJ, Wallich R, Simon MM. Granzyme B-induced and caspase 3-dependent cleavage of gelsolin by mouse cytotoxic T cells modifies cytoskeleton dynamics. J Biol Chem. 2010; 11;285(24):18918-27.

97. Martinvalet D, Zhu P, Lieberman J. Granzyme A induces caspase-independent mitochondrial damage, a required first step for apoptosis. Immunity. 2005; 22:355-70.

98. McIlwain DR, Berger T, Mak TW. Caspase functions in cell death and disease. Cold Spring Harb Perspect Biol. 2013; 1;5(4):a008656.

99. Michallet AS, Mondiere P, Taillardet M, Leverrier Y, Genestier L, Defrance T. Compromising the unfolded protein response induces autophagy-mediated cell death in multiple myeloma cells. PLoS One. 2011; 6:e25820.

100. Middleton MR, Grob JJ, Aaronson N, Fierlbeck G, Tilgen W, Seiter S, Gore M, Aamdal S, Cebon J, Coates A, Dreno B, Henz M, Schadendorf D, Kapp A, Weiss J, Fraass U, Statkevich P, Muller M, Thatcher N. Randomized phase III study of temozolomide versus dacarbazine in the treatment of patients with advanced metastatic malignant melanoma. J Clin Oncol. 2000a; 18:158-66.

101. Middleton MR, Lorigan P, Owen J, Ashcroft L, Lee SM, Harper P, Thatcher N. A randomized phase III study comparing dacarbazine, BCNU, cisplatin and tamoxifen with dacarbazine and interferon in advanced melanoma. Br J Cancer. 2000b; 82:1158-62.

102. Miranda S, González-Rodríguez Á, García-Ramírez M, Revuelta-Cervantes J, Hernández C, Simó R, Valverde ÁM. Beneficial effects of fenofibrate in retinal

pigment epithelium by the modulation of stress and survival signaling under diabetic conditions. J Cell Physiol. 2012; 227:2352-62.

103. Mouawad R, Sebert M, Michels J, Bloch J, Spano JP, Khayat D. Treatment for metastatic malignant melanoma: old drugs and new strategies. Crit Rev Oncol Hematol. 2010; 74:27-39.

104. Mozos A, Roué G, López-Guillermo A, Jares P, Campo E, Colomer D, Martinez A. The expression of the endoplasmic reticulum stress sensor BiP/GRP78 predicts response to chemotherapy and determines the efficacy of proteasome inhibitors in diffuse large b-cell lymphoma. Am J Pathol. 2011; 179:2601-10.

105. Nemes Z Jr, Friis RR, Aeschlimann D, Saurer S, Paulsson M, Fésüs L. Expression and activation of tissue transglutaminase in apoptotic cells of involuting rodent mammary tissue. Eur J Cell Biol. 1996; 70:125-33.

106. Newmeyer DD, Bossy-Wetzel E, Kluck RM, Wolf BB, Beere HM, Green DR. Bcl-xL does not inhibit the function of Apaf-1. Cell Death Differ. 2000; 7:402-7.

107. Nguyen DX, Bos PD, Massagué J. Metastasis: from dissemination to organ-specific colonization.Nat Rev Cancer. 2009; 9:274-84.

108. Nicholas B, Smethurst P, Verderio E, Jones R, Griffin M. Cross-linking of cellular proteins by tissue transglutaminase during necrotic cell death: a mechanism for maintaining tissue integrity. Biochem J. 2003; 15;371(Pt 2):413-22.

109. Noor R, Bedikian AY, Mahoney S, Bassett R Jr, Kim K, Papadopoulos N, Hwu WJ, Hwu P, Homsi J. Comparison of two dosing schedules of palonosetron for the prevention of nausea and vomiting due to interleukin-2-based biochemotherapy. Support Care Cancer. 2012; 20:2583-8.

110. North J, Mully T.Alpha-interferon induced sarcoidosis mimicking metastatic melanoma. J Cutan Pathol. 2011; 38:585-9.

111. Oda E, Ohki R, Murasawa H, Nemoto J, Shibue T, Yamashita T, Tokino T, Taniguchi T, Tanaka N. Noxa, a BH3-only member of the Bcl-2 family and candidate mediator of p53-induced apoptosis. Science. 2000; 288:1053-8.

112. Oh SH, Lim SC. Endoplasmic reticulum stress-mediated autophagy/apoptosis induced by capsaicin (8-methyl-N-vanillyl-6-nonenamide) and dihydrocapsaicin is regulated by the extent of c-Jun NH2-terminal kinase/extracellular signal-regulated kinase activation in WI38 lung epithelial fibroblast cells. J Pharmacol Exp Ther. 2009; 329:112-22.

113. Orlando KA, Pittman RN. Rho kinase regulates phagocytosis, surface expression of GlcNAc, and Golgi fragmentation of apoptotic PC12 cells. Exp Cell Res. 2006; 15;312(17):3298-311.

114. Park MA, Curiel DT, Koumenis C, Graf M, Chen CS, Fisher PB, Grant S, Dent P. PERK-dependent regulation of HSP70 expression and the regulation of autophagy. Autophagy. 2008; 4:364-7.

115. Penberthy KK, Ravichandran KS. Apoptotic cell recognition receptors and scavenger receptors. Immunol Rev. 2016; 269(1):44-59.

116. Periyasamy-Thandavan S, Jackson WH, Samaddar JS, Erickson B, Barrett JR, Raney L, Gopal E, Ganapathy V, Hill WD, Bhalla KN, Schoenlein PV. Bortezomib blocks the catabolic process of autophagy via a cathepsin-dependent mechanism, affects endoplasmic reticulum stress and induces caspase-dependent cell death in antiestrogen-sensitive and resistant ER+ breast cancer cells. Autophagy. 2010; 6:19-35.

117. Porter AG, Jänicke RU. Emerging roles of caspase-3 in apoptosis. Cell Death Differ. 1999; 6(2):99-104.

118. Portt L, Norman G, Clapp C, Greenwood M, Greenwood MT. Anti-apoptosis and cell survival: a review. Biochim Biophys Acta. 2011; 1813(1):238-59.

119. Rastogi RP, Sinha R. and Sinha RP. Apoptosis: molecular mechanisms and pathogenicity. EXCLI Journal 2009; 8:155-181.

120. Röckmann H, Schadendorf D. Drug resistance in human melanoma: mechanisms and therapeutic opportunities. Onkologie. 2003; 26:581-7.

121. Roos WP, Jöst E, Belohlavek C, Nagel G, Fritz G, Kaina B. Intrinsic anticancer drug resistance of malignant melanoma cells is abrogated by IFN-β and valproic acid. Cancer Res. 2011; 71:4150-60.

122. Russo SM, Tepper JE, Baldwin AS Jr, Liu R, Adams J, Elliott P, Cusack JC Jr. Enhancement of radiosensitivity by proteasome inhibition: implications for a role of NF-kappaB. Int J Radiat Oncol Biol Phys. 2001; 50:183-93.

123. Safa AR, Day TW, Wu CH. Cellular FLICE-like inhibitory protein (C-FLIP): a novel target for cancer therapy. Curr Cancer Drug Targets. 2008; 8(1):37-46.

124. Sahu SK, Gummadi SN, Manoj N, Aradhyam GK. Phospholipid scramblases: an overview. Arch Biochem Biophys. 2007; 1;462(1):103-14.

125. Sakahira H, Enari M, Nagata S. Cleavage of CAD inhibitor in CAD activation and DNA degradation during apoptosis. Nature. 1998; 391:96-9.

126. Schuler M, Green DR. Mechanisms of p53-dependent apoptosis. Biochem Soc Trans. 2001; 29:684-8.

127. Selimovic D, Hassan M, Haikel Y, Hengge UR. Taxol-induced mitochondrial stress in melanoma cells is mediated by activation of c-Jun N-terminal kinase (JNK) and p38 pathways via uncoupling protein 2. Cell Signal. 2008; 20:311-22.

128. Selimovic D, Ahmad M, El-Khattouti A, Hannig M, Haïkel Y, Hassan M. Apoptosis-related protein-2 triggers melanoma cell death by a mechanism including both endoplasmic reticulum stress and mitochondrial dysregulation. Carcinogenesis. 2011; 32:1268-78.

129. Selimovic D, Badura HE, El-Khattouti A, Soell M, Porzig BB, Sprenger A, Ghanjati F, Santourlidis S, Haikel Y, Hassan M. Vinblastine-induced apoptosis of melanoma cells is mediated by Ras homologous A protein (Rho A) via mitochondrial and non-mitochondrial-dependent mechanisms. Apoptosis. 2013; 18(8):980-97.

130. Selimovic D, Sprenger A, Hannig M, Haïkel Y, Hassan M. Apoptosis related protein-1 triggers melanoma cell death via interaction with the juxtamembrane region of p75 neurotrophin receptor. J Cell Mol Med. 2012; 16:349-61.

131. Shen HM, Codogno P. Autophagy is a survival force via suppression of necrotic cell death. Exp Cell Res. 2012; 318:1304-8.

132. Shirley S, Morizot A, Micheau O. Regulating TRAIL receptor-induced cell death at the membrane: a deadly discussion. Recent Pat Anticancer Drug Discov. 2011; 6(3):311-23

133. Slee EA, Adrain C, Martin SJ. Executioner caspase-3, -6, and -7 perform distinct, non-redundant roles during the demolition phase of apoptosis. J Biol Chem. 2001; 276:7320-6.

134. Soengas MS, Lowe SW. Apoptosis and melanoma chemoresistance.Oncogene. 2003; 22:3138-51.

135. Spagnolo F, Queirolo P. Upcoming strategies for the treatment of metastatic melanoma. Arch Dermatol Res. 2012; 304:177-84.

136. Spain L, Larkin J. Combination immune checkpoint blockade with ipilimumab and nivolumab in the management of advanced melanoma. Expert Opin Biol Ther. 2016. (Epub ahead of print)

137. Sun DY, Jiang S, Zheng LM, Ojcius DM, Young JD. Separate metabolic pathways leading to DNA fragmentation and apoptotic chromatin condensation. J Exp Med. 1994; 1;179(2):559-68.

138. Sun HQ, Yamamoto M, Mejillano M, Yin HL. Gelsolin, a multifunctional actin regulatory protein. J Biol Chem. 1999; 19;274(47):33179-82.

139. Susin SA, Daugas E, Ravagnan L, Samejima K, Zamzami N, Loeffler M, Costantini P, Ferri KF, Irinopoulou T, Prévost MC, Brothers G, Mak TW, Penninger J, Earnshaw WC, Kroemer G. Two distinct pathways leading to nuclear apoptosis. J Exp Med. 2000; 192:571-80.

140. Uong A, Zon LI. Melanocytes in development and cancer. J Cell Physiol. 2010; 222:38-41.

141. Verhoven B, Schlegel RA, Williamson P. Mechanisms of phosphatidylserine exposure, a phagocyte recognition signal, on apoptotic T lymphocytes. J Exp Med. 1995; 1;182(5):1597-601.

142. Verhoven B, Krahling S, Schlegel RA, Williamson P. Regulation of phosphatidylserine exposure and phagocytosis of apoptotic T lymphocytes. Cell Death Differ. 1999; 6(3):262-70.

143. Vink J, Cloos J, Kaspers GJ. Proteasome inhibition as novel treatment strategy in leukaemia. Br J Haematol. 2006; 134(3):253-62.

144. van der Wall E, Beijnen JH, Rodenhuis S. High-dose chemotherapy regimens for solid tumors. Cancer Treat Rev. 1995; 21:105-32.

145. van Engeland M, Nieland LJ, Ramaekers FC, Schutte B, Reutelingsperger CP. Annexin V-affinity assay: a review on an apoptosis detection system based on phosphatidylserine exposure. Cytometry. 1998; 1;31(1):1-9.

146. van Loo G, Saelens X, Matthijssens F, Schotte P, Beyaert R, Declercq W, Vandenabeele P. Caspases are not localized in mitochondria during life or death. Cell Death Differ. 2002; 9:1207-11.

147. Wang CY, Mayo MW, Baldwin AS Jr. TNF- and cancer therapy-induced apoptosis: potentiation by inhibition of NF-kappaB. Science. 1996; 274:784-7.

148. Wang Y, Singh R, Massey AC, Kane SS, Kaushik S, Grant T, Xiang Y, Cuervo AM, Czaja MJ. Loss of macroautophagy promotes or prevents fibroblast apoptosis depending on the death stimulus. J Biol Chem. 2008; 283:4766-77.

149. Wei MC, Zong WX, Cheng EH, Lindsten T, Panoutsakopoulou V, Ross AJ, Roth KA, MacGregor GR, Thompson CB, Korsmeyer SJ. Proapoptotic BAX and BAK: a requisite gateway to mitochondrial dysfunction and death. Science. 2001; 292:727-30.

150. Whalen GF, Sharif SF.Locally increased metastatic efficiency as a reason for preferential metastasis of solid tumors to lymph nodes. Ann Surg. 1992; 215:166-71.

151. Wilson EN, Bristol ML, Di X, Maltese WA, Koterba K, Beckman MJ, Gewirtz DA. A switch between cytoprotective and cytotoxic autophagy in the radiosensitization of breast tumor cells by chloroquine and vitamin D. Horm Cancer. 2011; 2:272-85.

152. Yang E, Zha J, Jockel J, Boise LH, Thompson CB, Korsmeyer SJ. Bad, a heterodimeric partner for Bcl-XL and Bcl-2, displaces Bax and promotes cell death. Cell. 1995; 80:285-91.

153. Yang QH, Church-Hajduk R, Ren J, Newton ML, Du C. Omi/HtrA2 catalytic cleavage of inhibitor of apoptosis (IAP) irreversibly inactivates IAPs and facilitates caspase activity in apoptosis. Genes Dev. 2003; 15;17(12):1487-96.

154. Yerlikaya A, Okur E, Eker S, Erin N. Combined effects of the proteasome inhibitor bortezomib and Hsp70 inhibitors on the B16F10 melanoma cell line. Mol Med Report. 2010; 3:333-339.

155. Yerlikaya A, Okur E, Ulukaya E. The p53-independent induction of apoptosis in breast cancer cells in response to proteasome inhibitor bortezomib. Tumour Biol. 2012; 33:1385-92.

156. Yip KW, Reed JC. Bcl-2 family proteins and cancer. Oncogene. 2008; 27:6398-406.

157. Zeng R, Chen Y, Zhao S, Cui GH. Autophagy counteracts apoptosis in human multiple myeloma cells exposed to oridonin in vitro via regulating intracellular ROS and SIRT1. Acta Pharmacol Sin. 2012; 33:91-100.

158. Zhu H, Zhang L, Dong F, Guo W, Wu S, Teraishi F, Davis JJ, Chiao PJ, Fang B. Bik/NBK accumulation correlates with apoptosis-induction by bortezomib (PS-341, Velcade) and other proteasome inhibitors. Oncogene. 2005; 24:4993-9.

159. Zwielly A, Mordechai S, Brkic G, Bogomolny E, Pelly IZ, Moreh R, Gopas J. Grading of intrinsic and acquired cisplatin-resistant human melanoma cell lines: an infrared ATR study. Eur Biophys J. 2011; 40:795-804.

Acknowledgements

First of all, I would like to thank PD Dr. rer. nat. Simeon Santourlidis, who gave me the opportunity to finish this study at the laboratories of the Institute for Transplantation Diagnostics and Cell Therapeutics, Heinrich Heine University of Düsseldorf.
Just as much, I would like to thank Dr. Mohamed Hassan for his untiring supervision of this work and his seemingly endless patience. His precious advice, love for science and sensitivity for the outstanding guided me through the jungle of scientific questions and kept me going on. His innumerable encouragements and continued support focused my work in numerous discussions to the results presented in this study. Thank you very much for the last 4 years, which have taught me very much in term of research and scientific work.

I would like to gratefully acknowledge the colleagues at the Clinic of Dermatology, where I started this work, as well as the colleagues of the Institute for Transplantation Diagnostics and Cell Therapeutics where I finished this work.

This work was financially supported in part by Dr. Mildred Scheel Foundation, Project Number: 10-2202-Ha1 (Deutsche Krebshilfe, Mildred Scheel Stiftung für Krebsforschung) and DFG (HA 5081/3-1) for which I want to express my greatest thanks.

Words cannot express my gratitude and love to my family who has always supported and encouraged me as long as I can think. Without your support and advice this work would never been realized. Your understanding, love and support are not measurable and will never be forgotten.

Eidesstattliche Versicherung

Ich versichere an Eides statt, dass die Dissertation selbstständig und ohne unzulässige fremde Hilfe erstellt worden ist und die hier vorgelegte Dissertation nicht von einer anderen Medizinischen Fakultät abgelehnt worden ist.

Düsseldorf, 21.05.2016
Ort, Datum

_____

Unterschrift Benjamin Bernhard Otto Wolfhart Porzig